Title
Defining Self-renewal in Human Hematopoietic Stem Cells

Author
Prashad, Sacha Leandra

Publication Date
2014

Peer reviewed|Thesis/dissertation

UNIVERSITY OF CALIFORNIA

Los Angeles

Defining Self-renewal in Human Hematopoietic Stem Cells

A dissertation submitted in partial satisfaction of the

requirements for the degree Doctor of Philosophy

in Molecular Biology

by

Sacha Leandra Prashad

2014

ABSTRACT OF THE DISSERTATION

Defining Self-renewal in Human Hematopoietic Stem Cells

by

Sacha Leandra Prashad

Doctor of Philosophy in Molecular Biology

University of California, Los Angeles, 2014

Professor Hanna K.A. Mikkola, Chair

Hematopoietic stem cells (HSC) are widely applicable for the treatment of blood disorders such as leukemias and anemias. However, only a fraction of patients can find a suitable HSC donor. As attempts to generate HSC from pluripotent cells or expand functional HSC in culture have met with limited success, it will be necessary to define the identity of the self-renewing HSC and key intrinsic and extrinsic factors utilized by the developing embryo for HSC self-renewal such that the conditions necessary for HSC development can be mimicked *in vitro*.

In this work, we first defined an *in vitro* HSPC (hematopoietic stem/progenitor cell) co-culture system on mesenchymal stem cell (MSC) stroma that sustains human multilineage hematopoietic hierarchy. We found that this culture system maintains undifferentiated, transplantable HSPC that retain a relatively stable HSPC surface phenotype and transcriptome over several weeks. However, we also discovered that dysregulation of PBX governed genetic networks may compromise the function of

cultured HSC, providing new insights on how to target the compromised HSC transcriptome to improve HSC expansion in culture.

This work also identified a novel surface marker that can be utilized to define the self-renewing HSC during human development. We discovered that the glycophosphatidylinositol-anchored surface protein GPI-80 (Vanin 2), previously implicated in leukocyte adhesion and diapedesis, identifies a functionally distinct subpopulation of human fetal HSPC that possess self-renewal ability. The GPI-80+ HSPC were the only population that maintained proliferative potential and undifferentiated state in MSC stroma co-culture, as well as displayed the ability to engraft in immunodeficient NSG mice. Through defining the identity of the human fetal HSC and characterizing the HSPC transcriptome in the in vivo niche and on mesenchymal stroma, we can determine the factors utilized in HSC self-renewal and identify those that are deficient in culture, which will bring us closer towards generation and expansion of HSC *in vitro*.

The dissertation of Sacha Leandra Prashad is approved.

Gay Crooks

April Pyle

Michael Teitell

Hanna K.A. Mikkola, Committee Chair

University of California, Los Angeles

2014

DEDICATION

This dissertation is dedicated to my parents, Vinny and Lakana, with love.

TABLE OF CONTENTS

Preliminary pages:

Dissertation research:

LIST OF FIGURES

Acknowledgements

Chapter 2 is a version of Magnusson M, Sierra MI, Sasidharan R, Prashad SL, Romero M, Saarikoski P, Van Handel B, Huang A, Li X, Mikkola HK. (2013). Expansion on stromal cells preserves the undifferentiated state of human hematopoietic stem cells despite compromised reconstitution ability. *Plos One* 8(1):e53912.

Chapter 3 is a version of Prashad SL**,** Yao CY*, Calvanese V*, Kaiser J, Sasidharan R, Magnusson M, and Mikkola HKA. GPI-80 Defines Self-renewal Ability in Hematopoietic Stem Cells During Human Development. (in submisson) * denotes equal contribution

Appendix is a version of Van Handel B, Prashad SL, Hassanzadeh-Kiabi N, Huang A, Magnusson M, Atanassova B, Chen A, Hamalainen E, and Mikkola H.K.A. (2010). The first trimester placenta is a site for the terminal maturation of primitive erythroid cells. *Blood* 116: 3321-3330.

I would like to thank the BSCRC Flow Cytometry Core for their assistance in FACS sorting. I would also like to acknowledge our funding sources. This work was supported by the NIH RO1 HL097766, CIRM New Faculty Award RN1-00557-1 and Leukemia &

Lymphoma Society (LLS) Scholar awards for H.K.A.M. S.L.P. was supported by the Howard Hughes Medical Institute Gilliam fellowship and the UCLA Whitcome Fellowship. C.Y. was supported by the Howard Hughes Undergraduate Research scholarship. V.C was supported by LLS Special Fellow Award. M.M. was supported by the Swedish Research Council and Tegger Foundation.

Biographical Sketch:

SACHA L. PRASHAD

EDUCATION

06/2008 B.S. Molecular, Cell, and Developmental Biology
University of California, Los Angeles

PUBLICATIONS

Prashad SL, Yao CY, Calvanese V, Sasidharan R, Kaiser J, Magnusson M, and Mikkola H. GPI-80 Defines Self-renewal Ability in Hematopoietic Stem Cells During Human Development (submitted)

Magnusson M, Sierra M, Sasidharan R, **Prashad SL**, Saarikoski P, Romero M, Van Handel B, Huang A, Li X, and Mikkola H. Ex vivo expansion on stroma preserves hematopoietic stem cell identity while compromising in vivo reconstitution ability. PLoS One. 8(1):e53912 (2013)

Van Handel B, **Prashad SL**, Hassanzadeh-Kiabi N, Huang A, Magnusson M, Atanassova B, Chen A, Hamalainen E, and Mikkola H. The first trimester human placenta is a site for terminal maturation of primitive erythroid cells. *Blood* 116 (17), 3321-3330 (2010)

Shih A, Schairer A, Barrett C, Geron I, Recart A, Goff D, **Prashad SL**, Wu J, Jiang F, Gotlib J, Balaian L, Minden M, Leu H, Wall R, Ma W, Shazand K, McPherson J, Kornblau S, Deichiate I, Pu M, Bao L, Martinelli G, Reya T, Morris S, VanArsdale T, Hudson T, Messer K, Mikkola H, Levin W, Frzer K, Carson D, Sadarangani A, Jamieson, C. Cycling Toward Leukemia Stem Cell Elimination with a Selective Sonic Hedgehog Antagonist (submitted)

FELLOWSHIPS/ACADEMIC HONORS

2011 International Society of Hematology (ISEH) travel grant

2009 Howard Hughes Gilliam Fellowship

2008 UCLA Molecular Biology Institute Whitcome Fellowship

2008 Department of Molecular, Cell, and Developmental Biology Senior Research Award

2008 Department of Molecular, Cell, and Developmental Biology: Highest Departmental Honors

2008 Fred Eiserling Prize for Outstanding Undergraduate Research 2006-2008 Howard Hughes Undergraduate Research Scholar 2004-2008 UCLA College Honors

2007 UCLA Dean's Prize

2004-2008 Dean's Honors List

POSTERS/TALKS (NON-UCLA)

Prashad S, Yao C, Sasidharan R, Magnusson M, Sasidharan R, Kaiser J and Mikkola, H. GPI-80 Distinguishes Transplantable Hematopoietic Stem Cells from Progenitors. Poster presented in Yokahama Japan at the International Society of Stem Cell Research Conference (ISSCR), June 2012.

Prashad S, Yao C, Sasidharan R, Magnusson M, Sasidharan R, Kaiser J and Mikkola, H. GPI-80 Distinguishes Transplantable Hematopoietic Stem Cells from Progenitors. Talk presented at the International Society of Hematology (ISEH), August 2011.

Prashad S, Yao C, Sasidharan R, Magnusson M, Sasidharan R, Kaiser J and Mikkola, H. GPI-80 Distinguishes Transplantable Hematopoietic Stem Cells from Progenitors. Talk presented at HHMI, August 2011.

Prashad S, Yao C, Sasidharan, R, Magnusson M, Sasidharan R, Kaiser J, and Mikkola, H. GPI-80 Distinguishes Transplantable Hematopoietic Stem Cells from Progenitors. Poster presented in San Diego at American Society of Hematology Conference (ASH), December 2011.

Prashad S, Van Handel B, Huang A, Magnusson M, Chen A, Bristol G, Zack J, Hamalainen E, and Mikkola H. Origins of Hematopoietic Stem Cells. Poster presented at Capitol Hill, May 2008.

Prashad S, Van Handel B, Huang A, Magnusson M, Chen A, Bristol G, Zack J, Hamalainen E, and Mikkola H. Origins of Hematopoietic Stem Cells. Poster presented at EXROP session at HHMI Conference Center, May 2008

WORK/EXTRACURRICULARS:

Junior Investigators Committee, International Society of Stem Cell Research
Fall 2013-present
Planned events fostering early career development for new independent scientists as part of the leading international stem cell society

Howard Hughes Medical Institute Ask-a-Scientist Program
Fall 2012- Spring 2013
Volunteer scientist for a special feature on HHMI website, focused on public education
Communicated scientific concepts in clear language to Web visitors with biology-related questions, specifically in topics of blood and stem cells

UCLA CityLab
Fall 2012 - present
Science education volunteer
Introduce disadvantaged high school students to biotechnology through hands- on laboratory experiences

Harvard Exceptional Research Opportunities Program (Harvard EXROP)
June 2007 – August 2007
Zon laboratory - Children's Hospital Boston
Executed chemical screen to study *TIF1gamma* function in zebrafish hematopoiesis

Howard Hughes Undergraduate Research Scholar
Fall 2006 – Spring 2008
Intensive training in research presentation/discussion of current scientific literature

UCLA Undergraduate Research Consortium in Functional Genomics: Advanced Research in Genes, Genomics, and Genetics
Fall 2005 – Spring 2007
Honors journal club meetings
Training in genetics and functional genomics employing the study of P-element mutations in *Drosophila*

Stroke Study – Student Clinical Research Program at UCLA Education Coordinator
June 2006 – Spring 2009
- **Stroke Student Educator**
- **Speaker** – stroke risk, prevention, recognition of stroke onset

• **Research associate** Educate/train new student researchers
Identify Emergency Department patients with acute neurological syndromes Identify patients meeting inclusion/exclusion criteria for acute and hyper-acute National Stroke Research Trials
Review stroke trials in progress

Quality Management Coordinator /Clinical Care Extender at Valley Presbyterian Hospital
June 2006 – October 2007
Training/selecting new Care Extender interns for rotations in Med/Surg, ER, Telemetry, Labor/Delivery
Administrator – managing interns, program improvement, peer review

Chapter 1:

Introduction

Preface

Stem cells have demonstrated great promise in the treatment of various human ailments. Clinical trials in multiple areas, such as heart disease (Doppler, Deutsch, Lange, & Krane, 2013), eye disease (Ramsden et al., 2013), and spinal cord injuries (J. Li & Lepski, 2013) are in the beginning stages of development and have shown early success, giving hope for novel stem cell therapies targeted towards previously incurable conditions. Hematopoietic stem cells (HSC) are unique in having been used for decades in clinic to replenish the blood system in the treatment of blood disorders (Bordignon, 2006). Arguably one of the most well studied type of stem cells, HSC represent an elegant model for the study of stem cell properties. However, a comprehensive understanding of the pathways responsible for the self-renewal of hematopoietic stem cells remains elusive. Thus, attempts to expand functional hematopoietic stem cells *in vitro*, or generate HSC from pluripotent stem cells to satisfy the unmet clinical need for HLA-matched HSC, have not yet been successful (Dravid & Crooks, 2011). Intensive study of both the niche and the cell intrinsic transcriptional machinery necessary to maintain stem cell properties will be critical for the construction of *in vitro* culture systems for HSC. A major obstacle impeding the investigation of programs utilized by human HSC is a lack of markers specific to self-renewing human HSC during development, a unique time period in which HSC are generated and expand in specialized niches created for HSC growth. We believe that investigation of fetal HSC and their niches will be particularly informative for expansion studies, as fetal HSC are in a state of active self-renewal and

expansion, while HSC in adult bone marrow are largely quiescent during homeostasis. Though specific surface markers exist for murine HSC (i.e. SLAM markers) the same genes are not expressed by human HSC (Kiel et al., 2005; Larochelle et al., 2011) . Therefore markers specific to human fetal HSC during development will be necessary to identify the cells of interest, as well as define the specific pathways employed for HSC production and expansion. Furthermore, as co-culture of HSC with supportive stromal cells has demonstrated limited success in maintenance of stem cell properties (Moore, Ema, & Lemischka, 1997; Nolta et al., 2002), scrutiny of HSC behavior in current co-culture systems, as well as molecular defects and transcriptional changes that occur in culture, will be conducive to the improvement of culture systems for the generation and expansion of HSC for clinical purposes.

1.1 The Hematopoietic Hierarchy

Hematopoietic stem cells (HSC) are tissue specific stem cells that reside atop a hierarchy of all myeloid and lymphoid precursor cells (Figure 1.1), and are maintained in specific anatomical sites known as niches that provide the signals necessary to protect stem cell properties.

It is thought that during homeostasis, hematopoietic stem cells replenish the HSC pool through asymmetric division; upon division, the HSC self-renew as well as give rise to hematopoietic progenitors, which may be multipotent, but have limited self-renewal ability, and lack engraftment ability (Weissman, 2000). Self-renewal of HSC must be tightly controlled, as many transcription factors that control HSC self-renewal can cause

hematopoietic malignancy if disturbed. HPC generate differentiated blood cells necessary for proper function of the blood and immune systems while proper maintenance of the HSC compartment ensures lifelong blood homeostasis. HPC may be divided into two major categories of progenitor cells; those that give rise to myeloid cells (myeloid progenitors), and those that specifically give rise to lymphoid cells (lymphoid progenitors). Downstream of HPC are precursors that have increasingly restricted differentiation potential, until reaching terminal differentiation.

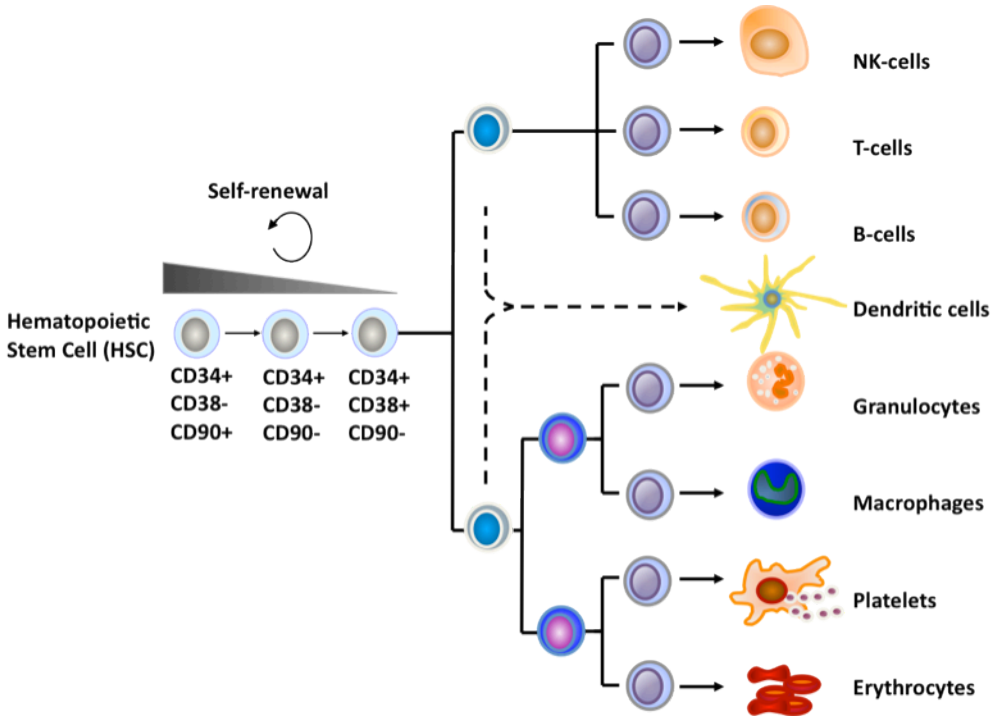

Figure 1.1: The Hematopoietic Hierarchy

1.2 Hematopoiesis in Development

De novo generation of HSC occurs only during embryonic development; thus, human development provides a unique window into the molecular events orchestrating formation of functional HSC. Though the vast majority of data regarding hematopoietic development has been determined based on mouse studies, the developmental program has corresponding niches in human. During development, the first hematopoietic cells that are generated are not hematopoietic stem cells, but primitive erythrocytes that are necessary to carry oxygen in the developing embryo. This first wave of hematopoiesis, referred to as the "primitive wave" occurs at approximately E7.0 in mice, which is approximately day 16 in human, and results in the generation of red cells and macrophages in the yolk sac (Mikkola & Orkin, 2006). Recently our work characterizing red blood cell development has demonstrated that human primitive red bloods enucleate in the placental villi (see Appendix). Red cells generated in the primitive way are distinguished by their expression of embryonic globins, which have a higher affinity for oxygen; as development progresses a switch to expression of adult globins occurs. Following the first wave of hematopoiesis, the second wave takes place and results in the generation of transient definitive progenitors in the yolk sac, AGM, vitelline and umbilical arteries, and the placenta (Figure 1.2). The cells generated in the second wave are progenitors that are thought to be transient myelo-erythroid progenitors; they lack the self-renewal ability that defines functional HSC, and their lymphoid potential is also limited. Definitive hematopoietic stem cells that can form all blood cell types are generated after the transient definitive wave from hemogenic endothelium in sites such as

the aorta-gonad-mesonephros region (AGM), yolk sack, and the placenta, after E8.0 (Alvarez-Silva, Belo-Diabangouaya, Salaün, & Dieterlen-Lièvre, 2003; Gekas, Dieterlen-Lièvre, Orkin, & Mikkola, 2005; Rhodes et al., 2008). Following the generation of HSC in the developing embryo and extra-embryonic tissues, the HSC migrate to the fetal liver, which acts as the major site of HSC expansion during development before HSC migrate to the bone marrow. During post-natal life, HSC reside in a quiescent state in the bone marrow and are activated as needed.

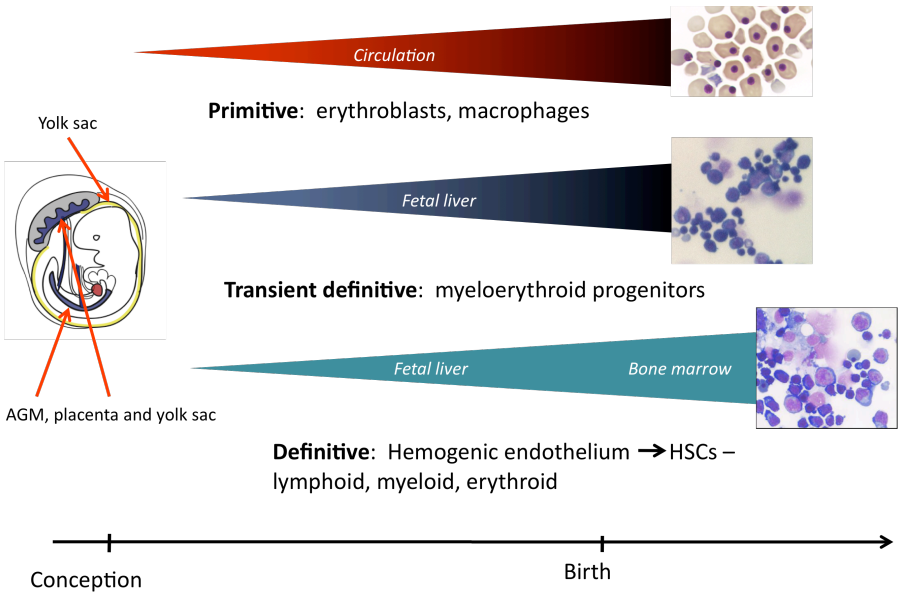

Figure 1.2: Waves of Developmental Hematopoiesis

HSC emerge from specialized endothelium known as "hemogenic" endothelium that has the ability to generate hematopoietic cells directly from endothelial cells in culture (Antas, Al-Drees, Prudence, Sugiyama, & Fraser, 2013). HSC emergence from hemogenic endothelium was first documented in the aorta-gonad-mesonephros region (AGM). It has then been shown that extraembryonic sites such as the yolk sac and the

placenta can also generate HSC (Alvarez-Silva et al., 2003; Gekas et al., 2005; Rhodes et al., 2008). Furthermore, recent studies have elegantly demonstrated the emergence of HSC from hemogenic endothelium in the zebrafish, using fluorescent reporters in conjunction with timelapse microscopy (Bertrand et al., 2010). Unexpectedly, some recent data suggests in mice, the endothelium in the head may have hemogenic potential as well; however these studies remain controversial, and other studies will reveal whether early endothelium in other sites may generate HSC (Z. Li et al., 2012).

As hematopoietic cells are derived from hemogenic endothelium, many surface markers and transcription factors are shared between HSC and endothelium. Surface markers CD31 and CD34 are expressed on both hematopoietic cells and the underlying endothelium and both hemogenic endothelium and hematopoietic cells express transcription SCL, RUNX-1 and GATA-2 (Goldie et. al, 2008).

While specific markers exist to distinguish mouse HSC from multipotent progenitors, such as the Lineage$^{-/low}$Sca-1^{+}c-Kit^{+} (LSK) and SLAM family, these markers are not expressed in human HSC (Kiel et al., 2005; Larochelle et al., 2011); few specific markers are known for human HSC. To further complicate matters, in both human and mouse, hematopoietic markers change throughout development and the same markers may not be conserved within different hematopoietic niches (McKinney-Freeman et al., 2009). In human there are no established HSC markers that can demarcate the HSC from endothelium; major hematopoietic stem cell markers CD34 and CD90 (Thy1) are expressed both on the HSC and the endothelium.

1.3 Identifying HSC: Current definition of HSCs: culture, expansion, CFU

Hematopoietic stem cells are defined by their function; in order to be defined as a mature, functional HSC, a cell must have the aforementioned properties: the ability to self-renew in long-term culture, have multi-lineage differentiation potential, and have the ability to engraft into adult bone marrow upon transplantation (Figure 1.3).

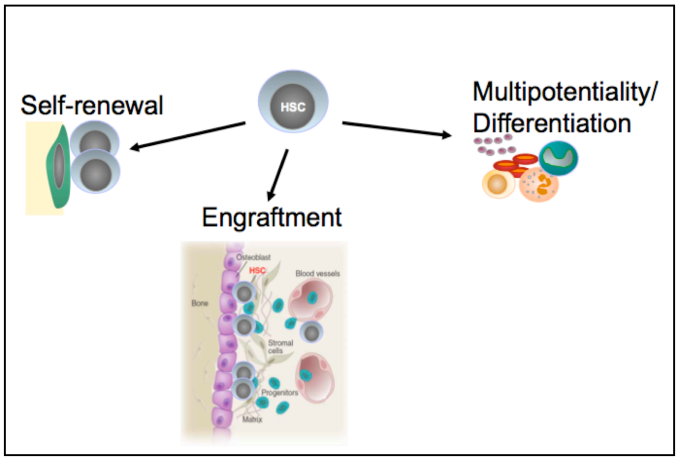

Figure 1.3: Hematopoietic Stem Cell Properties

While HSC self-renewal is most accurately assayed in vivo (see below), proliferative potential in long-term initialing culture can be used as a surrogate assay for self-renewal by using co-culture of HSC with supportive stromal lines such as OP9 (Nakano, Kodama, & Honjo, 1994), a stromal cell line derived from the calvaria of a macrophage-colony stimulating factor knockout mouse, or AFT024, a murine stromal cell line derived from fetal liver (Nolta, 2002). Myelo-erythroid differentiation potential is assessed through colony forming unit (CFU) assay on a semi-solid medium, methylcellulose, supplemented with cytokines that stimulate HSPC differentiation. Lymphoid

differentiation must be induced in co-culture with distinct conditions based on T-cell generation or B-cell generation. Generation of T-cells requires co-culture conditions that provide Notch ligands necessary for T-cell differentiation (Schmitt & Zúñiga-Pflücker, 2002). Finally, the gold standard for HSC function is the engraftment assay. HSC engraftment can be tested via transplantation into immune-deficient mice (Ishikawa, 2013). Retro-orbital or tail-vein injection is utilized to assess homing and engraftment into the bone marrow niche, and functional HSC are identified by possessing the unique ability to reconstitute the primary host, as well as reconstitute irradiated recipients in successive transplantations.

1.4 Current and Prospective Applications

Since the 1950's, hematopoietic stem cells have successfully been used to treat a variety of blood disorders. Patients can be treated with bone marrow transplants, or cord blood transplants from donors of matching HLA types (Bordignon, 2006; Shenoy, 2013). However, treatments are limited to finding successful matches; mismatch transplants may lead to rejection of the cells by the immune system and graft versus host disorder (GVHD); furthermore, data demonstrates that it may be particularly difficult for patients of mixed ethnic or minority backgrounds to find matching HLA donors (Dehn et al., 2008). Cord blood is a potential source for less immunogenic HSC for patient therapy (Ballen, Gluckman, & Broxmeyer, 2013); however the number of HSC in a single cord is sufficient only for the treatment of pediatric patients. Clinical studies have demonstrated that multiple cords can be pooled to generate sufficient numbers of HSC for transplant;

however pooling cords has the caveat of potentially leading to graft versus graft disorder. In an ideal system, HSC from cord blood could be expanded *in vitro* from the many cord blood units that have been frozen in cord blood banks. However, the regulation and maintenance of HSC is not understood well enough for expansion of HSC from cord blood. A second potential source of HSC would be specification of HSC from either embryonic stem (ES) cells or induced pluripotent cells (iPS). Unfortunately, efforts to generate functional HSC from pluripotent stem cells has met with limited success, largely due to limited knowledge of the emergence of HSC during development and the critical transcriptional programs that are necessary both for emergence and maintenance of HSC (Dravid & Crooks, 2011).

Significance and Aims of this Dissertation

Define an *In Vitro* System for Culturing Human HSC

Firstly, we aim to define the behavior of HSC during *in vitro* culture; particularly to analyze the stability of the transcriptome of HSC in co-culture with mesenchymal stem cells. In order to overcome the obstacles to HSC expansion in vitro, it will be critical to have a comprehensive understanding of the programs activated in the *in vivo* niche as compared to in vitro co-culture. Once discrepancies are identified, culture conditions can be adjusted accordingly to provide the proper niche signaling necessary for HSC expansion.

Identify the Self-renewing Human Fetal HSC Population

We aim to define a specific marker for human fetal HSC, conducive to the study of the key programs necessary for maintaining of stemness properties in HSC. Human fetal liver HSC, the most potent source of self-renewing HSC, will be utilized, as the fetal liver is the major site of HSC expansion during development. Purification and gene expression analysis of human fetal liver HSC would provide insight into the key factors that highly proliferative HSC utilize for niche interaction and expansion.

Bibliography

Alvarez-Silva, M., Belo-Diabangouaya, P., Salaün, J., & Dieterlen-Lièvre, F. (2003). Mouse placenta is a major hematopoietic organ. *Development (Cambridge, England)*, *130*(22), 5437–44.

Antas, V. I., Al-Drees, M. A., Prudence, A. J. A., Sugiyama, D., & Fraser, S. T. (2013). Hemogenic endothelium: a vessel for blood production. *The international journal of biochemistry & cell biology*, *45*(3), 692–5.

Ballen, K. K., Gluckman, E., & Broxmeyer, H. E. (2013). Umbilical cord blood transplantation: the first 25 years and beyond. *Blood*, *122*(4), 491–8.

Bertrand, J. Y., Chi, N. C., Santoso, B., Teng, S., Stainier, D. Y. R., & Traver, D. (2010). Haematopoietic stem cells derive directly from aortic endothelium during development. *Nature*, *464*(7285), 108–11.

Bordignon, C. (2006). Stem-cell therapies for blood diseases. *Nature*, *441*(7097), 1100–2.

Dehn, J., Arora, M., Spellman, S., Setterholm, M., Horowitz, M., Confer, D., & Weisdorf, D. (2008). Unrelated donor hematopoietic cell transplantation: factors associated with a better HLA match. *Biology of blood and marrow transplantation : journal of the American Society for Blood and Marrow Transplantation*, *14*(12),

Doppler, S. A., Deutsch, M.-A., Lange, R., & Krane, M. (2013). Cardiac regeneration: current therapies-future concepts. *Journal of thoracic disease*, *5*(5), 683–97.

Dravid, G. G., & Crooks, G. M. (2011). The challenges and promises of blood engineered from human pluripotent stem cells. *Advanced drug delivery reviews*, *63*(4-5), 331–41.

Gekas, C., Dieterlen-Lièvre, F., Orkin, S. H., & Mikkola, H. K. A. (2005). The placenta is a niche for hematopoietic stem cells. *Developmental cell*, *8*(3), 365–75.

Goldie, L., Lucitti, J., Dickinson, M., and Hirsch, K. Cell signaling directing the formation and function of hemogenic endothelium during murine embryogenesis. *Blood* 112(8), 3194-03.

Ishikawa, F. (2013). Modeling normal and malignant human hematopoiesis in vivo through newborn NSG xenotransplantation. *International journal of hematology*, *98*(6), 634–40.

Kiel, M. J., Yilmaz, O. H., Iwashita, T., Yilmaz, O. H., Terhorst, C., & Morrison, S. J. (2005). SLAM family receptors distinguish hematopoietic stem and progenitor cells and reveal endothelial niches for stem cells. *Cell*, *121*(7), 1109–21.

Larochelle, A., Savona, M., Wiggins, M., Anderson, S., Ichwan, B., Keyvanfar, K., … Dunbar, C. E. (2011). Human and rhesus macaque hematopoietic stem cells cannot be purified based only on SLAM family markers. *Blood*, *117*(5), 1550–4.

Li, J., & Lepski, G. (2013). Cell transplantation for spinal cord injury: a systematic review. *BioMed research international*, *2013*, 786475.

Li, Z., Lan, Y., He, W., Chen, D., Wang, J., Zhou, F., … Liu, B. (2012). Mouse embryonic head as a site for hematopoietic stem cell development. *Cell stem cell*, *11*(5), 663–75.

McKinney-Freeman, S. L., Naveiras, O., Yates, F., Loewer, S., Philitas, M., Curran, M., … Daley, G. Q. (2009). Surface antigen phenotypes of hematopoietic stem cells from embryos and murine embryonic stem cells. *Blood*, *114*(2), 268–78.

Mikkola, H. K. A., & Orkin, S. H. (2006). The journey of developing hematopoietic stem cells. *Development (Cambridge, England)*, *133*(19), 3733–44.

Moore, K. A., Ema, H., & Lemischka, I. R. (1997). In vitro maintenance of highly purified, transplantable hematopoietic stem cells. *Blood*, *89*(12), 4337–47.

Nakano, T., Kodama, H., & Honjo, T. (1994). Generation of lymphohematopoietic cells from embryonic stem cells in culture. *Science*, *265*(5175), 1098–1101.

Nolta, J. A., Thiemann, F. T., Arakawa-Hoyt, J., Dao, M. A., Barsky, L. W., Moore, K. A., … Crooks, G. M. (2002). The AFT024 stromal cell line supports long-term ex vivo maintenance of engrafting multipotent human hematopoietic progenitors. *Leukemia*, *16*(3), 352–61.

Ramsden, C. M., Powner, M. B., Carr, A.-J. F., Smart, M. J. K., da Cruz, L., & Coffey, P. J. (2013). Stem cells in retinal regeneration: past, present and future. *Development (Cambridge, England)*, *140*(12), 2576–85.

Rhodes, K. E., Gekas, C., Wang, Y., Lux, C. T., Francis, C. S., Chan, D. N., … Mikkola, H. K. A. (2008). The emergence of hematopoietic stem cells is initiated in the placental vasculature in the absence of circulation. *Cell stem cell*, *2*(3), 252–63.

Schmitt, T. M., & Zúñiga-Pflücker, J. C. (2002). Induction of T cell development from hematopoietic progenitor cells by delta-like-1 in vitro. *Immunity*, *17*(6), 749–56. Shenoy, S. (2013). Umbilical cord blood: an evolving stem cell source for sickle cell disease transplants. *Stem cells translational medicine*, *2*(5), 337–40.

Weissman, I. L. (2000). Stem cells: units of development, units of regeneration, and units in evolution. *Cell*, *100*(1), 157–68.

Chapter 2:

Expansion on stromal cells preserves the undifferentiated state of human hematopoietic stem cells despite compromised reconstitution ability

Expansion on stromal cells preserves the undifferentiated state of human hematopoietic stem cells despite compromised reconstitution ability

Mattias Magnusson[1], Maria I. Sierra[1], Rajkumar Sasidharan[1], Sacha L. Prashad[1], Melissa Romero[1], Pamela Saarikoski[1], Ben Van Handel[1], Andy Huang[1], Xinmin Li[2], Hanna K.A. Mikkola[1,3,4,5]

[1]Department of Molecular, Cell and Developmental Biology, University of California Los Angeles, Los Angeles, CA 90095, USA. [2]Department of Pathology and Laboratory Medicine, University of California Los Angeles, Los Angeles, CA 90095, USA. [3]Eli and Edythe Broad Center for Regenerative Medicine and Stem Cell Research, University of California Los Angeles, Los Angeles, CA 90095, USA. [4]Jonsson Comprehensive Cancer Center, University of California Los Angeles, Los Angeles, CA 90095, USA. [5]Molecular Biology Institute, University of California Los Angeles, Los Angeles, CA 90095, USA.

Corresponding author**:** Hanna K.A. Mikkola, 621 Charles E. Young Dr S, LSB 2204, Los Angeles, CA 90095; Telephone: 1-310-825-2565, **fax**: 1-310-206-5553 Email: hmikkola@mcdb.ucla.edu,

Abstract

Lack of HLA-matched hematopoietic stem cells (HSC) limits the number of patients with life-threatening blood disorders that can be treated by HSC transplantation. So far, insufficient understanding of the regulatory mechanisms governing human HSC has precluded the development of effective protocols for culturing HSC for therapeutic use and molecular studies. We defined a culture system using OP9M2 mesenchymal stem cell (MSC) stroma that protects human hematopoietic stem/progenitor cells (HSPC) from differentiation and apoptosis. In addition, it facilitates a dramatic expansion of multipotent progenitors that retain the immunophenotype (CD34+CD38-CD90+) characteristic of human HSPC and proliferative potential over several weeks in culture. In contrast, transplantable HSC could be maintained, but not significantly expanded, during 2-week culture. Temporal analysis of the transcriptome of the *ex vivo* expanded CD34+CD38-CD90+ cells documented remarkable stability of most transcriptional regulators known to govern the undifferentiated HSC state. Nevertheless, it revealed dynamic fluctuations in transcriptional programs that associate with HSC behavior and may compromise HSC function, such as dysregulation of *PBX1* regulated genetic networks. This culture system serves now as a platform for modeling human multilineage hematopoietic stem/progenitor cell hierarchy and studying the complex regulation of HSC identity and function required for successful *ex vivo* expansion of transplantable HSC.

Introduction

Hematopoietic stem cells (HSC) have been successfully used to treat leukemias, inherited immune deficiencies and other life-threatening blood diseases [1,2]. However, only a fraction of patients benefit from this therapy due to the lack of HLA-matched bone marrow donors, and low number of HSC in cord blood [3]. Therefore, a long-standing goal has been to establish culture protocols to facilitate HSC expansion. However, there has been little success in expanding human HSC for clinical purposes due to limited understanding of the complex mechanisms governing HSC properties, and how these programs become compromised in culture. Furthermore, most HSC regulators have been identified using gene-targeted mouse models [4], whereas mechanistic understanding of human hematopoiesis is lagging behind due to lack of suitable *in vitro* and *in vivo* model systems for manipulating human HSC or their niche. A major challenge in culturing HSC is the difficulty to recreate the specialized microenvironment that regulates self-renewal of HSC within hematopoietic tissues; as a result, cultured HSC are subjected to rapid differentiation or death [5].

The bone marrow HSC niche consists of multiple cell types, including mesenchymal stem cells (MSC), osteoblasts, adipocytes, endothelial cells and macrophages [6,7,8,9,10]. The microenvironment directs HSC fate decisions by mediating cell-cell interactions and secreting soluble growth factors [8,11,12]. Although several HSC supportive cytokines (e.g. SCF, IL-11, IL-3, FLT-3, TPO, angiopoietin-like proteins, and the Notch1 ligand Dl1) [13,14,15,16], cell-intrinsic

stimulators of HSC expansion (e.g. HOXB4) [16,17,18] and inhibitors of negative HSC regulators (e.g. AhR signaling [19]) have been identified, these have not yet led to the establishment of routine clinical protocols for HSC expansion. Several studies have assessed the suitability of various stromal cell lines from fetal and adult hematopoietic tissues to support murine and human hematopoiesis [20,21,22,23,24,25]; nevertheless, there has been little progress in expanding functional human HSC on these stroma lines. It is unclear to what extent the different HSC properties can be maintained in culture, and what molecular defects prevent robust expansion of transplantable HSC. Understanding how the *ex vivo* culture *per se* affects HSC function and molecular properties will be a critical step toward improving culture conditions for the expansion of HSC for clinical purposes, and also for the long-term goal to generate transplantable HSC in culture from human pluripotent stem cells.

To understand the behavior of human hematopoietic stem/progenitor cells (HSPC) in culture we established an MSC stroma based co-culture system for modeling human hematopoietic hierarchy, and defined the extent to which surface markers, functional properties and transcriptome characteristic for the primitive HSPC fraction can be preserved during culture. We show that OP9M2, a subclone of OP9 stroma cells, protects human fetal liver and cord blood HSPC from differentiation and apoptosis, facilitating a dramatic *ex vivo* expansion of multipotent hematopoietic cells that preserve the CD34+CD38-CD90+ surface immunophenotype that is characteristic for human HSC. This system also maintains the initial number of transplantable human fetal liver HSC (defined based on myelo-

lymphoid reconstitution in NSG mice) for at least 2 weeks in culture, but does not support their significant expansion. Genome-wide gene expression analysis of the expanded fetal liver CD34+CD38-CD90+ cells showed a remarkably stable transcription factor network associated with HSC entity, but revealed dynamic changes in distinct molecular programs that are sufficient to compromise HSC function. Thus, this co-culture offers a robust *ex vivo* system for studying the regulation of human multilineage hematopoiesis. Furthermore, the temporal gene expression data from *in vivo* derived and *ex vivo* expanded human CD34+CD38-CD90+ will serve as a resource to identify key regulatory mechanisms that control HSC identity *vs.* function, and to develop clinically applicable protocols for HSC expansion and *de novo* generation from pluripotent stem cells.

Materials and Methods

Ethical statement

This Study was carried out in strict accordance with the recommendations in the Guide for the Care and Use of Laboratory Animals of National Institutes of Health. The protocol was reviewed and approved by UCLA Animal Research Committee (Protocol number 2005-109). All efforts were made to minimize suffering.

This work does not involve research on human subjects based on the federal legislation (45 CFR 46.102(f)). Fetal livers were discarded material from elective terminations performed by Family Planning Associates. All material was obtained only after written informed consent and carried no personal identifiers. The consent form was

approved by Family Planning Associates. The project was evaluated by the UCLA Medical Institutional Board 2 who determined that no IRB approval is required.

Isolation of HSPC from human fetal liver

Fetal livers were discarded material from elective terminations of second trimester pregnancies (14-18 weeks of developmental age). Single cell suspension was prepared by dissociation using scalpels and syringes. Red cells were removed using Ficoll gradient (Stem Cell Technologies). CD34+ cells were isolated using magnetic beads (Miltenyi Biotech).

Stromal cell lines

OP9M2 subclone was generated by deriving a clonal line from OP9 stromal cells [26] plated at low density (0.32 cells/cm^2) in stroma media containing α-MEM (GIBCO/Invitrogen), 20% fetal bovine serum (Hyclone) and 1% penicillin/streptomycin (GIBCO/Invitrogen). The BFC012 and AFT024 mouse fetal liver stromal lines was kindly provided by Kateri A Moore and Ihor Lemischka (Mount Sinai School of Medicine, NYC) [27]. S17 [28] (obtained from Kenneth Dorshkind at UCLA) and the MS5 [29] mouse bone marrow stromal lines were also tested.

Hematopoietic stem/progenitor cell cultures

Stromal cells were irradiated (2000 rad) and plated (25,000 cells/cm^2) on tissue

culture treated wells in stroma media (see above) 24 hours before co-culture. HSPC were co-cultured with stroma (1000-5000 CD34+ cells/cm^2) in "HSC media" (stroma media supplemented with human SCF (25 ng/ml), FLT-3L (25 ng/ml) and TPO (25 ng/ml) (Peprotech) for 7-14 days before replating (100,000–200,000 cells/cm^2). Half the media was replaced every other day. For B-cell differentiation, the expanded cells were co-cultured on irradiated OP9M2 in stroma media supplemented with human SCF (50 ng/ml), FLT-3L (40 ng/ml) and IL-7 (100ng/ml) (Peprotech). Following expansion, cells were assayed by FACS and colony-forming assays (see below).

Flow cytometry

Mouse anti–human monoclonal antibodies for CD45, CD34, CD90, CD66b, CD235, CD13, CD14 and CD33 (BD Biosciences) and CD45, CD19, CD38 (eBioscience) were used for flow cytometry. Dead cells were excluded with 7-amino-actinomycin D (BD Biosciences). Cells were assayed on a BD LSRII flow cytometer and data was analyzed with FlowJo software (TreeStar). Cell sortings were performed on a BD Aria II.

Colony-forming assays

Single-cell suspensions were obtained as described and plated on MethoCult GF+ H4435 methylcellulose (Stem Cell Technologies) containing SCF, GM-CSF, IL-3 and EPO supplemented with TPO (10 ng/ml, Peprotech), 1% penicillin-streptomycin and 1% amphotericin B (GIBCO/Invitrogen). Colonies were scored after 14 days.

Transplantation assays

Transplantation assays were performed by intravenous (tail vein or retro-orbital) injection into sublethally (325 rad) irradiated 7-10 week female NOD-*scid IL2R*γ *null* mice (Jackson Laboratories) housed under pathogen-free conditions. For culture time course analysis, 50,000 CD34+ fetal liver cells or their expansion equivalent were transplanted. Peripheral blood was analyzed for human engraftment. Mice were sacrificed by CO_2 16 weeks post transplantation and bone marrow and spleen were analyzed for surface markers expressed in human HSPC and their differentiated progeny. The NSG repopulating cell (NSG-RC) frequency was determined using 5000, 1500 and 500 CD34+ fetal liver cells and their expansion equivalent after 2 weeks of co-culture on OP9M2. The cell dose was considered to contain at least one NSG-RC if human engraftment in the bone marrow exceeded 0.1%. The NSG-RC frequency was calculated on the basis of negative recipients using L-calc software (Stem Cell Technologies).

RNA purification and microarray

RNA was purified from 100,000 CD45+CD34+CD38-CD90+ fetal liver cells that were isolated freshly (day 0) or at different time points in culture (12 hours, 2 weeks and 5 weeks) using QIAshredder and RNEasy Mini Kit (QIAGEN). The RNA was amplified using the NuGen FFPE amplification kit (Roche) and hybridized on Affymetrix arrays (u133plus2.0 array) in the Clinical Microarray Core, Department of Pathology & Laboratory Medicine at UCLA. For the OP9M2 and BFC012 stromal cell lines the RNA was amplified using an Ambion kit and hybridized to Affymetrix mouse 430 2.0

array. Raw data will be available for download from Gene Expression Omnibus (http://ncbi.nlm.nih.gov/geo) (GSE34974).

Differential gene expression analysis

Bioconductor version 2.7 was used for computational analyses [30,31]. The samples were clustered using hierarchical clustering using Spearman rank correlation as the distance metric. Cluster 3.0 (for clustering) and Treeview (for visualization) were used. Limma package was used to obtain differentially expressed genes. The MAS5.0 algorithm through the R package Affy was used for calculating P/M/A detection calls for each array sample. The online resource DAVID was used to determine Gene Ontology (GO) statistically over-represented categories. The cellular location of the differentially expressed genes was annotated using Ingenuity Pathway Analysis software. Fuzzy c-means clustering was performed on microarray data from Day 0, 12 hours, 2 weeks and 5 weeks using Mfuzz. The probe sets included in the clustering were differentially expressed in at least one pair wise comparison at 5% FDR, and a fold change value of ±2.0. RMA derived expression values were standardized and clustered using Mfuzz for the probe sets that met the above criteria.

Results and Discussion

OP9M2 stroma supports expansion of human CD34+CD38-CD90+ cells and establishment of multilineage hematopoietic hierarchy *ex vivo*

One of the long-standing goals in the field has been to establish a culture system that maintains HSC properties. In the absence of such system, the ability to model human hematopoiesis *in vitro* has been limited, and little progress has been made in expanding transplantable human HSC for clinical applications. Moreover, in order to succeed in the generation of HSC from human pluripotent stem cells, we have to understand how culture affects HSC properties, and minimize the negative effects of culture. Therefore, it is crucial to develop culture systems that mimic the *in vivo* HSC niche, as well as to understand the molecular changes that HSC acquire during culture. To define the extent to which HSC properties can be maintained in culture, we first assessed the ability of different stromal cell lines to preserve the undifferentiated state of human HSC (Figure 2.1A, Figure S1 and data not shown

We chose second trimester fetal liver HSC as the primary cell type for this study, as they are highly self-renewing, similar to cord blood, and also represent a developmentally closer target cell for generation of HSC from human ES cells or IPS cells. Culture of CD34+ human fetal liver cells with standard "HSC cytokines" (SCF, TPO and FLT-3L) with no stroma for two weeks resulted in loss of the primitive CD34+CD38-CD90+ population that contains HSC (Figure 2.1A). Likewise, the mouse BFC012 fetal liver stroma line and most of the mouse and human stroma

lines tested resulted in complete loss or decrease of undifferentiated CD34+CD38-CD90+ cells during the two week culture (Figure 2.1A, Figure S1). In contrast, co-culture of CD34+ cells on OP9M2, a subclone of OP9 stroma maintained a robust population of CD34+CD38-CD90+ cells (Figure 2.1A). The parental OP9 also showed maintenance of CD34+CD38-CD90+ cells, albeit at slightly lower frequency (Figure S1). As the OP9M2 stroma is a clonal line and therefore more homogenous than the parental OP9 line, it was chosen for subsequent studies. Co-culture on OP9M2 cells also facilitated the generation of mature myeloid and erythroid cells, as well as B-cells if the culture was supplemented with IL-7 (Figure S2). These findings demonstrate that the OP9M2 stromal line maintains a population of human CD34+CD38-CD90+ cells in an undifferentiated state while supporting the establishment of multilineage hematopoietic hierarchy *ex vivo*. We found that the supportive OP9M2 stroma has MSC characteristics and can generate osteoblasts, adipocytes and chondrocytes (Figure S3), as also reported for the OP9 bulk cells [32], which is intriguing since MSCs and their derivatives are also key components of the bone marrow HSC niche *in vivo* [6,8,9].

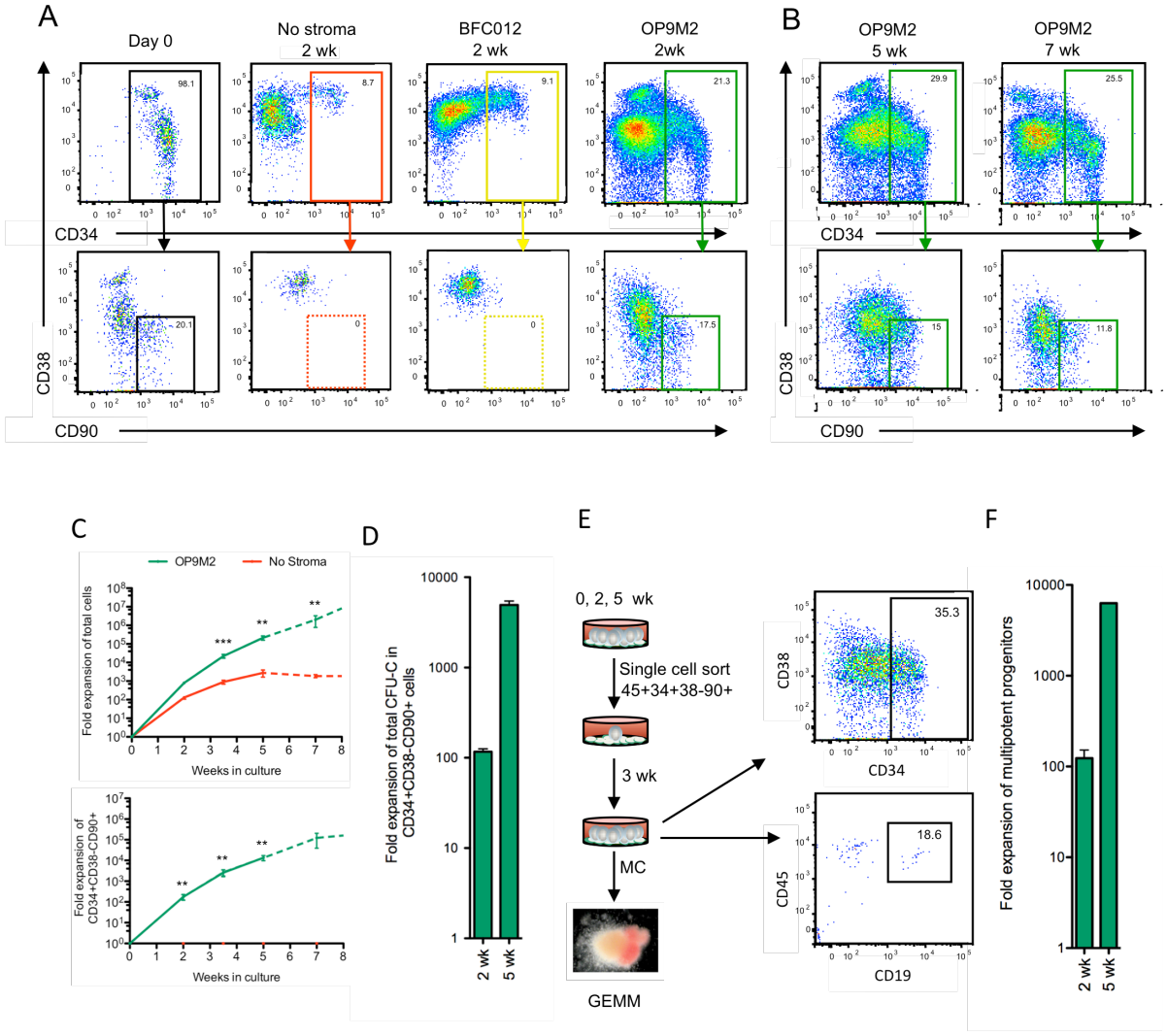

Figure 2.1: The OP9M2 MSC stromal cell line supports long-term expansion of multipotent human CD34+CD38-CD90+ cells.

Co-culture on OP9M2 stroma supports sustained *ex vivo* expansion of multipotent human CD34+CD38-CD90+ cells

We next assessed the ability of OP9M2 MSC stroma to sustain expansion of human CD34+CD38-CD90+ hematopoietic cells over time. Strikingly, CD34+CD38-CD90+ cells could be maintained on OP9M2 in similar frequencies for over 5 weeks, resulting in >10,000-fold expansion of cells with the surface immunophenotype associated with undifferentiated hematopoietic cells (Figure 2.1A-C). By 7-8 weeks of culture, the expansion potential of CD34+CD38-CD90+ cells had started to diminish (Figure 2.1C). Fractionation of the cultured (2 and 5 weeks) cells based on their surface phenotype showed long-term proliferative potential and capacity to expand phenotypic HSC exclusively within the CD34+CD38-CD90+ fraction (Figure S4), verifying that also during culture, the CD34+CD38-CD90+ phenotype identifies the most undifferentiated cells. Similar to human fetal liver, cord blood CD34+CD38-CD90+ cells could also be robustly expanded on OP9M2 (Figure S5A-C). Likewise, CD34+CD38-CD90+ cells were the only cells in cord blood expansion culture that that could regenerate hematopoietic cells with undifferentiated phenotype and long-term proliferative potential (Figure S5D-F).

To investigate the functional potential of the *ex vivo* expanded CD34+CD38-CD90+ cells, their colony forming potential and differentiation ability was assessed. Although there was a slight drop in frequency of clonogenic progenitors over time (CFU-C, as assessed on methylcellulose culture) among fetal liver CD34+CD38-CD90+ cells after culture (Figure S6A) a 110-fold and a 4900-fold total expansion of CD34+CD38-CD90+ clonogenic progenitors was obtained during 2 and 5 weeks,

respectively (Figure 2.1D). Similar expansion of CD34+CD38-CD90+ CFU-C (89-fold (±8)) was obtained during 2 weeks culture of cord blood cells (data not shown). In addition, the distribution of different colony types was maintained among the CD34+CD38-CD90+ cells expanded for 2 weeks, whereas by 5 wk, there was a slight decrease in GEMM colony frequency (Figure S6B). To assess multipotency of the expanded CD34+CD38-CD90+ cells at clonal level, CD34+CD38-CD90+ cells were isolated freshly or after 2 or 5-week culture and plated individually on OP9M2 (Figure 2.1E), after which the clones were split into myeloid- and B-lymphoid conditions. Likewise, there was a 2.3-fold decline in the frequency of clonally multipotent clonogenic cells among the CD34+CD38-CD90+ cells after 2 weeks in culture, (Figure S6C), nevertheless, a 100-fold expansion of clonally multipotent CD34+CD38-CD90+ cells was observed after 2 weeks (Figure 2.1F), and in one experiment, 8000-fold expansion after 5 weeks in culture. Importantly, the expanded CD34+CD38-CD90+ cells remained responsive to microenvironmental cues and differentiated rapidly upon removal from the supportive stroma (Figure S7).

These data demonstrate that the OP9M2 stroma supports long-term expansion of human HSPC that preserve key characteristics associated with HSC, including CD34+CD38-CD90+ surface immunophenotype, high proliferative potential and multipotency.

Transplantable HSC can be maintained on OP9M2 stroma

We next assessed the ability of the *ex vivo* expanded CD34+CD38-CD90+ cells to reconstitute the hematopoietic system *in vivo*. Transplantation of cells derived from 50,000 CD34+ fetal liver cells during 2-week culture into NSG mice demonstrated preservation of engraftable HSC on OP9M2 stroma. At 16 weeks post-transplantation, robust engraftment of human CD45+ cells was detected in both peripheral blood (2 wk: 14.55±8.51, Day 0: 29.93±7.67) and bone marrow (2 wk: 43.02±11.48, Day 0: 63.90±10.14) with contribution to undifferentiated CD34+CD38- cells, myeloid cells and B-cells (Figure 2.2A-B and Table S1). Furthermore, human T-cells were detected in the spleen (Figure 2.2B and Table S1). Multilineage human bone marrow engraftment was also observed from cells cultured for 3 weeks (18.26±12.35) (Table S1), whereas by 5 weeks in culture, their reconstitution ability had dropped dramatically (0.04%±0.015) (Figure 2.2A). Transplantation of *ex vivo* expanded cells fractionated into cells with the immunophenotype associated with undifferentiated HSPC (CD34+CD38-CD90+) and downstream progenitors (CD34+CD38-CD90-, CD34+CD38+CD90- and CD34-) confirmed that CD34+CD38-CD90+ cells in the cultured fetal liver possessed most of the *in vivo* HSC activity (Figure 2.2C and Table S1) as previously shown for cord blood HSC [33]. These results demonstrate that transplantable human HSC that retain the characteristic surface immunophenotype (CD34+CD38-CD90+) can be maintained *ex vivo* on OP9M2 stroma for over 2 weeks. Notably, previous work has suggested that CD38 is an unreliable differentiation marker in hematopoietic cells cultured *in vitro* [34]. However, this discrepancy could potentially be explained by

different culture conditions, such as the lack of using OP9 MSC stromal cells. To investigate whether expansion of engraftable HSC was achieved, limiting dilution transplantation assay was performed. The number of NSG repopulating cells (NSG-RC) among cultured HSPC was similar to that before the expansion (Day 0: 1 in 2610 (lower 1413 and upper 4821) and at 2 wk in culture: 1 in 3003 (lower 1515 and upper 5953))(Figure 2.2D and Table S1). As there was a dramatic expansion of CD34+CD38-CD90+ cells during culture (Figure 2.1C) but no increase in engraftable HSC, the frequency of NSR-RCs among CD34+CD38-CD90+ cells was estimated to drop from 1 in 522 to 1 in 63504. These data indicate that although HSC activity can be preserved during culture, majority of the expanded CD34+CD38-CD90+ cells fail to reconstitute the recipient's hematopoietic system.

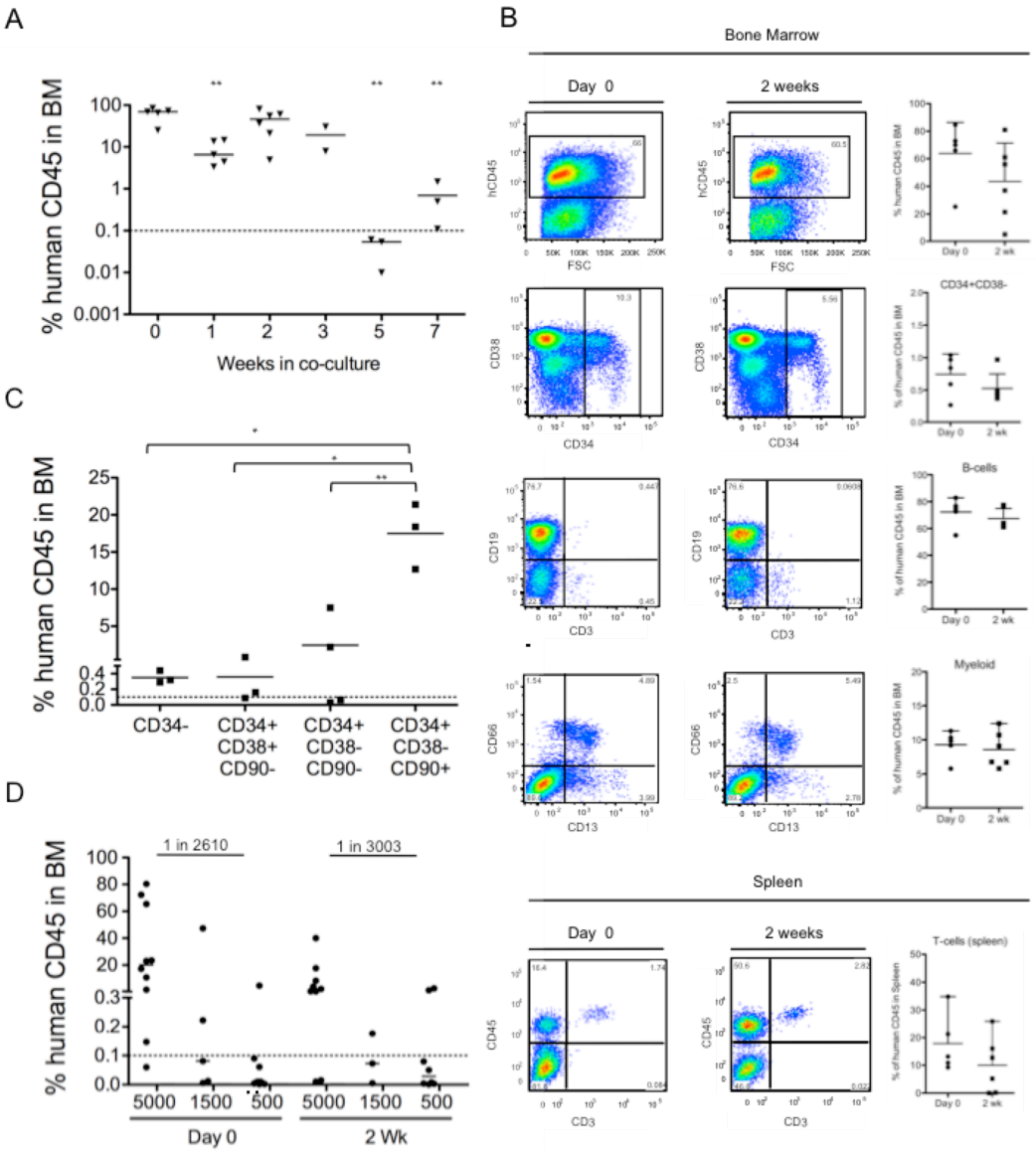

Figure 2.2: The OP9M2 stromal cell line supports maintenance of engraftable HSC.

Microarray analysis of *ex vivo* expanded CD34+CD38-CD90+ cells demonstrates stable expression of HSC transcriptional regulators

Despite the dramatic expansion of multipotent CD34+CD38-CD90+ cells on OP9M2 MSC stroma, there was no significant expansion of transplantable HSC, suggesting that most expanded CD34+CD38-CD90+ cells are functionally compromised. To define at the molecular level the degree to which "HSC transcriptional identity" can be preserved during culture and to identify the molecular blocks preventing successful expansion of fully functional HSC, we performed a genome-wide gene expression analysis of sorted CD34+CD38-CD90+ cells isolated at different stages of co-culture. To distinguish between molecular changes acquired immediately upon exposure to culture *versus* over prolonged culture, gene expression in sorted CD34+CD38-CD90+ cells was assessed after 12 hours, 2 weeks and 5 weeks in culture. Cultured CD34+CD38-CD90+ cells were compared to freshly isolated CD34+CD38-CD90+ cells and the more differentiated CD34+CD38+CD90- progenitors. Hierarchical clustering grouped all replicates together, demonstrating high reproducibility of gene expression in cultured CD34+CD38-CD90+ cells (Figure 2.3A). Spearman rank correlation and principal component analysis revealed that all cultured CD34+CD38-CD90+ cells were more similar to the freshly isolated CD34+CD38-CD90+ cells than the freshly isolated CD34+CD38+CD90- progenitors (Figure 2.3A-B), indicating that the transcriptome of the expanded CD34+CD38-CD90+ cells is highly preserved throughout the culture. Strikingly, CD34+CD38-CD90+ cells sorted after 2 weeks of co-culture were more similar to freshly isolated

CD34+CD38-CD90+ cells than those cultured for only 12 hours (Figure 2.3A-B), suggesting that CD34+CD38-CD90+ cells have the capacity to adopt to their new stromal niche upon continued culture. However, the number of differentially expressed genes among CD34+CD38-CD90+ cells increased again substantially after prolonged culture (5 weeks) (Figure 2.3C).

We next investigated whether the expression of 33 transcriptional regulators that are known to be required for HSC development and/or maintenance were maintained in CD34+CD38-CD90+ cells sorted after culture. 26 of them (*SCL/TAL1, RUNX1, GFI1, BMI, HOXB4, HOXA9* etc.) remained stably expressed (<2-fold differentially expressed) throughout the entire 5-week culture (Figure 2.3D and Table S2). Strikingly, at 2 weeks in culture, *PBX1* was the only one of the known HSC transcription factors assessed that was downregulated more than 2-fold ($p<0.05$) (Table S2), documenting a remarkable stability of HSC regulators in *ex vivo* expanded CD34+CD38-CD90+ cells.

In line with these data, lineage specific transcription factors that are known to be crucial in initiating lymphoid, myeloid or megakaryocyte/erythroid linage differentiation (*PAX5, BCL11A, PU.1, CEBPα*, *NFE2* and *GATA1* etc. [35,36,37,38] were not upregulated in CD34+CD38-CD90+ cells during 2 weeks of culture, and even by 5 weeks, only *CEBPα* was marginally activated (Figure 2.3E). This suggests that co-culture of human CD34+CD38-CD90+ cells on OP9M2 not only preserves a remarkably stable expression of HSC regulators but also suppresses the activation of canonical differentiation programs, thereby highly preserving the HSPC transcriptome during culture.

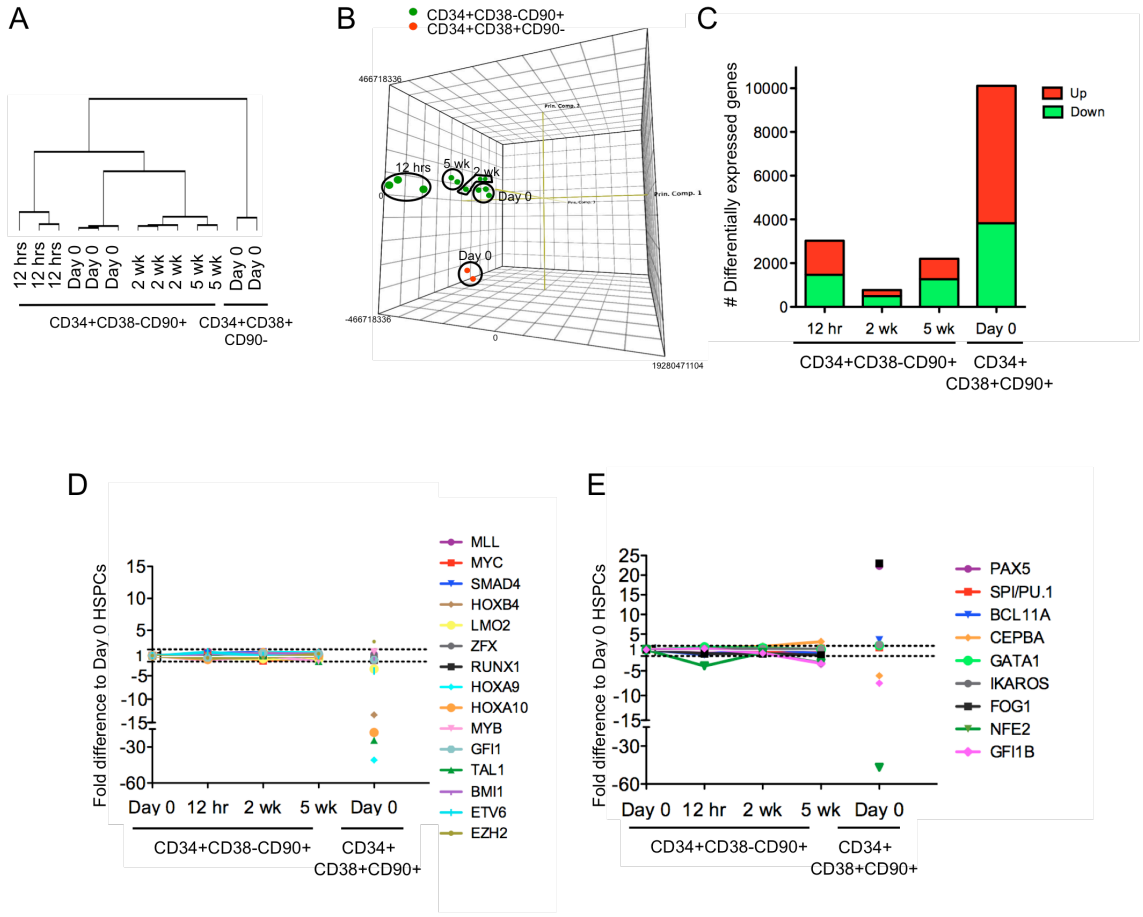

Figure 2.3: *Ex vivo* expanded CD34+CD38-CD90+ cells demonstrate high preservation of the HSC transcriptional program.

In order to understand the nature of the transcriptional changes in CD34+CD38-CD90+ cells sorted after culture, we analyzed the 3110 genes identified as >2-fold differentially expressed at least in one time point during the 5-week culture (Table S3). To identify patterns of co-regulation within the differentially expressed genes, a fuzzy c-means cluster analysis was performed. Eight distinct temporally changing gene expression patterns with unique GO categories were identified (Figure 2.4A-C,

2.5A-C and 2.6A-B). This analysis demonstrated that, despite their shared surface phenotype, stability of most known HSC transcription factors and ability to resist premature differentiation, the *ex vivo* expanded CD34+CD38-CD90+ cells undergo dynamic gene expression changes during culture.

CD34+CD38-CD90+ cells display a transient "culture shock" upon exposure to culture

Interestingly, three clusters (A-C) contained genes whose expression changed already by 12 hours in culture, but was largely restored by 2 weeks (Figure 2.4A-C, Table S3). GO analysis of clusters A and B which showed a transient upregulation revealed enrichment for genes regulating cell proliferation and apoptosis (Figure 2.4A-B). Cluster A genes included *CDKN1A* (*p21*), *TP63* and members of the TNF signaling pathway, all known regulators of cell cycle arrest and cell death (Figure 2.4D) [39,40,41], suggesting that OP9M2 stroma can provide signals that protect the primitive CD34+CD38-CD90+ cells from apoptosis. Furthermore, several members of the aryl hydrocarbon receptor (AhR) signaling pathway (*AHRR*, *CYP1A1* and *CYP1B*), which has been recently identified as a negative regulator of HSC expansion [19], were upregulated at 12 hours, while at 2 weeks, the levels were remarkably similar to non-cultured CD34+CD38-CD90+ cells (Figure 2.4E). Analysis of published data of genes suppressed upon blocking AhR signaling in culture using SR1 (Stemregulin 1) [19] revealed that 9 out of 11 of the AhR signaling responsive genes became transiently induced in CD34+CD38-CD90+ cells on OP9M2 MSC stroma, but were a least temporarily restored during continued culture (Figure S8). These data indicate that the OP9M2 stroma can provide critical niche signals to

suppress the AhR pathway that would negatively affect HSC function. Moreover, a transient decrease in gene expression was observed in other factors previously associated with HSC function such as *CDKN1C, HLF* and *FLT3* (Figure 2.4F) [42,43,44]. The immediate fluctuation in gene expression of negative and positive HSC regulators, followed by restoration to almost normal levels upon further culture suggests that cultured CD34+CD38-CD90+ cells experience an initial "culture shock" after which they are still capable of adapting to a new supportive niche on OP9M2 stroma with a transcriptome that highly resembles freshly isolated CD34+CD38-CD90+ cells.

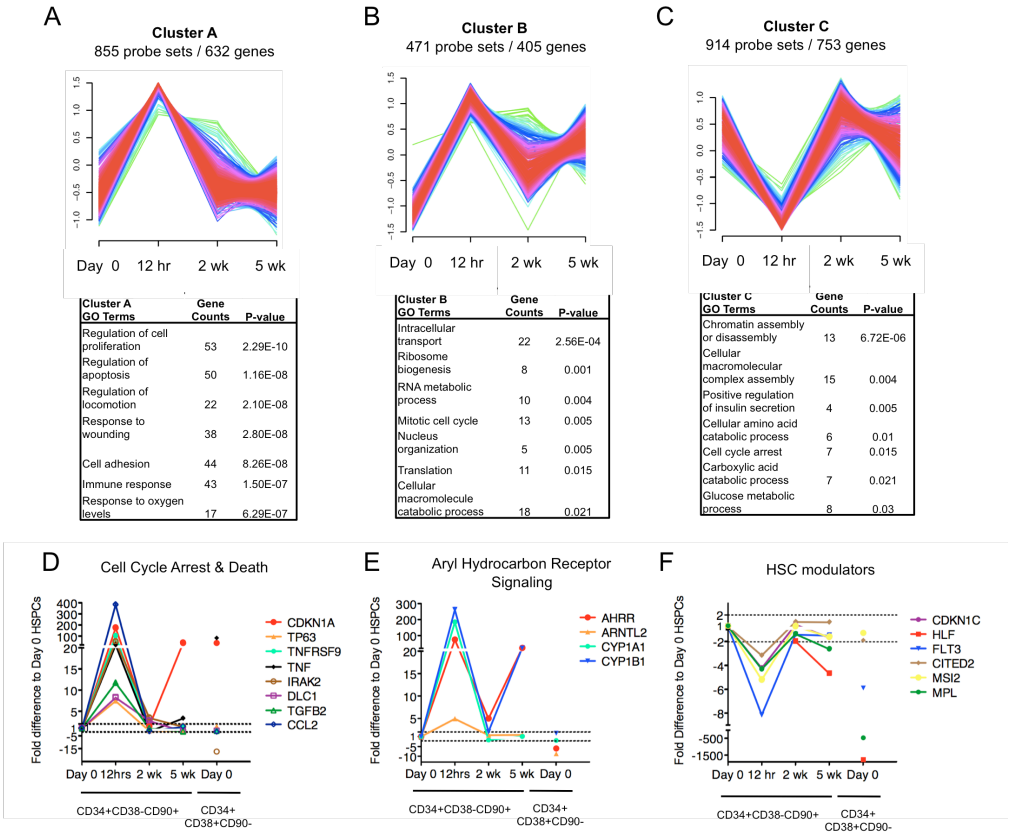

Figure 2.4: CD34+CD38-CD90+ cells display a transient "culture shock" upon exposure to culture.

Ex vivo culture of CD34+CD38-CD90+ cells induces dynamic changes in cellular state

Clusters D, E and F contained genes that were upregulated at some point in culture (Figure 2.5A-C, Table S3). Cluster D genes that showed a trend for upregulation already by 12 hours and mostly stayed upregulated throughout the culture were enriched for genes involved in kinase activity and DNA repair (Figure 2.5D-E). However, the expression changes for genes in these categories were only modest, and mainly observed at 5 weeks of culture, providing little evidence for compromised genomic integrity in the expanded CD34+CD38-CD90+ cells or other explanation for their dysfunction.

Cluster E, which showed upregulation by 2 weeks of culture when the transcriptome of CD34+CD38-CD90+ cells was otherwise highly reminiscent of the freshly isolated CD34+CD38-CD90+ cells (Figure 2.5B), revealed alterations in metabolic genes. Many of these genes were involved in glucose metabolism and specifically in glycolysis (Figure 2.5F). This is intriguing, as HSC are known to utilize glycolytic metabolism rather than oxidative phosphorylation as their preferred energy metabolism [45]. Although it is not known whether increased expression of glycolytic genes would compromise HSC function, this data draws attention to the culture conditions (e.g. glucose content, oxygen tension etc.) that change significantly between the *in vivo* niches and *ex vivo* culture, and may impact HSC function.

Cluster F genes that were upregulated gradually during prolonged culture were enriched for genes involved in cell cycle regulation and immune response (Figure 2.5C, 2.5G-H). Notably, the expression of genes involved in cell cycle regulation (e.g. E2F7, which is induced by p53 upon genotoxic stress and negatively regulates cell cycle [46], and CCNB2 and NEK2 which accumulate during S phase and G2, etc.) was only marginally upregulated by 2 weeks when the CD34+CD38-CD90+ cells still possessed high proliferative potential, but increased by 5 weeks when the expansion potential of CD34+CD38-CD90+ cells had started to plateau (Figure 2.5G). Interestingly, specific genes normally expressed in mature myeloid (*MPO and BPI*) [47,48,49] or lymphoid cells (*IL7R, RAG1* and *RAG2*) [50,51] as well as toll like receptors (TLR4 and TLR7) and their agonists, S100 proteins, were significantly upregulated already by 2 weeks in culture (Figure 2.5H). Importantly, induction of the inflammatory genes in CD34+CD38-CD90+ cells does not seem to reflect promiscuous activation of the canonical differentiation programs, as the key lineage specific transcription factors (e.g. *PAX5, BCL11A, PU.1*, *GATA1, NFE2* etc.) remained suppressed in CD34+CD38-CD90+ cells throughout the culture period (Figure 2.3E). The etiology and significance of the upregulation of these immune response genes is unknown, as MSCs have been shown to rather have immunosuppressive properties and even reduce the risk for graft failure when transplanted together with HSC [52,53]. If the species mismatch between human HSPC and mouse stroma or fetal calf serum can elicit an immune response in cultured human CD34+CD38-CD90+ cells, it will be important to recreate similar the supportive culture conditions using non-animal products.

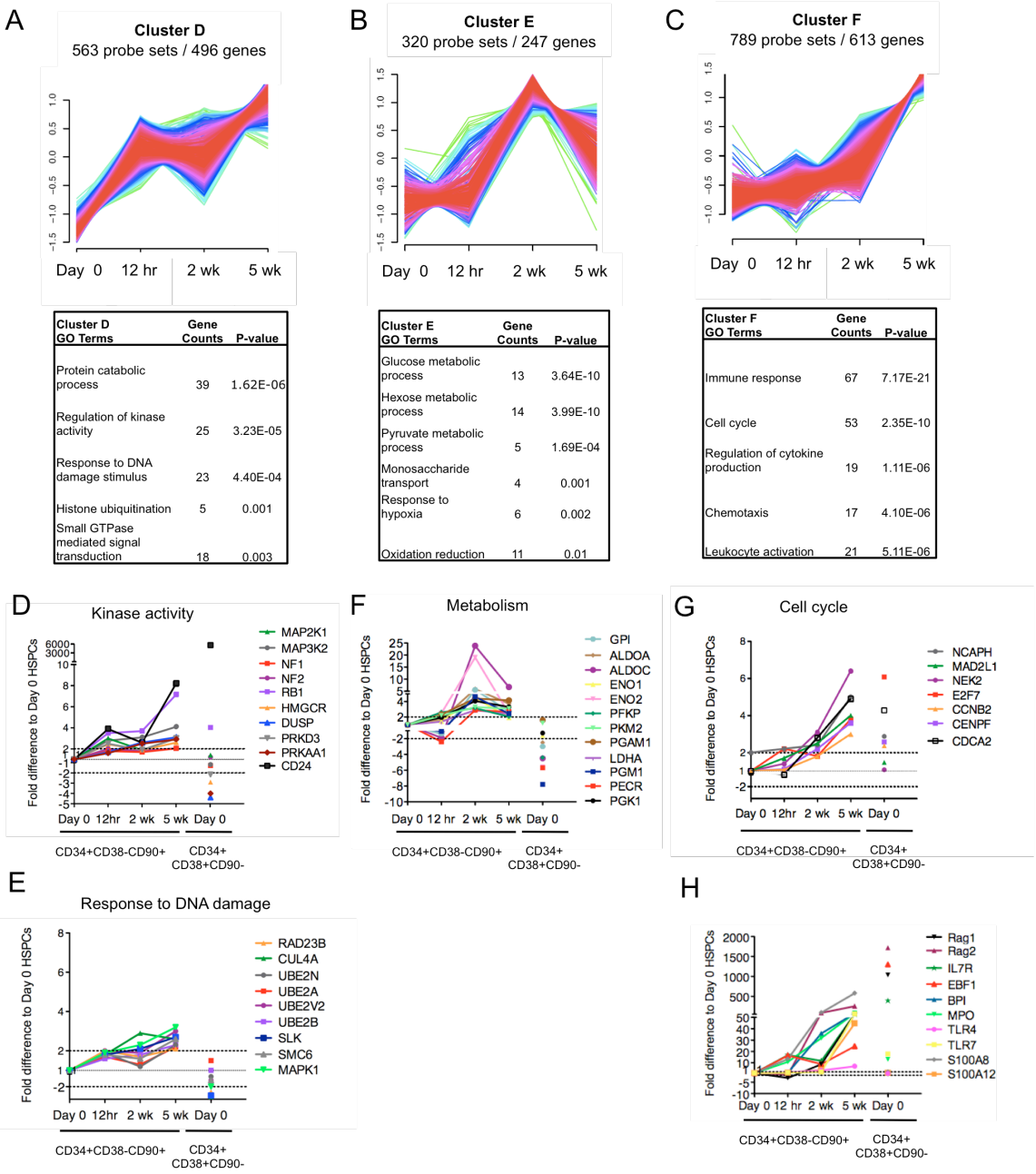

Cluster D GO Terms	Gene Counts	P-value
Protein catabolic process	39	1.62E-06
Regulation of kinase activity	25	3.23E-05
Response to DNA damage stimulus	23	4.40E-04
Histone ubiquitination	5	0.001
Small GTPase mediated signal transduction	18	0.003

Cluster E GO Terms	Gene Counts	P-value
Glucose metabolic process	13	3.64E-10
Hexose metabolic process	14	3.99E-10
Pyruvate metabolic process	5	1.69E-04
Monosaccharide transport	4	0.001
Response to hypoxia	6	0.002
Oxidation reduction	11	0.01

Cluster F GO Terms	Gene Counts	P-value
Immune response	67	7.17E-21
Cell cycle	53	2.35E-10
Regulation of cytokine production	19	1.11E-06
Chemotaxis	17	4.10E-06
Leukocyte activation	21	5.11E-06

Figure 2.5: *Ex vivo* expanded CD34+CD38-CD90+ cells show dynamic changes in transcriptional programs associated with cellular state.

Ex vivo expansion results in downregulation of transcription factors and adhesion molecules in CD34+CD38-CD90+ cells

Our findings indicate that even though *ex vivo* expanded CD34+CD38-CD90+ cells demonstrate dynamic changes in "cell state" (e.g. kinase activity, metabolism, cell cycle etc.), based on the transcriptional regulators that govern "cell identity" (e.g. undifferentiated HSC *vs.* lineage committed cell), they still maintain the identity of an HSC. As such, these data provided little clues to why the majority of the *ex vivo* expanded CD34+CD38-CD90+ cells do not function properly upon transplantation. However, the two remaining clusters of differentially expressed genes contained genes that were progressively downregulated during culture, either immediately by 12 hours (cluster G) or during prolonged culture (cluster H)(Figure 2.6A-B). Interestingly, both clusters were enriched for transcriptional regulators, including *PBX1* (cluster G) that is crucial for HSC function [54], *EGR1* (cluster G) that is required to maintain HSC in the niche although its loss does not compromise HSC function [55], and GATA3 (cluster H) (Figure 2.6C-D). GATA3 is required for proper T-cell development and implicated in the regulation of adult HSC function, although gata3 deficient HSC from neonatal mice or fetal liver demonstrated no functional defect [56,57]. Moreover, cluster G and H genes that were downregulated during culture also included several surface proteins that have been implicated to participate in HSC-niche interactions, such as *TEK (TIE2)* and *N-CADHERIN* (Figure

2.6E) [11,12], as well as molecules associated with cell projections, polarity, asymmetric division (*DCHS1* and *PARD3*) and implantation (TRO) [58,59,60] (Figure 2.6F). By 5 weeks, many of these genes had been downregulated to levels comparable to the more differentiated CD34+CD38+CD90- cells (Figure 2.6C-F). This indicates that, despite maintaining the characteristic HSC surface immunophenotype and most known HSC transcription factors as well as suppressing lineage differentiation, the expanded CD34+CD38-CD90+ cells have altered the expression of a unique subset of transcriptional regulators and cell surface proteins, which may impair their ability to fully maintain HSC function upon transplantation.

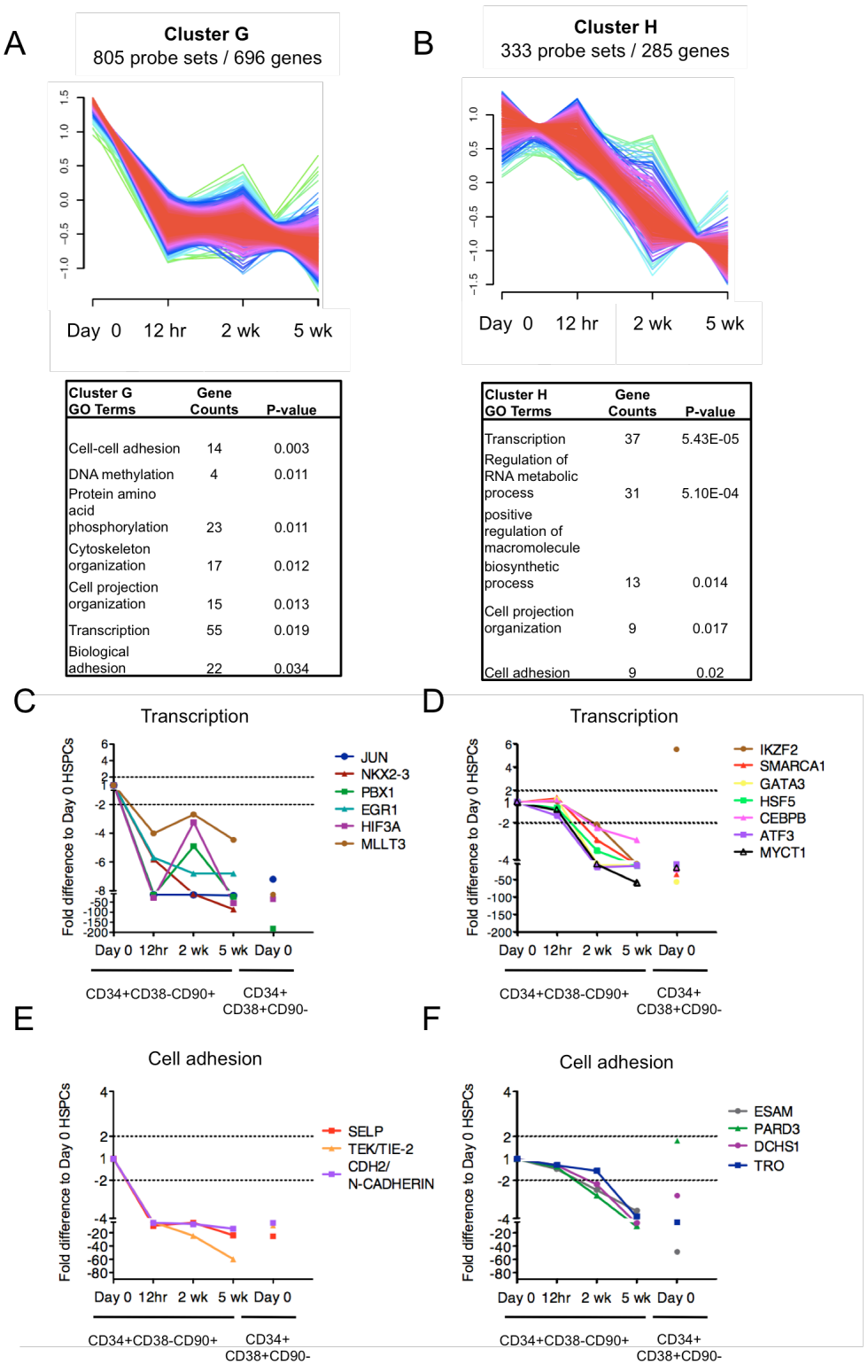

Cluster G GO Terms	Gene Counts	P-value
Cell-cell adhesion	14	0.003
DNA methylation	4	0.011
Protein amino acid phosphorylation	23	0.011
Cytoskeleton organization	17	0.012
Cell projection organization	15	0.013
Transcription	55	0.019
Biological adhesion	22	0.034

Cluster H GO Terms	Gene Counts	P-value
Transcription	37	5.43E-05
Regulation of RNA metabolic process	31	5.10E-04
positive regulation of macromolecule biosynthetic process	13	0.014
Cell projection organization	9	0.017
Cell adhesion	9	0.02

Figure 2.6: *Ex vivo* expanded CD34+CD38-CD90+ cells show temporal changes in transcriptional programs associated with HSPC function and cell adhesion.

Dysregulation of *PBX1* compromises the transcriptome of *ex vivo* expanded CD34+CD38-CD90+ cells

Our finding that the cultured CD34+CD38-CD90+ cells showed a remarkably stable expression of most known HSC transcription factors suggests that "HSC identity" *per se* is not lost upon *ex vivo* expansion. An exception to this was *PBX1*, which was downregulated already at 12 h and never fully recovered, indicating that *PBX1* expression is highly dependent on microenvironmental signals that were not recapitulated in culture. *Pbx1* deficiency in mice disrupts HSC self-renewal due to loss of stem cell quiescence and severely compromises their *in vivo* repopulation ability [54]. Therefore, we sought to define the extent to which the transcriptional changes in cultured CD34+CD38-CD90+ cells correlate with those dysregulated in *Pbx1* deficient mouse HSC. Indeed, gene set enrichment analysis (GSEA) showed a very high statistically significant correlation between *Pbx1* deficient mouse LSKCD34-Flt3- cells (Lin-Sca1+cKit+CD34-Flt3-) cells and cultured human CD34+CD38-CD90+ cells (Figure 2.7A). Direct comparison of the differentially expressed genes showed that 24 of the genes downregulated (>1.5-fold) and 54 genes upregulated in *Pbx1* deficient HSC (LSKCD34-Flt3-) showed similar dysregulation with respect to genes that changed in culture (Figure 2.7B-C). These included many downregulated transcriptional regulators, some of which are known to regulate hematopoiesis such as *MLLT3, MSI2, MEIS1, DNMT3A* and *HLF* [42,61,62,63,64] while others have so far not been associated with a clear function

in HSPC biology (*MYCT1, HMGA2, SMARCA2* etc) (Figure 2.7B). The shared upregulated genes included many cell cycle- and mitosis genes *(NCAPH, NEK2, CCNB2, CDCA2* etc.)(Figure 2.5G and 2.7C). Although the specific function of many of the Pbx1 dependent gene in HSC still remains to be investigated, these data identify dysregulation of *PBX1* as a factor compromising the otherwise highly stable HSC transcriptional network in human CD34+CD38-CD90+ cells during expansion on MSC stroma, and nominate loss of *PBX1* as a possible defect contributing to the functional limitations in cultured HSPC (Figure 2.7D).

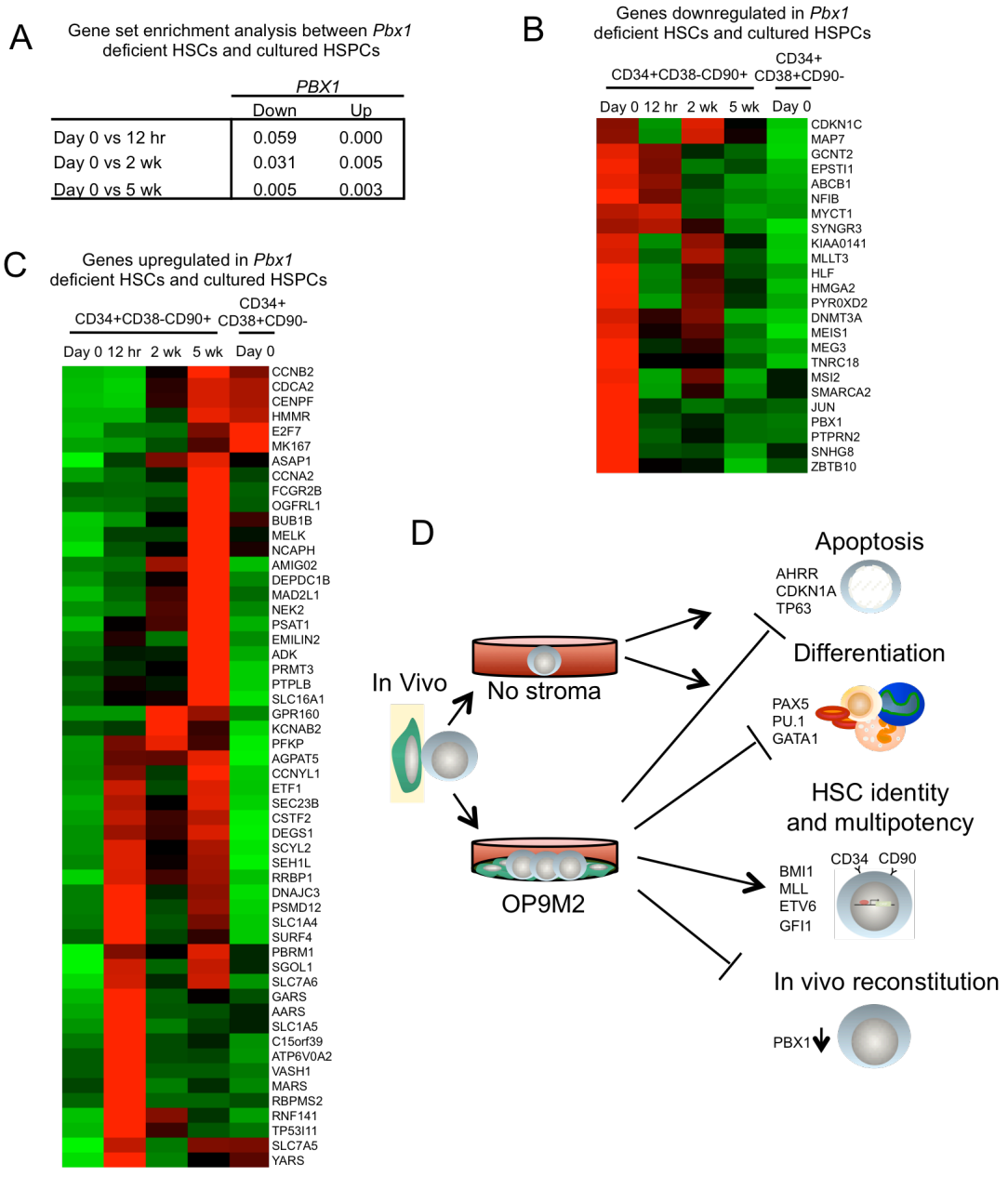

Figure 2.7: Cultured human CD34+CD38-CD90+ cells show shared gene expression changes with *Pbx1* deficient mouse HSC.

Conclusion

We have defined a MSC co-culture system that expands clonally multipotent human hematopoietic cells that are protected from adverse effects that normally occur during culture (e.g. activation of aryl hydrocarbon receptor signaling, apoptosis, and immediate differentiation), and retain the CD34+CD38-CD90+ HSC surface immunophenotype and remarkably stable HSC transcription factor network for several weeks in culture. These data revealed that the identity of human HSC is highly preserved during *ex vivo* expansion on supportive MSC stroma despite the dynamic fluctuations in gene expression programs reflecting different cellular states (cell cycle, metabolism, etc). However, the fact that transplantable HSC could only be maintained, but not significantly expanded, during culture, indicated that most of the *ex vivo* expanded CD34+CD38-CD90+ cells are functionally compromised. Downregulation of *PBX1* was identified as a possible factor contributing to the dysregulated gene expression programs and the functional limitations in cultured CD34+CD38-CD90+ cells. It is important to note that the microarray analysis of cultured CD34+CD38-CD90+ cells was performed on human fetal liver cells, which are functionally different from HSC from adult bone marrow or cord blood as they have the highest self-renewal potential [65]. However, although fetal liver HSC are rarely used for clinical purposes due to ethical and legal considerations, they are developmentally the closest target for generation of HSC from ES or IPS cells, and therefore these data not only give important clues about the mechanisms regulating self-renewal but also how to improve the culture conditions for the generation of

self-renewing HSC *de novo* from pluripotent cells.

This culture system serves now both as a useful platform for studying the regulation of human HSPC and multilineage hematopoietic hierarchy *ex vivo*, and as a starting point to develop protocols for the expansion or *de novo* generation of transplantable HSC for clinical applications. To achieve this goal, it will be critical to identify the signals that would help preserve the dysregulated HSC transcription factors identified in the study, such as *PBX1.* Notably, one report demonstrated that by knocking down *pbx1* in *HOXB4* over-expressing mouse HSC improved HSC expansion as compared to overexpression of *HOXB4* alone [66], although other studies had documented loss of HSC function upon knockdown of *pbx1* [54]. Notably, HOXB4 expression was not altered during our expansion culture. These data suggest that the effects of loss or overexpression of individual transcription factors may be context dependent, and also influenced by the time how long the gene is suppressed. Future overexpression and knockdown studies will be required to determine the degree to which *PBX1,* or the other transcription factors and signaling pathways dysregulated in culture, contribute to the loss of HSC function. However, as many of the transcription factors that were downregulated during culture are also putative oncogenes, their mere over-expression is unlikely to provide a clinically viable option for expanding functional HSC. Instead, future studies should focus on complementing the OP9M2 co-culture with other niche cells or extrinsic cues to better recapitulate the *in vivo* niche, such as Akt-activated endothelial cells, which express HSC supportive angiocrine factors IGFB2 and FGF2 [10] that are not expressed by OP9M2 stroma (data not shown). Moreover, as we

also observed dynamic changes in HSPC metabolism during the culture, these findings suggest that optimization of the physiological parameters such as glucose and oxygen levels could further improve HSC function. Indeed, the HSC niche is hypoxic and culture of HSC in low oxygen levels has been reported to increase HSPC function [67,68].

The fact that excessive proliferation of HSC *in vivo* in mice has been associated with decreased HSC function[69] inevitably raises the question whether the cell divisions in culture cause a reversible dysfunction in engraftment, or have already led to permanent loss of "stemness". Nevertheless, our discovery of the high preservation of "HSC identity" in human CD34+CD38-CD90+ cells cultured on MSC stroma provides hope that by modulating the culture conditions to preserve, or even return, the *ex vivo* expanded CD34+CD38-CD90+ cells to the correct "cellular state" that allows efficient engraftment *in vivo* will take us closer to expanding functional HSC for the treatment of leukemia and other blood diseases.

Acknowledgments

The authors thank Gay Crooks for helpful comments on the manuscript and Kelly Wagner for excellent technical assistance. The authors also thank the staff at UCLA Warren hall for excellent animal care and the JCCC and BSCRC FACS Core Facilities for assistance with cell sorting.

References

1. Bordignon C (2006) Stem-cell therapies for blood diseases. Nature 441: 1100-1102.
2. Weissman IL (2000) Stem cells: units of development, units of regeneration, and units in evolution. Cell 100: 157-168.
3. Stanevsky A, Goldstein G, Nagler A (2009) Umbilical cord blood transplantation: pros, cons and beyond. Blood Rev 23: 199-204.
4. Teitell MA, Mikkola HK (2006) Transcriptional activators, repressors, and epigenetic modifiers controlling hematopoietic stem cell development. Pediatr Res 59: 33R-39R.
5. Nakauchi H, Sudo K, Ema H (2001) Quantitative assessment of the stem cell self-renewal capacity. Ann N Y Acad Sci 938: 18-24; discussion 24-15.
6. Naveiras O, Nardi V, Wenzel PL, Hauschka PV, Fahey F, et al. (2009) Bone-marrow adipocytes as negative regulators of the haematopoietic microenvironment. Nature 460: 259-263.
7. Chow A, Lucas D, Hidalgo A, Mendez-Ferrer S, Hashimoto D, et al. (2011) Bone marrow CD169+ macrophages promote the retention of hematopoietic stem and progenitor cells in the mesenchymal stem cell niche. J Exp Med 208: 261-271.
8. Calvi LM, Adams GB, Weibrecht KW, Weber JM, Olson DP, et al. (2003) Osteoblastic cells regulate the haematopoietic stem cell niche. Nature 425: 841-846.
9. Mendez-Ferrer S, Michurina TV, Ferraro F, Mazloom AR, Macarthur BD, et al. (2010) Mesenchymal and haematopoietic stem cells form a unique bone marrow niche. Nature 466: 829-834.
10. Kobayashi H, Butler JM, O'Donnell R, Kobayashi M, Ding BS, et al. (2010) Angiocrine factors from Akt-activated endothelial cells balance self-renewal and differentiation of haematopoietic stem cells. Nat Cell Biol 12: 1046-1056.
11. Arai F, Hirao A, Ohmura M, Sato H, Matsuoka S, et al. (2004) Tie2/angiopoietin-1 signaling regulates hematopoietic stem cell quiescence in the bone marrow niche. Cell 118: 149-161.
12. Zhang J, Niu C, Ye L, Huang H, He X, et al. (2003) Identification of the haematopoietic stem cell niche and control of the niche size. Nature 425: 836-841.
13. Bryder D, Jacobsen SE (2000) Interleukin-3 supports expansion of long-term multilineage repopulating activity after multiple stem cell divisions in vitro. Blood 96: 1748-1755.
14. Zhang CC, Kaba M, Ge G, Xie K, Tong W, et al. (2006) Angiopoietin-like proteins stimulate ex vivo expansion of hematopoietic stem cells. Nat Med 12: 240-245.

15. Miller CL, Eaves CJ (1997) Expansion in vitro of adult murine hematopoietic stem cells with transplantable lympho-myeloid reconstituting ability. Proc Natl Acad Sci U S A 94: 13648-13653.
16. Delaney C, Heimfeld S, Brashem-Stein C, Voorhies H, Manger RL, et al. (2010) Notch-mediated expansion of human cord blood progenitor cells capable of rapid myeloid reconstitution. Nat Med 16: 232-236.
17. Antonchuk J, Sauvageau G, Humphries RK (2002) HOXB4-induced expansion of adult hematopoietic stem cells ex vivo. Cell 109: 39-45.
18. Amsellem S, Pflumio F, Bardinet D, Izac B, Charneau P, et al. (2003) Ex vivo expansion of human hematopoietic stem cells by direct delivery of the HOXB4 homeoprotein. Nat Med 9: 1423-1427.
19. Boitano AE, Wang J, Romeo R, Bouchez LC, Parker AE, et al. (2010) Aryl hydrocarbon receptor antagonists promote the expansion of human hematopoietic stem cells. Science 329: 1345-1348.
20. Oostendorp RA, Harvey KN, Kusadasi N, de Bruijn MF, Saris C, et al. (2002) Stromal cell lines from mouse aorta-gonads-mesonephros subregions are potent supporters of hematopoietic stem cell activity. Blood 99: 1183-1189.
21. Moore KA, Ema H, Lemischka IR (1997) In vitro maintenance of highly purified, transplantable hematopoietic stem cells. Blood 89: 4337-4347.
22. Shimakura Y, Kawada H, Ando K, Sato T, Nakamura Y, et al. (2000) Murine stromal cell line HESS-5 maintains reconstituting ability of Ex vivo-generated hematopoietic stem cells from human bone marrow and cytokine-mobilized peripheral blood. Stem Cells 18: 183-189.
23. Nolta JA, Thiemann FT, Arakawa-Hoyt J, Dao MA, Barsky LW, et al. (2002) The AFT024 stromal cell line supports long-term ex vivo maintenance of engrafting multipotent human hematopoietic progenitors. Leukemia 16: 352-361.
24. Vanheusden K, Van Coppernolle S, De Smedt M, Plum J, Vandekerckhove B (2007) In vitro expanded cells contributing to rapid severe combined immunodeficient repopulation activity are CD34+38-33+90+45RA. Stem Cells 25: 107-114.
25. Sutherland HJ, Eaves CJ, Eaves AC, Dragowska W, Lansdorp PM (1989) Characterization and partial purification of human marrow cells capable of initiating long-term hematopoiesis in vitro. Blood 74: 1563-1570.
26. Nakano T, Kodama H, Honjo T (1994) Generation of lymphohematopoietic cells from embryonic stem cells in culture. Science 265: 1098-1101.
27. Hackney JA, Charbord P, Brunk BP, Stoeckert CJ, Lemischka IR, et al. (2002) A molecular profile of a hematopoietic stem cell niche. Proc Natl Acad Sci U S A 99: 13061-13066.
28. Collins LS, Dorshkind K (1987) A stromal cell line from myeloid long-term bone marrow cultures can support myelopoiesis and B lymphopoiesis. J Immunol 138: 1082-1087.
29. Itoh K, Tezuka H, Sakoda H, Konno M, Nagata K, et al. (1989) Reproducible establishment of hemopoietic supportive stromal cell lines from murine bone marrow. Exp Hematol 17: 145-153.

30. Gentleman RC, Carey VJ, Bates DM, Bolstad B, Dettling M, et al. (2004) Bioconductor: open software development for computational biology and bioinformatics. Genome Biol 5: R80.
31. Wettenhall JM, Simpson KM, Satterley K, Smyth GK (2006) affylmGUI: a graphical user interface for linear modeling of single channel microarray data. Bioinformatics 22: 897-899.
32. Gao J, Yan XL, Li R, Liu Y, He W, et al. (2010) Characterization of OP9 as authentic mesenchymal stem cell line. J Genet Genomics 37: 475-482.
33. Majeti R, Park CY, Weissman IL (2007) Identification of a hierarchy of multipotent hematopoietic progenitors in human cord blood. Cell Stem Cell 1: 635-645.
34. Dorrell C, Gan OI, Pereira DS, Hawley RG, Dick JE (2000) Expansion of human cord blood CD34(+)CD38(-) cells in ex vivo culture during retroviral transduction without a corresponding increase in SCID repopulating cell (SRC) frequency: dissociation of SRC phenotype and function. Blood 95: 102-110.
35. Nutt SL, Heavey B, Rolink AG, Busslinger M (1999) Commitment to the B-lymphoid lineage depends on the transcription factor Pax5. Nature 401: 556-562.
36. Iwasaki H, Somoza C, Shigematsu H, Duprez EA, Iwasaki-Arai J, et al. (2005) Distinctive and indispensable roles of PU.1 in maintenance of hematopoietic stem cells and their differentiation. Blood 106: 1590-1600.
37. Pevny L, Simon MC, Robertson E, Klein WH, Tsai SF, et al. (1991) Erythroid differentiation in chimaeric mice blocked by a targeted mutation in the gene for transcription factor GATA-1. Nature 349: 257-260.
38. Zhang P, Iwasaki-Arai J, Iwasaki H, Fenyus ML, Dayaram T, et al. (2004) Enhancement of hematopoietic stem cell repopulating capacity and self-renewal in the absence of the transcription factor C/EBP alpha. Immunity 21: 853-863.
39. Liu ZG (2005) Molecular mechanism of TNF signaling and beyond. Cell Res 15: 24-27.
40. Dohn M, Zhang S, Chen X (2001) p63alpha and DeltaNp63alpha can induce cell cycle arrest and apoptosis and differentially regulate p53 target genes. Oncogene 20: 3193-3205.
41. Cheng T, Rodrigues N, Shen H, Yang Y, Dombkowski D, et al. (2000) Hematopoietic stem cell quiescence maintained by p21cip1/waf1. Science 287: 1804-1808.
42. Shojaei F, Trowbridge J, Gallacher L, Yuefei L, Goodale D, et al. (2005) Hierarchical and ontogenic positions serve to define the molecular basis of human hematopoietic stem cell behavior. Dev Cell 8: 651-663.
43. Mackarehtschian K, Hardin JD, Moore KA, Boast S, Goff SP, et al. (1995) Targeted disruption of the flk2/flt3 gene leads to deficiencies in primitive hematopoietic progenitors. Immunity 3: 147-161.
44. Matsumoto A, Takeishi S, Kanie T, Susaki E, Onoyama I, et al. (2011) p57 is required for quiescence and maintenance of adult hematopoietic stem cells. Cell Stem Cell 9: 262-271.

45. Suda T, Takubo K, Semenza GL (2011) Metabolic regulation of hematopoietic stem cells in the hypoxic niche. Cell Stem Cell 9: 298-310.
46. Carvajal LA, Hamard PJ, Tonnessen C, Manfredi JJ (2012) E2F7, a novel target, is up-regulated by p53 and mediates DNA damage-dependent transcriptional repression. Genes Dev 26: 1533-1545.
47. Radomska HS, Huettner CS, Zhang P, Cheng T, Scadden DT, et al. (1998) CCAAT/enhancer binding protein alpha is a regulatory switch sufficient for induction of granulocytic development from bipotential myeloid progenitors. Mol Cell Biol 18: 4301-4314.
48. Austin GE, Chan WC, Zhao W, Racine M (1994) Myeloperoxidase gene expression in normal granulopoiesis and acute leukemias. Leuk Lymphoma 15: 209-226.
49. Elsbach P (1998) The bactericidal/permeability-increasing protein (BPI) in antibacterial host defense. J Leukoc Biol 64: 14-18.
50. Sudo T, Nishikawa S, Ohno N, Akiyama N, Tamakoshi M, et al. (1993) Expression and function of the interleukin 7 receptor in murine lymphocytes. Proc Natl Acad Sci U S A 90: 9125-9129.
51. Oettinger MA, Schatz DG, Gorka C, Baltimore D (1990) RAG-1 and RAG-2, adjacent genes that synergistically activate V(D)J recombination. Science 248: 1517-1523.
52. Ball LM, Bernardo ME, Roelofs H, Lankester A, Cometa A, et al. (2007) Cotransplantation of ex vivo expanded mesenchymal stem cells accelerates lymphocyte recovery and may reduce the risk of graft failure in haploidentical hematopoietic stem-cell transplantation. Blood 110: 2764-2767.
53. Le Blanc K, Ringden O (2007) Immunomodulation by mesenchymal stem cells and clinical experience. J Intern Med 262: 509-525.
54. Ficara F, Murphy MJ, Lin M, Cleary ML (2008) Pbx1 regulates self-renewal of long-term hematopoietic stem cells by maintaining their quiescence. Cell Stem Cell 2: 484-496.
55. Min IM, Pietramaggiori G, Kim FS, Passegue E, Stevenson KE, et al. (2008) The transcription factor EGR1 controls both the proliferation and localization of hematopoietic stem cells. Cell Stem Cell 2: 380-391.
56. Ku CJ, Hosoya T, Maillard I, Engel JD (2012) GATA-3 regulates hematopoietic stem cell maintenance and cell-cycle entry. Blood 119: 2242-2251.
57. Buza-Vidas N, Duarte S, Luc S, Bouriez-Jones T, Woll PS, et al. (2011) GATA3 is redundant for maintenance and self-renewal of hematopoietic stem cells. Blood 118: 1291-1293.
58. Mao Y, Tournier AL, Bates PA, Gale JE, Tapon N, et al. (2011) Planar polarization of the atypical myosin Dachs orients cell divisions in Drosophila. Genes Dev 25: 131-136.
59. Bultje RS, Castaneda-Castellanos DR, Jan LY, Jan YN, Kriegstein AR, et al. (2009) Mammalian Par3 regulates progenitor cell asymmetric division via notch signaling in the developing neocortex. Neuron 63: 189-202.
60. Fukuda MN, Sato T, Nakayama J, Klier G, Mikami M, et al. (1995) Trophinin and tastin, a novel cell adhesion molecule complex with potential involvement in embryo implantation. Genes Dev 9: 1199-1210.

61. Pina C, May G, Soneji S, Hong D, Enver T (2008) MLLT3 regulates early human erythroid and megakaryocytic cell fate. Cell Stem Cell 2: 264-273.
62. Challen GA, Sun D, Jeong M, Luo M, Jelinek J, et al. (2012) Dnmt3a is essential for hematopoietic stem cell differentiation. Nat Genet 44: 23-31.
63. Hope KJ, Cellot S, Ting SB, MacRae T, Mayotte N, et al. (2010) An RNAi screen identifies Msi2 and Prox1 as having opposite roles in the regulation of hematopoietic stem cell activity. Cell Stem Cell 7: 101-113.
64. Cai M, Langer EM, Gill JG, Satpathy AT, Albring JC, et al. (2012) Dual actions of Meis1 inhibit erythroid progenitor development and sustain general hematopoietic cell proliferation. Blood 120: 335-346.
65. Holyoake TL, Nicolini FE, Eaves CJ (1999) Functional differences between transplantable human hematopoietic stem cells from fetal liver, cord blood, and adult marrow. Exp Hematol 27: 1418-1427.
66. Krosl J, Beslu N, Mayotte N, Humphries RK, Sauvageau G (2003) The competitive nature of HOXB4-transduced HSC is limited by PBX1: the generation of ultra-competitive stem cells retaining full differentiation potential. Immunity 18: 561-571.
67. Ivanovic Z, Dello Sbarba P, Trimoreau F, Faucher JL, Praloran V (2000) Primitive human HPCs are better maintained and expanded in vitro at 1 percent oxygen than at 20 percent. Transfusion 40: 1482-1488.
68. Danet GH, Pan Y, Luongo JL, Bonnet DA, Simon MC (2003) Expansion of human SCID-repopulating cells under hypoxic conditions. J Clin Invest 112: 126-135.
69. Jude CD, Gaudet JJ, Speck NA, Ernst P (2008) Leukemia and hematopoietic stem cells: balancing proliferation and quiescence. Cell Cycle 7: 586-591.

Figure legends

Figure 2.1. The OP9M2 MSC stromal cell line supports long-term expansion of multipotent human CD34+CD38-CD90+ cells. Co-culture of human fetal liver CD34+ cells on OP9M2 stroma maintains cells with the characteristic CD34+CD38-CD90+ surface immunophenotype that HSC express. (A) Representative FACS plots of CD34+ fetal liver cells after co-culture either without stroma, on BFC012 stromal cells or on OP9M2 stromal cells are shown. (B) Representative FACS plots of fetal liver CD34+ cells co-cultured for 5 and 7 weeks on the OP9M2 stromal cell line are shown. (C) Upper chart shows total fold expansion of all hematopoietic cells from

input CD34+ cells with or without OP9M2. Lower chart shows total fold expansion of CD34+CD38-CD90+ cells. Bold line represents 7 experiments (n=7) while dashed lines represent 3 experiments (n=3), as in some experiments HSPC cultured beyond 5 weeks had started to lose proliferative potential. (D) Fold expansion of CD34+CD38-CD90+ clonogenic progenitors (CFU-C, assessed in methylcellulose cultures) is shown. Error bars represent SEM (* $p < 0.05$, n = 3). (E) Single cell assay documenting expansion of CD34+CD38-CD90+ cells that retain both myeloid and lymphoid differentiation potential is shown. 96-well plates were coated with OP9M2 stroma, and individual CD34+CD38-CD90+ fetal liver cells (freshly isolated or *ex vivo* expanded) were sorted directly into each well and cultured for 3 weeks to assess for recreating the CD34+CD38-CD90+ immature population and for myelo-lymphoid differentiation potential. (F) Total fold expansion of clonally multipotent progenitors in co-culture with OP9M2 is shown. Error bars represent SEM (* $p < 0.05$, 2 weeks n=3, and 5 weeks n=1).

Figure 2.2. The OP9M2 stromal cell line supports maintenance of engraftable HSC. (A) Summary of total human reconstitution in the bone marrow of NSG mice 16 weeks post transplantation of all the progeny cells from 50,000 CD34+ input cells that were transplanted freshly (Day 0) or co-cultured for up to 7 weeks. Shown are all individual recipients and mean value. P value was calculated for each time-point in comparison to Day 0. (** $p < 0.01$). (B) Representative FACS plot of bone marrow and spleen from NSG recipient mice showing long-term multilineage engraftment of 50,000 input CD34+ FL cells that were isolated freshly or co-cultured 2 weeks on

OP9M2. (C) Comparison of engraftment capacity between purified CD34+CD38-CD90+, CD34+CD38-CD90-, CD34+CD38+CD90+ and CD34- cells 2 weeks after co-culture demonstrates that the engraftable HSC are maintained only in the CD34+CD38-CD90+ fraction. Each mouse was transplanted with the respective population derived from 50,000 input CD34+ human fetal liver cells in culture. Shown are all individual recipients and mean value from one experiment (** $p < 0.01$, * $p < 0.05$). (D) Limited dilution assays (n= 2) was performed to estimate NSG-RC frequency among fetal liver CD34+ cells that were transplanted freshly or after 2 week culture. Mice were transplanted with equal number of input CD34+ cells at different concentrations and analyzed 16 weeks post transplantation. No significant difference in NSG-RC number (Day 0: 1 in 2610, upper 4821, lower 1413 and 2 wk: 1 in 3003, upper 5953, lower 1515) ($p=0.77$) was detected.

Figure 2.3. *Ex vivo* expanded CD34+CD38-CD90+ cells demonstrate high preservation of the HSC transcriptional program. (A) Hierarchical clustering using spearman rank correlation and (B) principal component analysis comparing freshly isolated CD34+CD38-CD90+ cells (Day 0) to CD34+CD38+CD90- differentiated progenitors and to *ex-vivo* expanded CD34+CD38-CD90+ cells demonstrate high conservation of the HSC transcriptome during culture on OP9M2 stroma. (C) Number of genes with more than 2-fold change in gene expression compared to Day 0 CD34+CD38-CD90+ cells is shown. (D) Graph showing the relative expression of transcription factors known to regulate HSC development or maintenance. (E) Graph showing the relative expression of transcription factors

known to initiate hematopoietic lineage commitment. Values represent a fold difference to freshly isolated CD34+CD38-CD90+ cells. Raw data is available for download from Gene Expression Omnibus (http://ncbi.nlm.nih.gov/geo) (GSE34974).

Figure 2.4. CD34+CD38-CD90+ cells display a transient "culture shock" upon exposure to culture. Fuzzy C cluster analysis identified three temporal gene expression patterns consisting of genes whose expression became transiently altered by 12 hrs in culture. (A) Cluster of genes upregulated at 12 hrs is shown together with their Gene ontology (GO) analysis. (B) Cluster of genes upregulated at 12 hrs and at 5 wk is shown with their GO analysis, (C) Cluster of genes downregulated at 12 hrs is shown with their GO analysis. (D) Transient upregulation of cell cycle arrest and cell death genes selected from clusters in A and B is shown. (E) Aryl hydrocarbon receptor signaling genes selected from cluster A are shown. (F) A temporary decrease in gene expression was observed in known HSC regulators; individual genes selected from cluster C are shown. Shown are fold differences in gene expression of *ex vivo* expanded CD34+CD38-CD90+ cells relative to freshly isolated (day 0) control CD34+CD38-CD90+ cells. CD34+CD38+CD90- indicates gene expression changes for differentiated progenitors relative to Day 0 control CD34+CD38-CD90+ cells.

Figure 2.5. *Ex vivo* expanded CD34+CD38-CD90+ cells show dynamic changes in transcriptional programs associated with cellular state. Fuzzy C cluster

analysis identified three temporal gene expression patterns describing genes that were either upregulated (A) immediately upon culture, (B) predominantly at 2 weeks of culture or (C) gradually during prolonged culture. The GO analysis of genes in (A), (B) and (C) is shown below each cluster respectively. The GO analysis from cluster D identified several genes associated with (D) Kinase activity and (E) response to DNA damage that were modestly upregulated during culture. (F) GO analysis from cluster E identified several genes regulating glucose metabolism. GO analysis of cluster F identified several genes associated with (G) Cell cycle and (H) Immune response that were upregulated during prolonged culture. Shown are fold difference in gene expression of CD34+CD38-CD90+ cells at each time point relative to Day 0 control CD34+CD38-CD90+ cells. CD34+CD38+CD90- indicates gene expression changes for differentiated progenitors relative to Day 0 control CD34+CD38-CD90+ cells.

Figure 2.6. ***Ex vivo*** **expanded CD34+CD38-CD90+ cells show temporal changes in transcriptional programs associated with HSPC function and cell adhesion.** Fuzzy C cluster analysis identified two temporal gene expression patterns describing genes that were either (A) immediately downregulated upon culture or (B) downregulated progressively during culture. GO analysis of genes in (A) and (B) (shown below each cluster respectively) identified numerous transcription factors that were downregulated, either (C) immediately or (D) progressively during culture. Similarly, several cell adhesion molecules implicated in HSC-niche interactions were downregulated either (E) immediately or (F) progressively during

the culture. Shown are fold difference in gene expression of CD34+CD38-CD90+ cells at each time point relative to Day 0 control CD34+CD38-CD90+ cells. CD34+CD38+CD90- indicates gene expression changes for differentiated progenitors relative to Day 0 control CD34+CD38-CD90+ cells.

Figure 2.7. Cultured human CD34+CD38-CD90+ cells show shared gene expression changes with *Pbx1* deficient mouse HSC. Differential gene expression analysis was performed comparing HSC (LSKCD34-Flt3-) from control and *Pbx1* deficient mice (GEO series GSE9188). (A) Table showing the FDR-q values from the GSEA analysis on pairwise expression data comparing freshly isolated CD34+CD38-CD90+ human cells with each time point in culture to the differentially expressed genes from *Pbx1* deficient mouse LSKCD34-Flt3- cells. (B) Heat map showing 24 genes downregulated both in Pbx1 deficient LSKCD34-Flt3- cells and at least in one of the culture time points (right) (>1.5-fold with respect to freshly isolated CD34+CD38-CD90+ cells, FDR of 5%). (C) Heat map of 54 genes that were upregulated both in *Pbx1* deficient HSC and at least in one of the culture time points (left), (>1.5-fold with respect to freshly isolated CD34+CD38-CD90+ cells, FDR of 5%). (D) A summary figure illustrating the HSC properties that are preserved or lost in the presence or absence of supportive stromal cells.

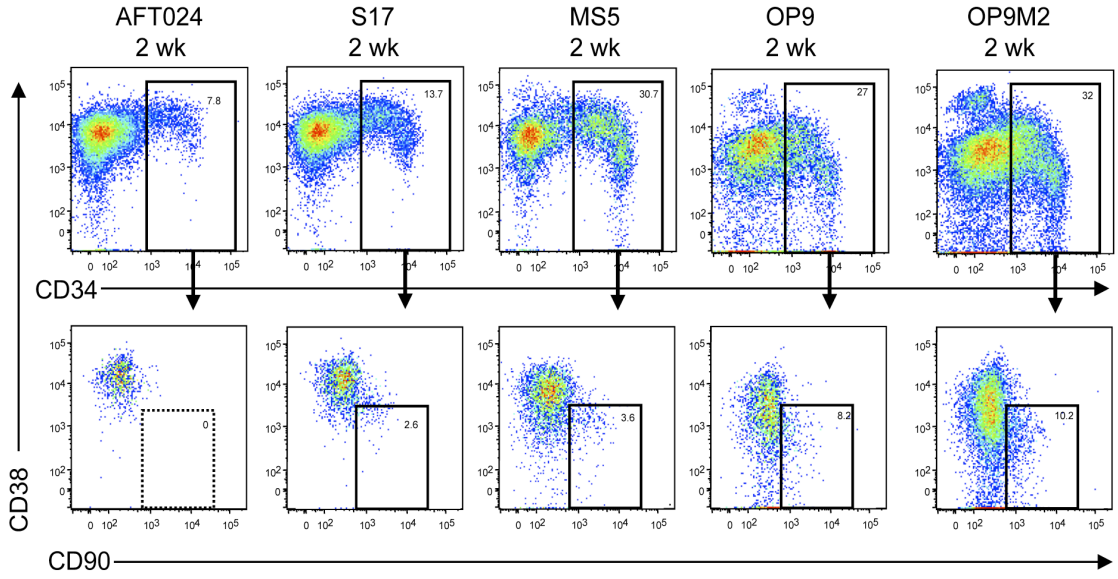

Figure S1. Co-culture of human CD34+ fetal liver on different stromal cell lines. Representative FACS plots of CD34+ fetal liver cells after 2 weeks of co-culture on different mouse stroma cell lines. Presence of CD34+CD38-CD90+ cells indicates maintenance of undifferentiated human hematopoietic cells.

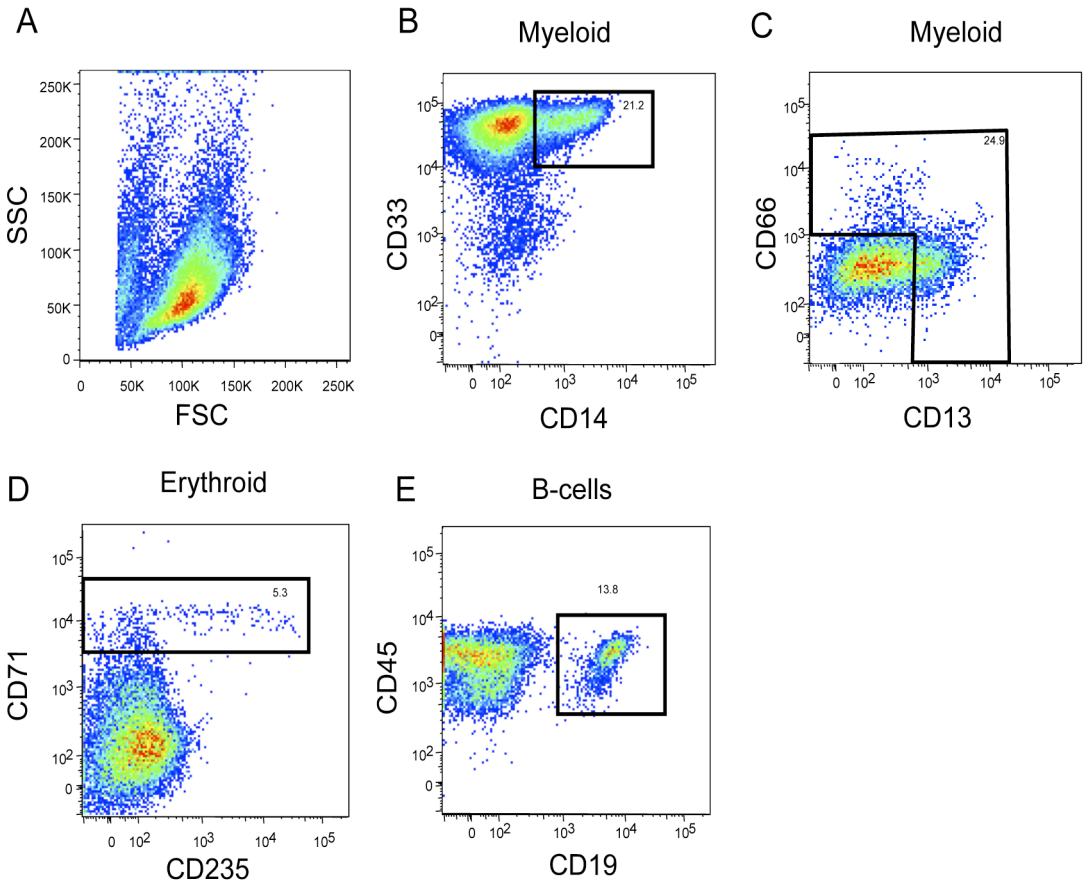

Figure S2. The OP9M2 stroma line facilitates establishment of a multilineage human hematopoietic hierarchy *ex vivo*. FACS analysis of CD34+ FL cells cultured on OP9M2 supplemented with SCF, TPO and FLT3L demonstrating,(A) forward and side scatter of cultured cells ,(B and C) presence of HSPC (CD33) and various myeloid progenitors , monocytes and granulocytes (CD33, CD14, CD66 and CD13) as well as (D) erythroid cells (CD71). (E) CD34+ FL cells co-cultured on OP9M2 with IL-7, FLT-3L and SCF demonstrating robust generation of B-cells (CD19).

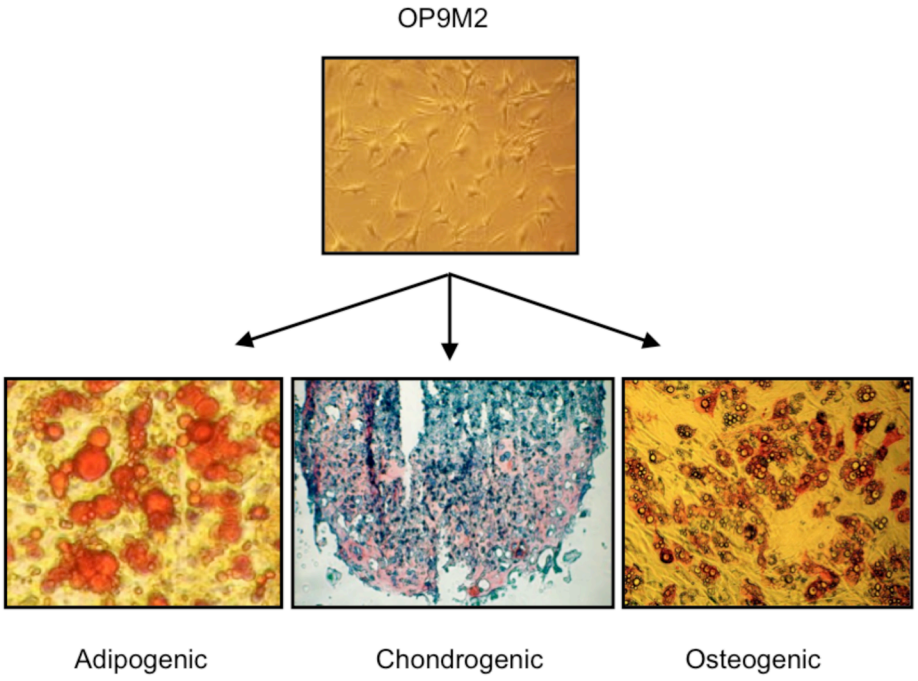

Figure S3. The OP9M2 stroma line has mesenchymal stem cell properties. OP9M2 stromal cells exhibit tri-lineage differentiation capacity into adipocytes, chondrocytes and osteoblasts. Adipocyte potential was determined by Oil Red O stain; chondrogenic potential by Safranin O stain; and osteocytic potential by Alizarin red stain. Images were acquired at 20x original magnification using an Axiovert 40CL microscope and a Canon Powershot G6 camera.

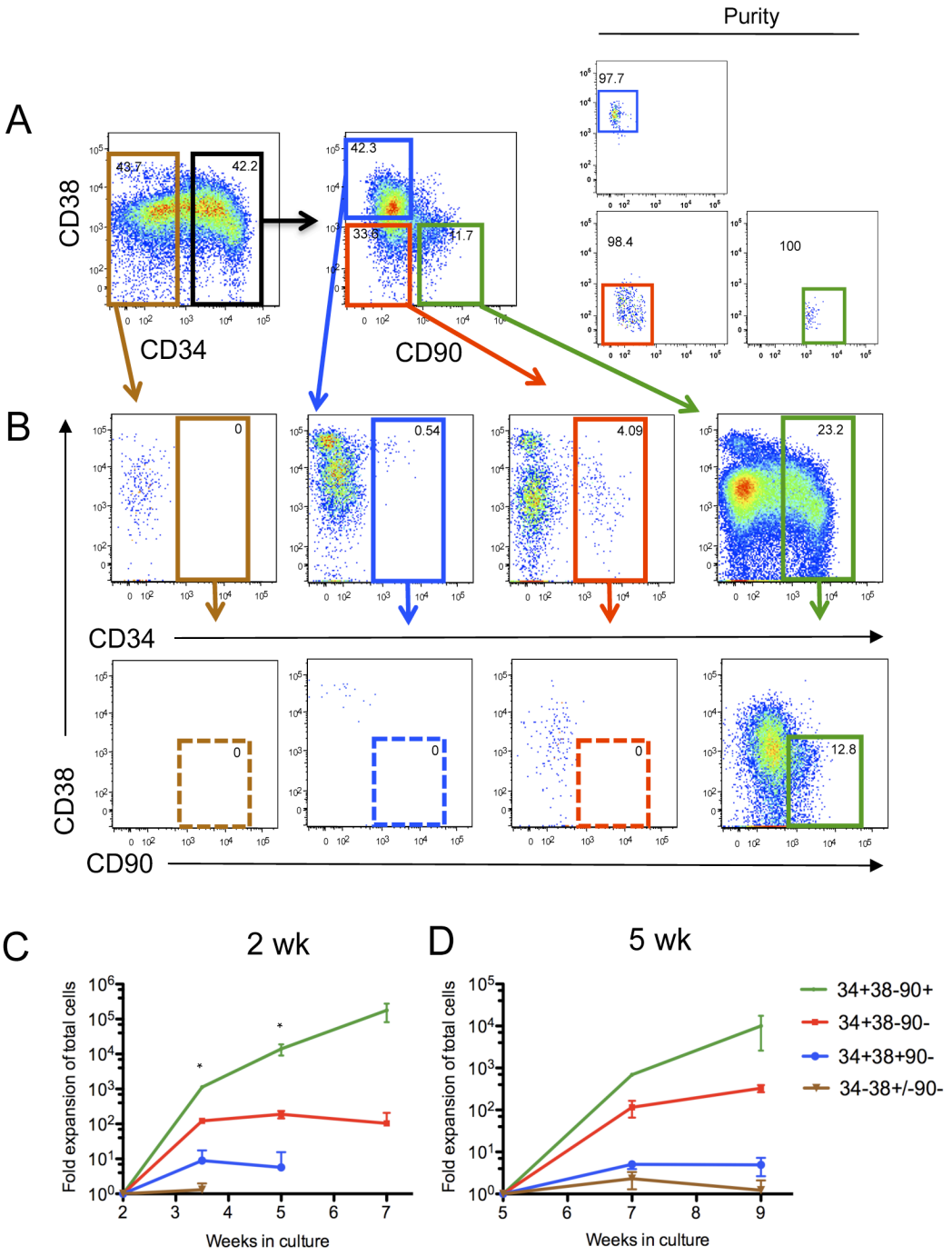

Figure S4. Long-term proliferative potential and capacity to maintain hematopoietic cells with undifferentiated surface phenotype remains entirely within the CD34+CD38-CD90+ fraction of cultured cells. Fractionation of CD34+CD38-CD90+ cells after 2 weeks of culture based on surface phenotype demonstrates sustained expansion of CD34+CD38-CD90+ cells during re-plating only within the CD34+CD38-CD90+ population. (A) Upper FACS plots represent the cells and gates used for the fractionation at 2 weeks and purity plots. (B) FACS plots in the middle show the immunophenotype of the fractions after additional 2 weeks of culture and the charts below summarize the total fold expansion of hematopoietic cells fractionated at (C) 2 weeks and (D) 5 weeks of culture. Error bars represent SEM (* $p < 0.05$, $n = 3$).

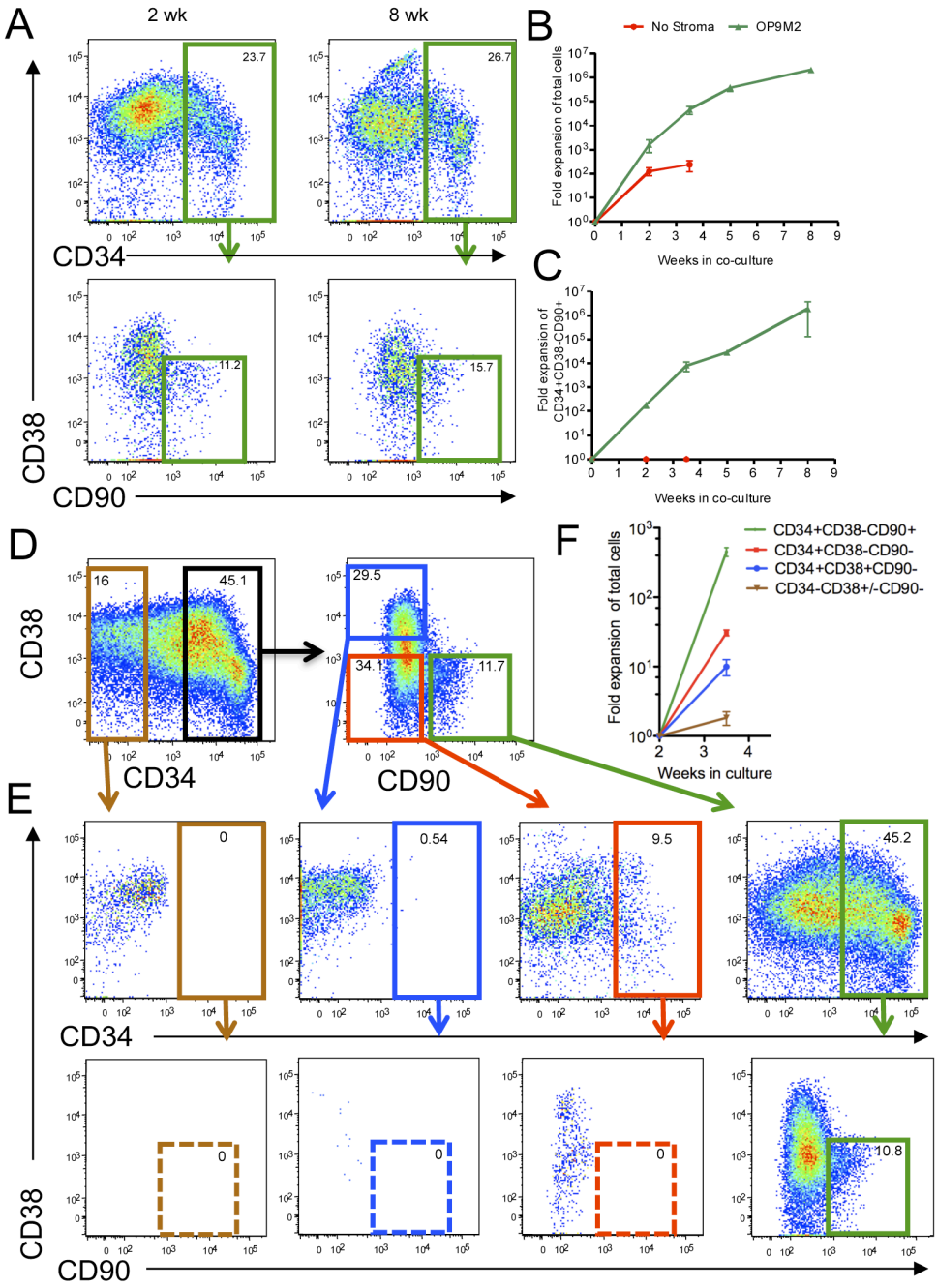

Figure S5. OP9M2 supports the expansion of cord blood (CB) CD34+CD38-CD90+ cells. (A) Representative FACS plots of CD34+ CB cells after 2 and 8 weeks of co-culture on OP9M2 are shown. (B) Summary of total fold expansion of all CB cells from input cells cultured with or without OP9M2. (C) Summary of fold expansion of CD34+CD38-CD90+ CB cells cultured with or without OP9M2. Fractionation of cultured CB cells after 2 weeks of culture demonstrates sustained expansion of the undifferentiated CD34+CD38-CD90+ cells during re-plating only within the CD34+CD38-CD90+ population. (D) FACS plots represent the cells and gates used for the fractionation at 2 weeks. (E) FACS plots show the immunophenotype of the fractions after additional 2 weeks of culture and (F) summarize the total fold expansion of hematopoietic cells fractionated at 2 weeks and additional 2 weeks of culture (Error bars represent SEM (* $p < 0.05$, $n = 3$).

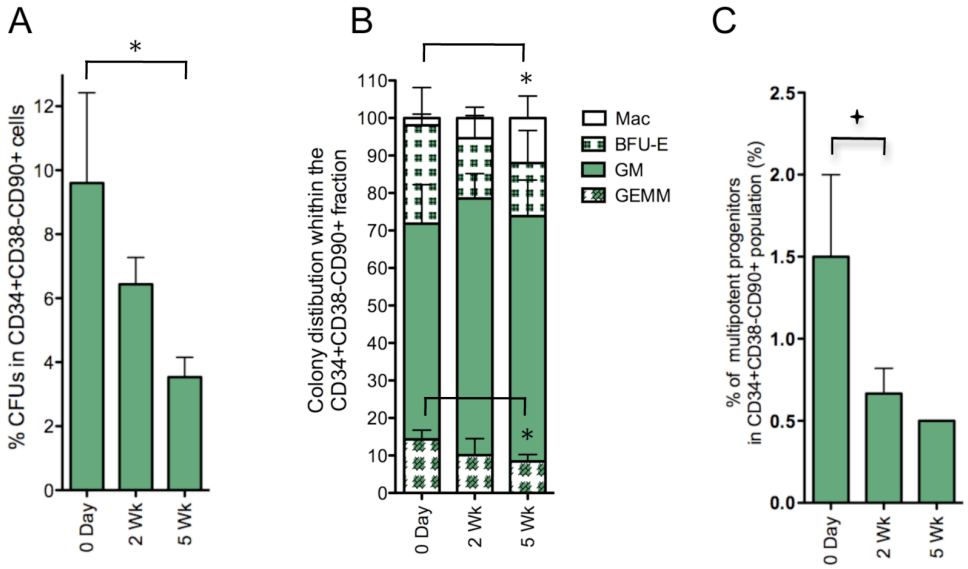

Figure S6. CD34+CD38-CD90+ cells expanded on OP9M2 demonstrate slight relative decrease in the frequency of hematopoietic progenitors. (A) Frequency of CFUs among *ex vivo* expanded CD34+CD38-CD90+ cells. (B) Colony distribution among *ex vivo* expanded CD34+CD38-CD90+ cells. (C) Frequency of multipotent progenitors among *ex vivo* expanded CD34+CD38-CD90+ cells as measured by single cell assay. Error bars represent SEM (* $p < 0.05$, ✦ $p=0.051$, $n = 3$ independent experiments, except for C, only one experiment showed robust proliferation of single CD34+CD38-CD90+ cells sorted and re-plated at 5 weeks)

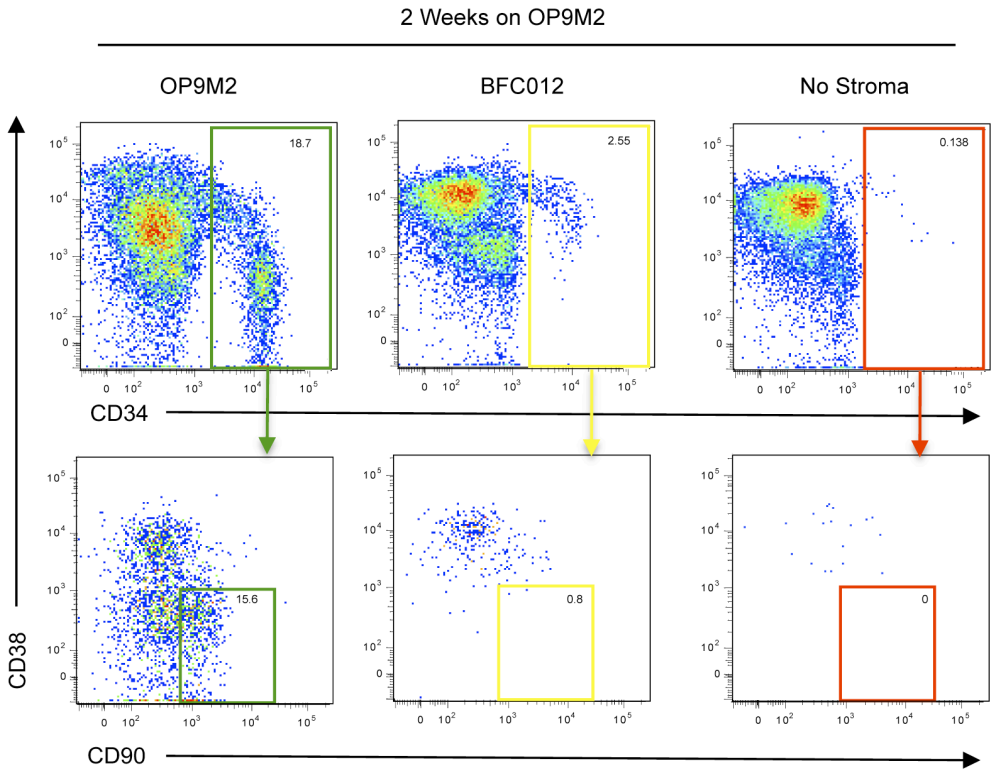

Figure S7. *Ex vivo* expanded CD34+CD38-CD90+ cells demonstrate continued dependence on OP9M2 niche signals. CD34+ FL cells cultured on OP9M2 for 2 weeks rapidly differentiate when transferred to non-supportive BFC012 stroma or no stroma. Left FACS plot: cells replated on OP9M2, Middle FACS plot: cells replated on BFC012, Right FACS plot: cells replated without stroma.

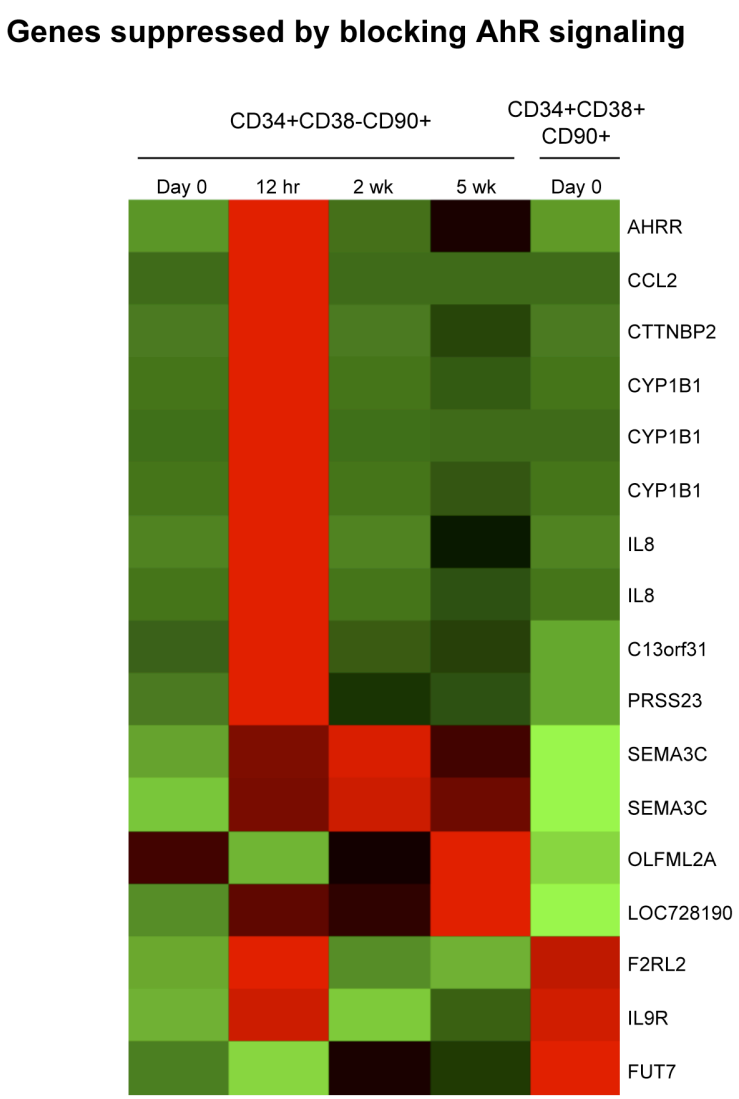

Figure S8. CD34+CD38-CD90+ cells expanded on OP9M2 stroma undergo an initial culture shock resulting in transient activation of the aryl hydrocarbon receptor (AhR) signaling pathway. Heat map showing genes in cultured fetal CD34+CD38-CD90+ cells, selected if they were at least two-fold downregulated in CD34+ cells treated with SR1 (inhibitor of AhR signaling) (GEO series GSE28359)[1], and at least two-fold up-regulated in cultured fetal liver CD34+CD38-CD90+ cells. All five arrays (untreated, and treated with four different concentrations of SR1) from Boitano et al[1] were normalized using RMA method and fold change was calculated comparing SR1 treated cells to the untreated control. Thirteen genes were at least 2-fold down-regulated in two or more concentrations of SR1 treated cells. Of those, 9 were differentially expressed in our dataset of cultured CD34+CD38-CD90+ cells (illustrated in heat map above). The heat map was generated on probe sets called as "Present" using the MAS5 algorithm in at least in one sample and if the absolute expression level was above 50. Several of these genes are known members of the AHR signaling pathway, which is a negative regulator of HSC function[1,2]. Robust activation of this pathway was observed in CD34+CD38-CD90+ cells cultured for 12 hours, with restoration to almost normal levels by 2 weeks. AHRR negatively regulates AHR, however, it's own transcription is regulated by AHR activation[3,4]. CYP1B1 is also regulated by AHR activation[1]. Interestingly, the inflammatory cytokine, CCL2, has been linked to activation of mTOR[5], which compromises HSC function. Therefore, activation of AHR signaling and inflammatory pathways at the onset of *ex vivo* culture may trigger downstream effectors that negatively regulate CD34+CD38-CD90+ cell function.

Chapter 3:

GPI-80 Defines Self-renewal Ability in Hematopoietic Stem Cells During Human Development

GPI-80 Defines Self-renewal Ability in Hematopoietic Stem Cells During Human Development

Prashad SL[1, 2, 3], **Yao CY***[1, 2], **Calvanese V***[1, 2], **Kaiser J**[1, 2], **Sasidharan R**[1, 2], **Magnusson M**[1, 2], **Mikkola HKA**[1, 2, 3]

[1]Department of Molecular, Cell and Developmental Biology, University of California Los Angeles, Los Angeles, CA 90095, USA. [2]Eli and Edythe Broad Center for Regenerative Medicine and Stem Cell Research. [3]Molecular Biology Institute, UCLA.

Contact: hmikkola@mcdb.ucla.edu, 621 Charles E. Young Dr S, Los Angeles, CA 90095

Running title
Self-renewing HSPC express GPI-80.

*These authors contributed equally to this work.

Highlights

- Human fetal HSC with self-renewal ability express GPI-80, a myeloid adhesion factor
- The migration of HSPC between fetal hematopoietic sites can be tracked by GPI-80
- GPI-80 and ITGAM co-localize on the cell surface to facilitate HSC self-renewal

Summary

Advances in pluripotent stem cell (PSC) and reprogramming technologies have given hope of generating hematopoietic stem cells (HSC) in culture. To succeed, greater understanding of the self-renewing HSC during human development is required. We discovered that glycophosphatidylinositol-anchored surface protein GPI-80 (Vanin 2) defines a subpopulation of human fetal hematopoietic stem/progenitor cells (HSPC) with self-renewal ability. $CD34^{+}CD38^{-}CD90^{+}GPI\text{-}80^{+}$ HSPC were the sole population that maintained proliferative potential and undifferentiated state in bone marrow stroma co-culture and engrafted in immunodeficient mice. GPI-80 expression also enabled tracking of HSPC emergence from endothelium and migration between human fetal hematopoietic niches. $GPI\text{-}80^{+}$ co-localized on the surface of HSPC with Integrin alpha-M (ITGAM), which in leukocytes cooperates with GPI-80 to support migration; knockdown of either GPI-80 or ITGAM was sufficient to perturb HSPC expansion in stroma co-culture. These findings indicate that human fetal HSC employ mechanisms used in leukocytes for cell-cell interactions governing HSC self-renewal.

Introduction

The ability to replenish blood and immune cells relies on a rare population of hematopoietic stem cells (HSC) that can differentiate into all blood cell types, self-renew and engraft upon transplantation (Morrison, Uchida, & Weissman, 1995; Weissman, 2000). HSC hold immense therapeutic value for treating hematological disorders (Bordignon, 2006; Shenoy, 2013); however, there is a shortage of immunocompatible HSC donors, particularly for patients of minority descent or mixed ethnic background (Dehn et al., 2008). Use of induced pluripotent stem (iPS) cells or lineage reprogramming strategies provide a promising avenue for the generation of patient specific HSC, although attempts to create functional HSC have not yet been successful (Dravid & Crooks, 2011; Risueño et al., 2012). Better understanding of HSC emergence and expansion during human development is critical for identifying programs necessary for the generation and maintenance of HSC *in vitro*.

The first hematopoietic cells in the embryo emerge in yolk sac blood islands, initially generating a cohort of primitive erythroblasts, followed by a burst of erythro-myeloid progenitors that seed the fetal liver (Mikkola & Orkin, 2006). Subsequently, functional HSC emerge in the dorsal aorta, vitelline and umbilical arteries, the yolk sac and the placenta (Alvarez-Silva, Belo-Diabangouaya, Salaün, & Dieterlen-Lièvre, 2003; Gekas, Dieterlen-Lièvre, Orkin, & Mikkola, 2005; Rhodes et al., 2008) from a specialized, "hemogenic" endothelium (Eilken, Nishikawa, & Schroeder, 2009; Lancrin et al., 2009). HSC then seed the fetal liver, the major site that supports copious HSC expansion during development. Following expansion in the fetal liver, HSC migrate to their lifelong niche

in the bone marrow where they shift into a predominantly quiescent state (Ciriza, Thompson, Petrosian, Manilay, & García-Ojeda, 2013). Although the sites for HSC emergence and expansion have first been established in mice, the same anatomical sites have been shown to support hematopoiesis during human development (Robin et al., 2009; Tavian, Biasch, Sinka, Vallet, & Péault, 2010; Van Handel et al., 2010).

Despite being one of the best-characterized adult stem cells, insufficient knowledge of the surface proteins specific to human HSC has hampered studies of their regulation. Many well-established murine HSC markers such as Sca1 and the SLAM markers are not conserved in human HSC (Larochelle, Savona, Wiggins, Anderson, Ichwan, Keyvanfar, Morrison, & Dunbar, 2011). Further challenges for investigating HSC properties are posed by the change of HSC surface markers during development, as observed in mouse embryos (McKinney-Freeman et al., 2012; Mikkola & Orkin, 2006). Previous studies suggest that in human, long-term repopulating HSC are enriched in the $CD34^{+}CD38^{-}CD90^{+}$ population in both cord blood and fetal hematopoietic tissues (Baum, Weissman, Tsukamoto, Buckle, & Péault, 1992; Mayani & Lansdorp, 1994; Tavian & Péault, 2005; Magnusson et al., 2013). However, as both endothelium and HSC co-express CD34 and CD90, these markers alone do not allow distinction of HSC from the endothelium during endothelial-hematopoietic transition. Therefore, specific markers that demarcate human HSC from short-lived progenitors or endothelium remain elusive.

Here we define a select population that harbors HSC during human development and uncover novel HSC regulatory factors by functionally validating surface proteins highly

enriched in the most undifferentiated fetal liver HSPC. Our studies reveal that *VNN2*/GPI-80 distinguishes a population of self-renewing HSC, and allows tracking HSC in multiple developmental niches. Molecular analysis of GPI-80 HSPC provides new insight into the regulatory machinery in the highly self-renewing fetal HSC, and reveals that fetal HSC preserve their self-renewal ability using mechanisms that are utilized in leukocyte adhesion and migration.

Results

GPI-80 expression defines a subpopulation of human fetal liver HSPC

Our goal was to define the identity and molecular properties of fetal liver HSC, which are functionally the most potent human HSC (Holyoake, Nicolini & Eaves, 1999), and ontologically, closer to PSC-derived hematopoietic cells than adult bone marrow or cord blood, thereby representing a more relevant model to study molecular blocks hampering *in vitro* HSC generation. Therefore fetal liver HSC serve as an ideal target for studying self-renewal. To identify novel candidate surface markers for the highly self-renewing fetal HSC, we performed gene expression analysis on HSPC subsets isolated from second trimester (week 15-17 of developmental age) human fetal liver. An HSC enriched population and their downstream progeny were isolated using a combination of previously established HSPC surface markers: $CD34^+CD38^-CD90^+$ (P1, most undifferentiated), $CD34^+CD38^-CD90^-$ (P2), and $CD34^+CD38^+CD90^-$ (P3) (Figure 3.1A). Sixteen weeks after transplantation into NOD-*scid IL2Rγ-null* (NSG) mice, robust engraftment was detected only in the bone marrow of mice transplanted with P1 cells (Figure 3.1B and Table S1). These data verified that fetal liver HSC engraftment ability is restricted to $CD34^+CD38^-CD90^+$ (P1) population, henceforth referred to as $CD90^+$ HSPC, while P2 and P3 consist of only hematopoietic progenitor cells (HPC).

To generate candidates for further purification of HSC, we used Affymetrix microarray analysis to identify surface proteins highly expressed in $CD34^+CD38^-CD90^+$ HSPC as compared to downstream HPC. A total of 1274 genes were upregulated > 2-fold and

1369 genes were > 2 fold down-regulated in the P1 HSPC population as compared to P2 HPC (p=0.05). Quantile-Quantile (Q-Q) analysis of differentially expressed genes confirmed that the P1 population was more similar to P2 than P3, indicating an increase in differentially expressed genes concomitant with CD38 upregulation (Figure 3.1C). Candidate HSC surface proteins were selected from the most highly up-regulated membrane proteins on $CD90^+$ HSPC (Figure 3.1D, Table S2). Of these, EMCN (Endomucin) and PROCR (or Endothelial Protein C Receptor, EPCR) have been previously implicated as useful markers to enrich for HSC (Balazs, Fabian, Esmon, & Mulligan, 2006; Matsubara et al., 2005).

Vanin-2 (*VNN2*, or glycosylphosphatidylinositol-anchored surface protein GPI-80; Figure 3.1D) a molecule that governs neutrophil adhesion and transendothelial migration (Suzuki et al., 1999), was 16.7-fold upregulated in $CD90^+$ HSPC. Upregulation of GPI-80 mRNA in HSPC (P1) as compared to the downstream HPC (P2 and P3) was verified by q-RT-PCR (Figure 3.1E). Flow cytometry analysis indicated that GPI-80 subfractionated $CD90^+$ HSPC into a distinct GPI-80^+ population (32%±7.0% of P1) (Figure 3.1F). We also confirmed GPI-80 expression in myeloid cells from adult peripheral blood (Figure S1A) and fetal liver (Figure S1B). These data implied that, in addition to having a function in the myeloid compartment, GPI-80 may also play a role in a subset of human fetal HSPC.

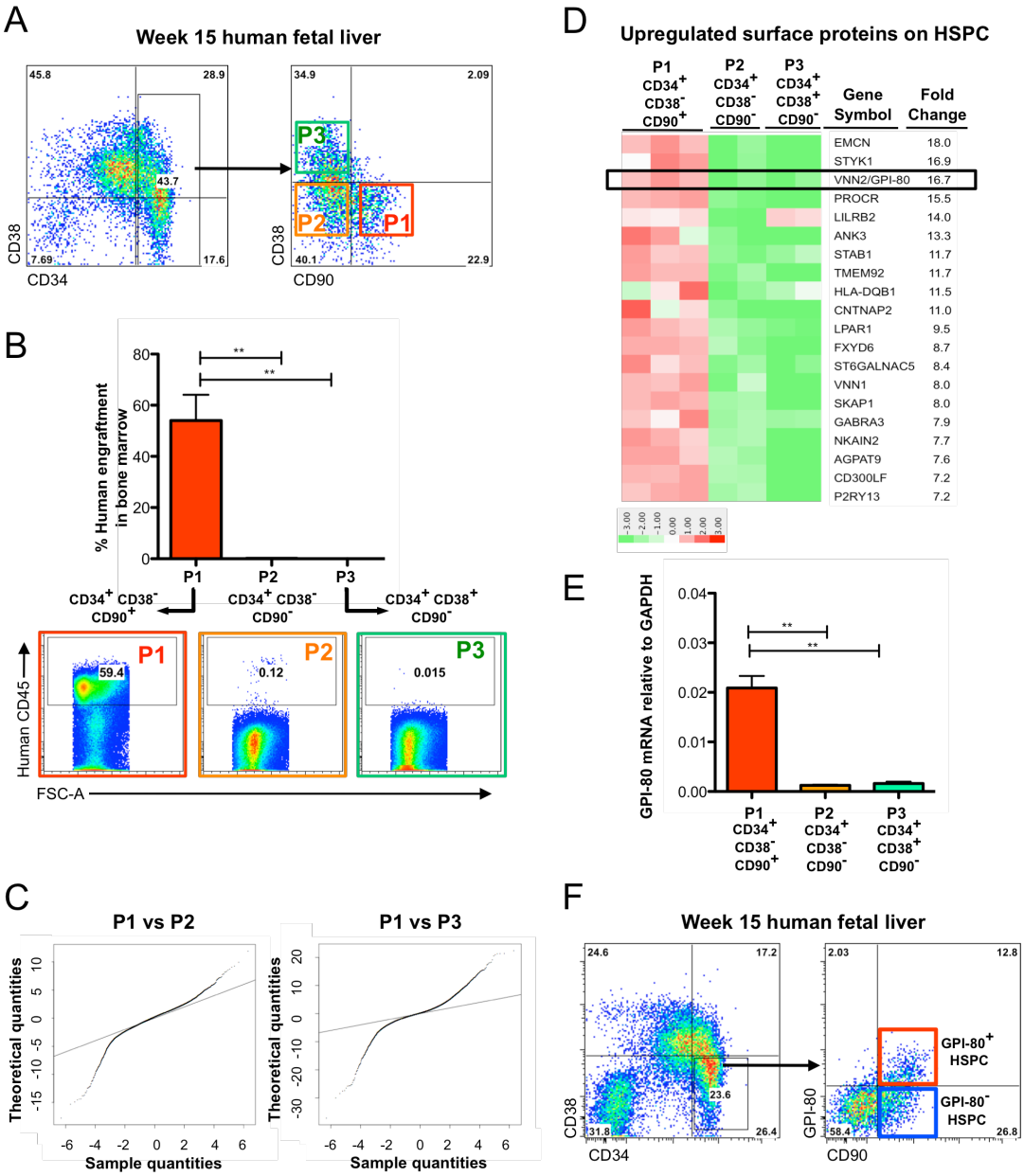

Figure 3.1: A subpopulation of human fetal liver hematopoietic stem and progenitor cells express GPI-80/VNN2

GPI80$^+$ HSPC exhibit robust multi-lineage differentiation potential

GPI-80 positive and negative fractions of fetal liver HSPC were FACS sorted and evaluated for the presence of key HSC properties: multipotency, self-renewal and engraftment ability. Both the GPI-80$^+$ and GPI-80$^-$ fractions of HSPC were able to generate colonies of myeloid and erythroid lineage in methylcellulose, although the GPI-80$^+$ HSPC consistently formed fewer colonies than GPI-80$^-$ cells (Figure S2A). B- and T-lymphoid differentiation potential was assayed *in vitro* on OP9M2 (Magnusson et al., 2013; Nakano, Kodama, & Honjo, 1994) and OP9DL1 stroma (Schmitt & Zúñiga-Pflücker, 2002), respectively; in bulk cultures, both GPI-80$^+$ and GPI-80$^-$ cells formed comparable populations of CD19$^+$ B-cells (Figure S2B) and CD4/CD8$^+$ T-cells (Figure S2C).

To further investigate multilineage differentiation ability at a clonal level, GPI-80$^+$ HSPC and GPI-80$^-$ HSPC were sorted as single cells and cultured on OP9M2 in conditions that support both myeloid and B-cell differentiation. After two weeks in culture, expanded clones were enumerated and scored as myeloid (CD13$^+$, CD14$^+$ or CD66$^+$ cells), lymphoid (CD19$^+$ cells), myelo-lymphoid (both myeloid and lymphoid cells) or undifferentiated if there was a robust CD34$^+$ population (>30%) with minimal expression of differentiation markers. A significant enrichment of proliferating clones (defined as >200 daughter cells after 14 days) was observed in GPI-80$^+$ HSPC (35%) as compared to GPI-80$^-$ HSPC (17%) (Figure S2D). Furthermore, GPI-80$^+$ cells demonstrated enrichment in clones that remained largely undifferentiated or displayed myelo-lymphoid differentiation potential, as compared to GPI-80$^-$ HSPC clones that predominantly gave

rise to myeloid progeny in OP9M2 co-culture. These data imply that, although both GPI-80^+ and GPI-80^- HSPC possess multilineage differentiation ability in bulk culture, only GPI-80^+ HSPC display robust multipotency at clonal level.

In vitro expansion ability is restricted to GPI-80^+ HSPC

We next evaluated *in vitro* self-renewal ability of GPI-80^+ and GPI-80^- HSPC on OP9M2 stroma; we have previously shown that this mesenchymal stem cell (MSC)-like stroma line supports robust expansion of human fetal liver HSPC over 5 weeks and maintains transplantable HSC for over 2 weeks in culture (Magnusson et al., 2013). After 14 and 28 days, the differentiation status of GPI80^+ and GPI-80^- HSPC was assessed based on cell surface phenotype. Strikingly, only GPI-80^+ HSPC showed robust expansion of undifferentiated $CD34^+CD38^-CD90^+$ HSPC (>1000 fold in 4 weeks), of which a subpopulation continued to express GPI-80 (Figure 3.2A). In contrast, GPI-80^- cells had no ability to expand or maintain $CD34^+CD38^-CD90^+$ HSPC in culture. Quantification of total cell expansion showed that cultures seeded with GPI-80^- HSPC exhibited more limited proliferative potential than those seeded with GPI-80^+ cells. Altogether, these data indicate that the GPI-80^+ subpopulation is fully responsible for the *in vitro* expansion of undifferentiated HSPC.

Cell cycle analysis using BrdU incorporation in HSPC in OP9M2 co-culture (Figure 3.2B) revealed that both GPI-80^+ and GPI-80^- HSPC exhibit similar distribution between cell cycle phases, while $CD34^+CD38^-CD90^-$ cells exhibit a significant reduction of

cycling/S-phase cells. These data suggest that the poor expansion of GPI-80$^-$ HSPC in culture is not due to lower proliferation rate, but rather due to inability of GPI-80$^-$ HSPC to undergo self-renewal divisions to maintain/expand undifferentiated HSPC.

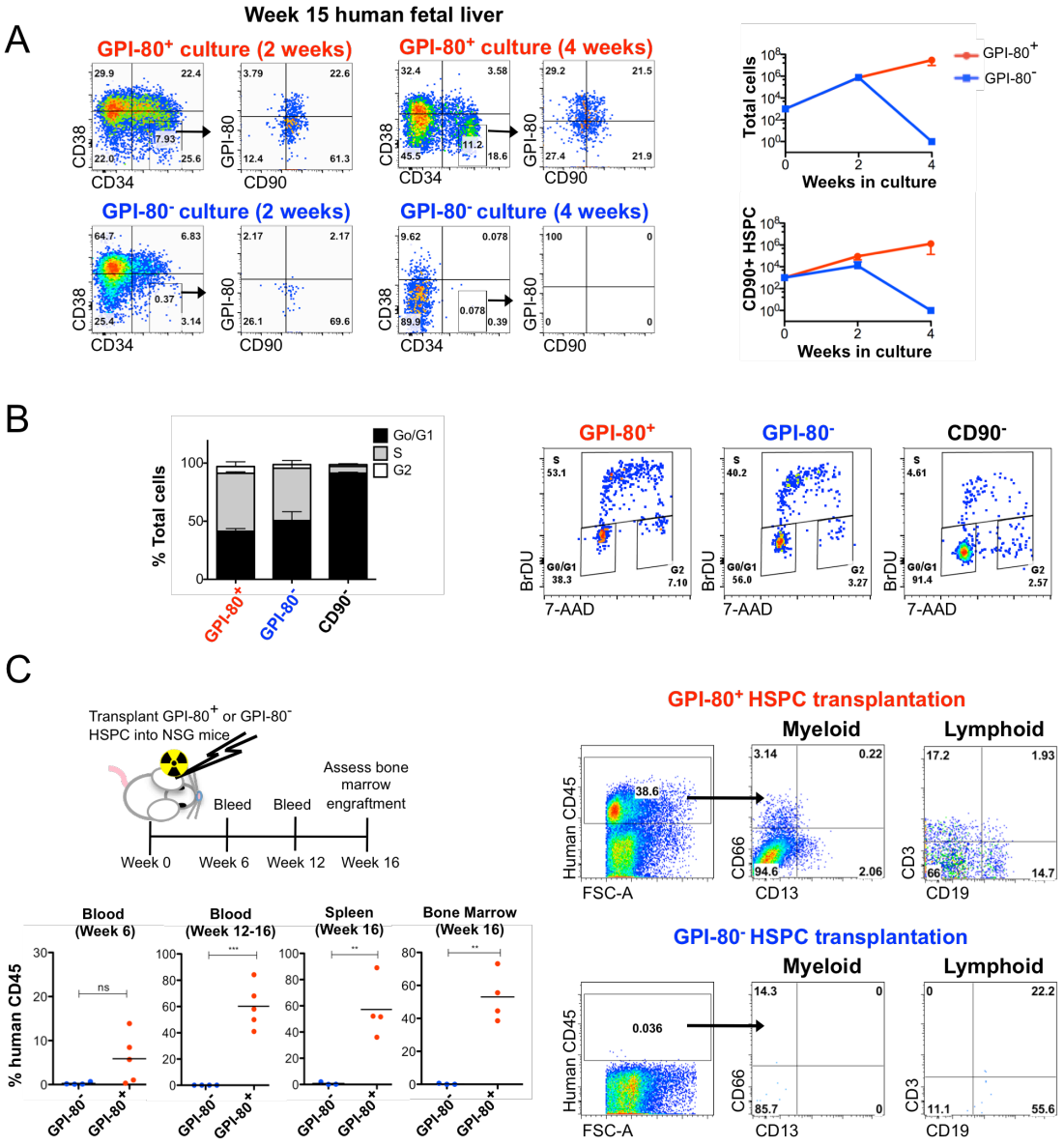

Figure 3.2: GPI-80 expression defines HSPC with self-renewal and engraftment ability

GPI-80 identifies *in vivo* engraftable fetal hematopoietic stem cells

To assess the *in vivo* engraftment and reconstitution ability of GPI-80$^+$ HSPC, xenotransplantation assays were performed. NSG mice were sublethally irradiated and transplanted with either GPI-80$^+$ or GPI-80$^-$ HSPC (respective populations originating from 50,000 CD34$^+$ cells) via tail vein injection (Figure 3.2C). Mice were bled retro-orbitally at 6 weeks and 12-16 weeks to track peripheral blood reconstitution, and the hematopoietic organs were assessed for human engraftment at 16 weeks. Robust populations of human CD45$^+$ cells were detected in peripheral blood of all mice transplanted with GPI-80$^+$ HSPC. The average human CD45$^+$ bone marrow chimerism of GPI-80$^+$ transplants after 16 weeks was 53.0%; of total cells, CD13$^+$or CD66$^+$ myeloid cells constituted 16.7%, CD19$^+$ B cells 26.9% and CD3$^+$ T-cells 1.4% (Table S3). In contrast, GPI-80$^-$ HSPC transplants did not yield detectable cells at any time-point. These results indicate that only the GPI-80$^+$ population of human fetal liver HSPC displays capacity for *in vivo* engraftment and multilineage hematopoietic reconstitution.

GPI-80 expression can be used to track self-renewing HSPC throughout early human development

We next assessed whether GPI-80 expression marks undifferentiated HSPC also in fetal bone marrow, which becomes colonized after the fetal liver. FACS analysis demonstrated the presence of a distinct population of GPI-80$^+$ HSPC in the fetal bone marrow by 15 weeks of development. *In vitro* expansion assays revealed that also in fetal bone marrow,

only the GPI-80 expressing HSPC harbor *in vitro* expansion ability, whereas GPI-80$^-$ HPSC are progenitors that are not sustained in culture (Figure 3.3A).

To assess GPI-80 expression in first trimester hematopoietic tissues, fetal livers between 7 and 10 weeks were analyzed. FACS analysis showed the presence of GPI-80$^+$ HSPC in fetal liver also earlier during human development (Figures S3A and 3.3B). Analysis of *in vitro* expansion ability of 10 week fetal liver HSPC sorted based on GPI-80 confirmed that, similar to the second trimester fetal liver and bone marrow, *in vitro* self-renewal capacity was restricted to GPI-80$^+$ HSPC (Figure S3A). In contrast, 8-10 week bone marrow showed absence of GPI-80$^+$ HSPC (n=4, Figure 3.3B). Even though CD34$^+$CD38$^-$CD90$^+$ cells were present in the bone marrow and a subset of them expressed the pan-hematopoietic marker CD45, there was no expansion of CD34$^+$ cells in culture (data not shown), consistent with the concept that *in vitro* expansion potential is restricted to GPI-80$^+$ HSPC.

Expression analysis of CD45 and GPI-80 indicated that both in fetal liver and bone marrow, GPI-80$^+$ cells were confined to the hematopoietic population (CD34$^+$CD45$^+$) (Figure S3B). Thus, unlike many other established HSC markers, GPI-80 expression can distinguish HSPC from endothelium.

To determine whether GPI-80 is expressed and similarly restricted to hematopoietic cells at a site of HSPC emergence, first trimester human placentas were analyzed. The first GPI-80$^+$ HSPC appeared in the placenta between 4 and 5 weeks of development; by 5

weeks in development, a robust population of GPI-80$^+$ HSPC was reproducibly observed (Figure 3.3C). Moreover, co-staining for CD45 showed that GPI-80 expression is restricted to the hematopoietic population also in the placenta. Coinciding with the presence of a GPI-80$^+$ HSPC, cultured CD34$^+$ cells from derived from 5 week placenta maintained undifferentiated HSPC, many of which co-expressed GPI-80 (Figure 3.3C).

In summary, analysis of fetal hematopoietic tissues during early human development indicates that in all niches studied, GPI-80 expression correlates with the acquisition of HSPC high proliferative potential, and can be used to track the migration of HSPC from the human placenta to fetal liver during early first trimester, and, eventually, to fetal bone marrow by the beginning of the second trimester (Figure 3.3D).

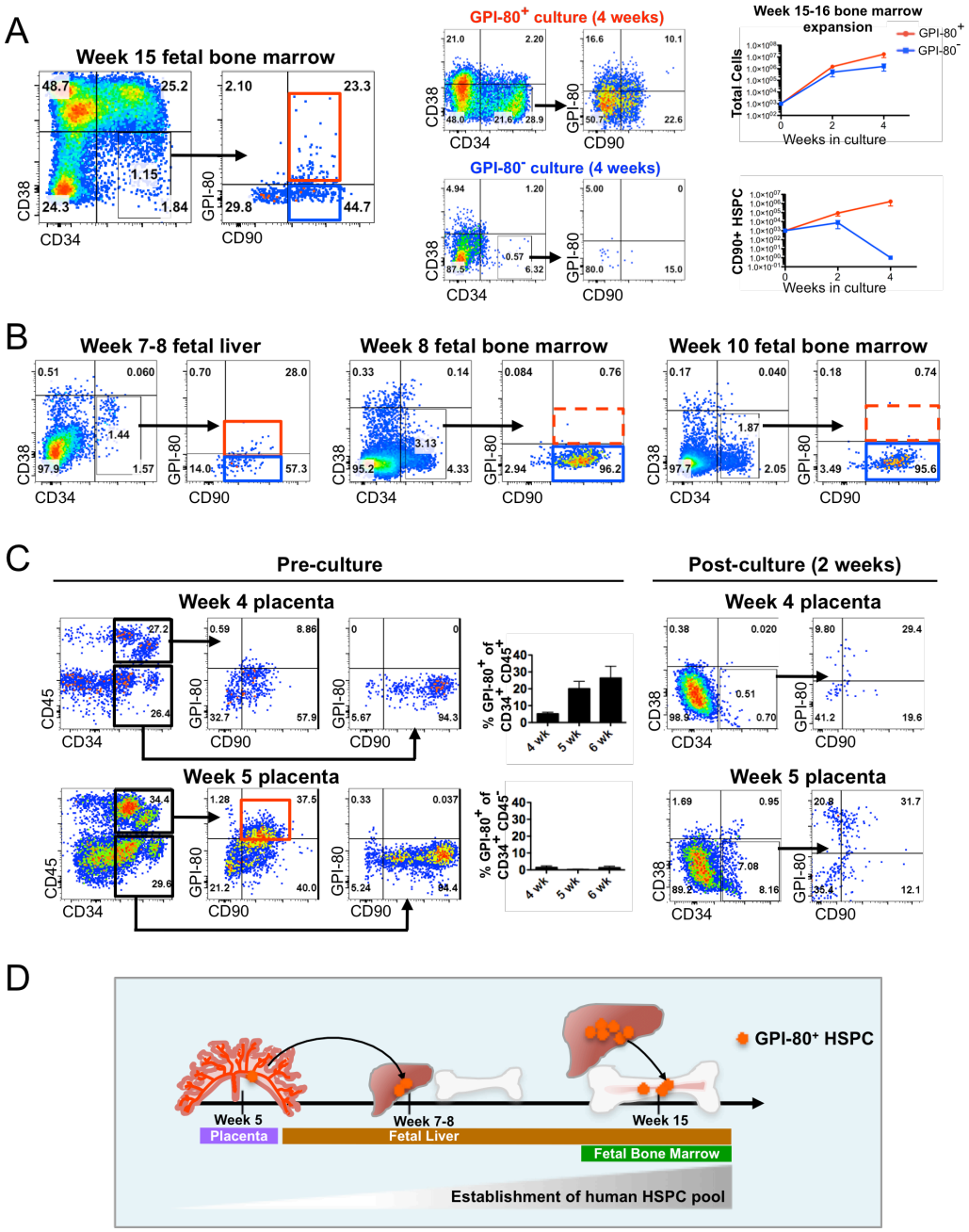

Figure 3.3: GPI-80 tracks self-renewing HSPC during human development

GPI-80 and ITGAM are critical for fetal HSPC expansion

To provide insights into the mechanisms of how human fetal HSC sustain self-renewal and expansion, Affymetrix microarray analysis was performed to identify genetic networks enriched in GPI-80$^+$ as compared to their immediate progeny. Q-Q probability plot reveals remarkable similarity between GPI-80$^+$ and GPI-80$^-$ HSPC (Figure 3.4A), in contrast to the more obvious differences observed when comparing CD90$^+$ HSPC and downstream HPC (Figure 3.1C). Similar expression levels of known transcription factors governing HSC specification (*TAL1/SCL, LMO2, RUNX1/AML, MYB*) and maintenance (*MLL1, MYC, SMAD4, HOXB4, HOXA9, BMI1, GFI1, ETV6/TEL* etc.; Figure 3.4B) or lineage commitment (*PU.1, BCL11A, CEPBA, GATA1, IKAROS* etc.; Figure 3.4C) was observed, indicating that GPI-80$^-$ HSPC have not yet committed to specific downstream fates. Only 574 genes were found to be upregulated on GPI-80$^+$ HSPC while 246 genes were downregulated (> 2 fold, $p<0.05$; Table S4). Of the top 20 differentially expressed annotated genes, three were transcription factors or other nuclear proteins (*HIF3α, TOB1, KLF4*) with no previously described function in HSC.

The second most highly upregulated transcript was ITGAM (Integrin α-M) (Figure 3.4D), an α integrin component of the MAC-1 complex. ITGAM is known to co-localize with GPI-80 on neutrophils, enabling leukocyte adherence and extravasation (Huang et al., 2004). Flow cytometry of fetal liver and placental HSPC demonstrated robust co-expression of ITGAM on GPI-80$^+$ HSPC (Figure 3.4E). ImageStream analysis was used

to define the localization of ITGAM relative to GPI-80 on GPI-80^{+} HSPC surface; distinct regions of co-localization between GPI-80 and ITGAM were visualized, as previously described on neutrophils (Huang et al., 2004). In contrast, there was only limited co-localization between GPI-80 and CD90, another GPI-anchored surface protein (Figure 3.4F). These data suggested that GPI-80 and ITGAM may function together also in HSC.

To assess whether GPI-80 and/or ITGAM are functionally required for maintaining HSC properties, lentiviral-mediated shRNA knockdown of GPI-80 and ITGAM was performed on fetal liver CD34^{+} cells. FACS analysis and q-RT-PCR confirmed a reduction of GPI-80 and ITGAM by 1 week in culture (Figure S4). Moreover, knockdown of either protein lead to progressive loss of the undifferentiated HSPC on OP9M2 stroma (Figure 3.4G). Collectively, these data suggest that GPI80 and ITGAM are not only markers for the highly self-renewing fetal HSC, but also required for their proper function.

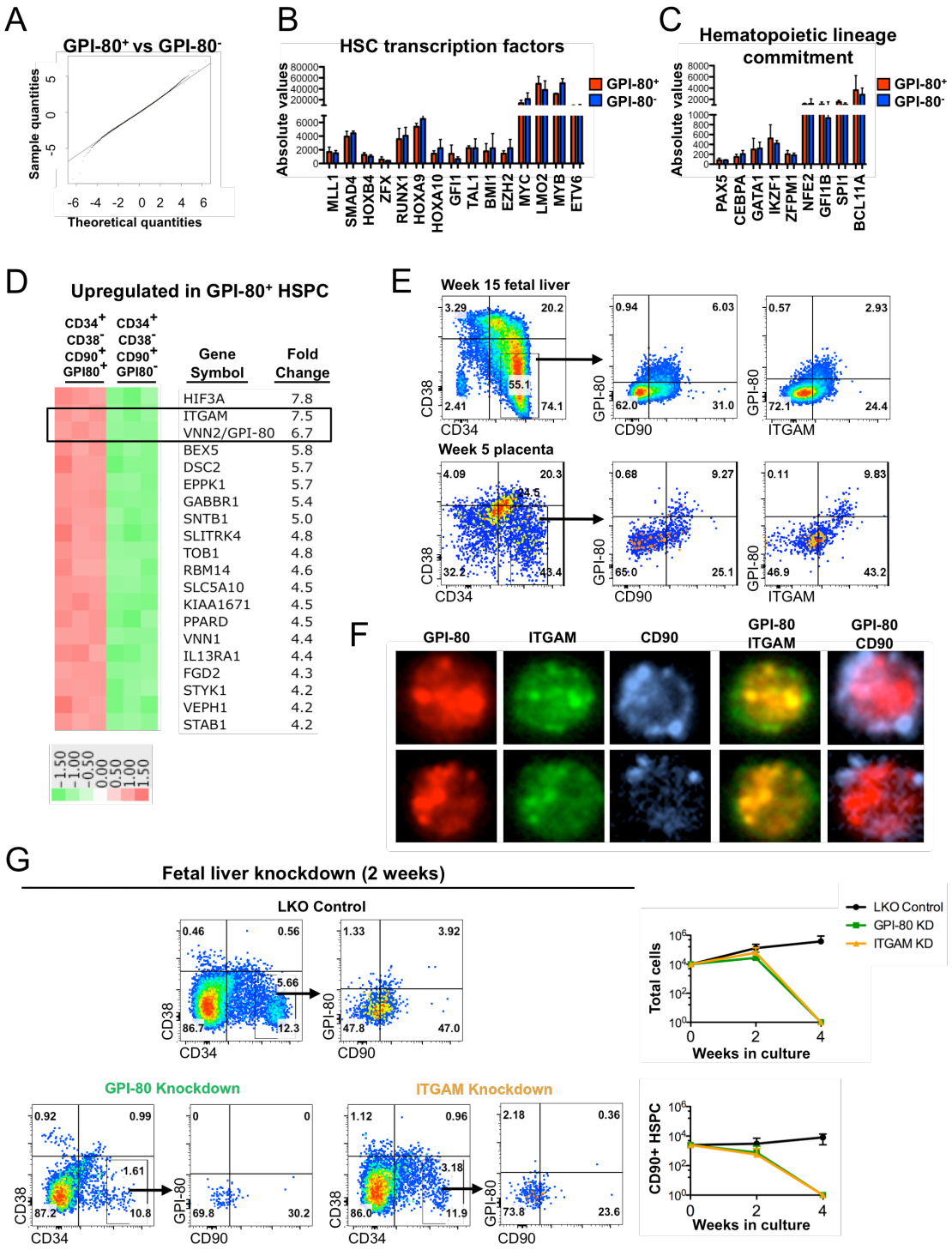

Figure 3.4: GPI-80 and ITGAM are required for the maintenance of undifferentiated HSPC

Discussion

Uncovering the identity and regulation of the self-renewing HSC as they emerge and expand during embryogenesis is of paramount significance, both for the understanding of the fundamental mechanisms governing "stemness", and for bringing pluripotent stem cell derivatives toward clinical applications. Our work identified GPI-80 as a novel surface protein that demarcates the HSC lineage from non-self-renewing progenitors during human development. Although the GPI-80$^-$ subset of HSPC also expresses other established HSC surface markers (e.g. CD34$^+$, CD90$^+$, CD38$^-$) and exhibits striking similarity with GPI-80$^+$ HSPC in global gene expression, they are profoundly different functionally by lacking the ability to self-renew and engraft.

In contrast to CD34 and CD90 that, similar to many other HSC markers, are even more highly expressed in the endothelium than in HSC, GPI-80 expression was observed only after HSPC have been specified from hemogenic endothelium and co-express the pan-hematopoietic marker CD45. GPI-80$^+$ HSPC first appear in the human placenta by 5 weeks of development, which parallels the time of HSC emergence in mouse placenta (E11.5) (Gekas et al., 2005). Analysis of GPI-80 expression at different stages and anatomical sites during human development revealed a remarkable correlation with GPI-80 expression and with the capacity to expand undifferentiated HSPC in MSC stroma niche, and ultimately engraft *in vivo*. In contrast, presence of CD45$^+$ hematopoietic cells expressing CD34$^+$ and CD90$^+$, in absence of GPI-80, was not an accurate predictor of

HSPC with high proliferative potential in the placenta or fetal bone marrow. Thus, GPI-80 expression provides a unique tool for temporal and spatial tracking of the self-renewing HSPC as they migrate between fetal hematopoietic tissues.

Notably, our studies show that GPI-80 is not expressed in hemogenic endothelial precursors isolated from embryoid bodies during human ES cell differentiation; however, GPI-80 can be induced in a subset of $CD34^{+}CD38^{-}CD90^{+}CD45^{+}$ cells during their developmental maturation on OP9M2 stroma (Dou, Mikkola, manuscript in preparation). The finding that GPI-80 expression can be detected in PSC derived HPC that are defective in self-renewal implies that GPI-80 expression is necessary, but not sufficient, for self-renewal ability. Nevertheless, GPI-80 now represents an attractive candidate to track the appearance and developmental maturation of PSC-derived HSC precursors.

An intriguing property of GPI-80 as compared to many other known HSC surface markers is that it is also functionally required for HSC self-renewal; this observation opens new avenues for future studies to understand the self-renewal mechanisms utilized during human development. Although GPI-80 does not possess an intracellular domain that could convey a signal from the niche to sustain HSC self-renewal, it associates with the Mac1 (CR3) integrin complex that consists of ITGAM/CD11b and ITGB2/CD18, which in leukocytes co-operate with GPI-80 to mediate their migration and extravasation (Huang et al., 2004). Mac1 is also expressed on mouse fetal hematopoietic stem cells (Morrison, Hemmati, Wandycz, & Weissman, 1995) and down-regulated in adult bone marrow HSC (Morrison & Weissman, 1994). Our finding that GPI-80 and ITGAM are

co-expressed and co-localize on highly self-renewing human fetal HSPC, and that disruption of the expression of either leads to loss of undifferentiated HSPC, implies that they function together to protect HSC. These findings introduce the unanticipated concept that HSC, the most undifferentiated cells in hematopoietic hierarchy, utilize mechanisms employed by terminally differentiated leukocytes during immune response, for maintaining "stemness".

In stark contrast to the profound functional differences between GPI-80^+ versus GPI-80^- HSPC, gene expression profiling showed striking similarity in overall gene expression, including the fundamental hematopoietic programs known to be essential for HSC specification and function. Nevertheless, our analysis uncovered unique differentially expressed genes that are novel candidates for governing HSC self-renewal. As an example, HIF3-α, a transcription factor whose expression also declines during culture (Magnusson et al., 2013) when HSPC begin to lose their functional properties, was the most differentially expressed gene between GPI-80^+ and GPI-80^- HSPC. We believe that deciphering the function of the genes upregulated in highly self-renewing GPI-80^+ fetal HSC will provide an invaluable resource for dissecting the genetic programs that govern "stemness" in HSC. Inducing these programs in human ES and iPSC-derived HSPC may bring us closer to creating self-renewing HSC *in vitro* for clinical applications.

Acknowledgements

The authors thank the FACS Core facilities at BSCRC and JCCC at UCLA, and Children's Hospital Los Angeles, for assistance with cell sorting and Imagestream analysis; the UCLA Clinical Microarray Core for performing the microarray analysis; UCLA Warren hall staff for outstanding animal care; and UCLA Tissue and Pathology Core and Novogenix LLC for provision of human hematopoietic tissue. This work was supported by the NIH RO1 HL097766, CIRM New Faculty Award RN1-00557-1 and Leukemia & Lymphoma Society (LLS) Scholar awards for H.K.A.M. S.L.P. was supported by the Howard Hughes Medical Institute Gilliam fellowship. C.Y. was supported by the Howard Hughes Undergraduate Research scholarship. V.C was supported by LLS Special Fellow Award. M.M. was supported by the Swedish Research Council and Tegger Foundation.

Authorship:

Contributions: S.L.P., C.Y., V.C., M.M. and H.K.A.M. designed experiments. S.L. P., C.Y., V.C., J.K., R.S. and M.M. performed experiments. S.L.P., C.Y., V.C and H.K.A.M. wrote the manuscript, which all authors edited and approved.

Conflict-of-interest disclosure: M.M. is a cofounder of and own significant financial stakes in Novogenix Laboratories, LLC. The remaining authors declare no competing financial interests.

EXPERIMENTAL PROCEDURES

Ethical statement. Experimental protocols involving mice were reviewed and approved by the UCLA Animal Research Committee (Protocol number 2005-109). Fetal hematopoietic tissues were discarded material devoid of personal identifiers obtained from elective terminations performed by Family Planning Associates or UCLA Medical Center. All material was used with written informed consent.

Tissues, cell culture and hematopoietic assays. *In vitro* cell expansion was performed on OP9M2 stroma with the addition of SCF, Flt3-l and TPO, each at 25ng/ml. B and T cell assays were performed on OP9M2 and OP9DL1 respectively, in the presence of SCF 25 ng/ml, Flt3-l 10 ng/ml and IL-7 20ng/ml (Invitrogen). Fetal liver, placenta, bone marrow and peripheral blood processing and transplantation are described in supplemental material.

Lentiviral shRNA knockdown. pLKO lentiviral vectors from the TRC library (TRCN0000158666 and TRCN0000029051, Open Biosystems) were produced and transduced in fetal liver $CD34^+$ cells as described in supplemental material.

Graphical and Statistical Analysis. Graphs were generated and statistics were analyzed using GraphPad Prism software. Student's t tests were used to calculate p values.

Gene expression, FACS analysis and Image Stream: see supplemental material.

REFERENCES

Alvarez-Silva, M., Belo-Diabangouaya, P., Salaün, J., & Dieterlen-Lièvre, F. (2003). Mouse placenta is a major hematopoietic organ. Development, 130(22), 5437–44.

Balazs, A. B., Fabian, A. J., Esmon, C. T., & Mulligan, R. C. (2006). Endothelial protein C receptor (CD201) explicitly identifies hematopoietic stem cells in murine bone marrow. Blood, 107(6), 2317–21.

Baum, C. M., Weissman, I. L., Tsukamoto, A. S., Buckle, A. M., & Peault, B. (1992). Isolation of a candidate human hematopoietic stem-cell population. Proc Natl Acad Sci USA, 89(7), 2804–8.

Bordignon, C. (2006). Stem-cell therapies for blood diseases. Nature, 441(7097), 1100–2.

Ciriza, J., Thompson, H., Petrosian, R., Manilay, J. O., & García-Ojeda, M. E. (2013). The migration of hematopoietic progenitors from the fetal liver to the fetal bone marrow: lessons learned and possible clinical applications. Exp Hemat, 41(5), 411–23.

Dehn, J., Arora, M., Spellman, S., Setterholm, M., Horowitz, M., Confer, D., & Weisdorf, D. (2008). Unrelated donor hematopoietic cell transplantation: factors associated with a better HLA match. Biol Blood Marrow Transplant, 14(12), 1334–40.

Dravid, G. G., & Crooks, G. M. (2011). The challenges and promises of blood engineered from human pluripotent stem cells. Adv Drug Deliv Rev, 63(4-5), 331–41.

Eilken, H. M., Nishikawa, S.-I., & Schroeder, T. (2009). Continuous single-cell imaging of blood generation from haemogenic endothelium. Nature, 457(7231), 896–900.

Gekas, C., Dieterlen-Lièvre, F., Orkin, S. H., & Mikkola, H. K. A. (2005). The placenta is a niche for hematopoietic stem cells. Dev Cell, 8(3), 365–75.

Holyoake, T. L., Nicolini, F. E., Eaves, C. J.(1999), Functional differences between transplantable human hematopoietic stem cells from fetal liver, cord blood, and adult marrow. Exp Hemat, Sep;27(9):1418-27

Huang, J.-B., Takeda, Y., Araki, Y., Sendo, F., & Petty, H. R. (2004). Molecular proximity of complement receptor type 3 (CR3) and the glycosylphosphatidylinositol-linked protein GPI-80 on neutrophils: effects of cell adherence, exogenous saccharides, and lipid raft disrupting agents. Mol immunol, 40(17), 1249–56.

Lancrin, C., Sroczynska, P., Stephenson, C., Allen, T., Kouskoff, V., & Lacaud, G. (2009). The haemangioblast generates haematopoietic cells through a haemogenic endothelium stage. Nature, 457(7231), 892–5.

Larochelle A, Savona M, Wiggins M, Anderson S, Ichwan B, Keyvanfar K, Morrison SJ, Dunbar CE. (2011). Human and rhesus macaque hematopoietic stem cells cannot be purified based only on SLAM family markers. Blood, 117(5):1550-4.

Magnusson, M., Sierra, M. I., Sasidharan, R., Prashad, S. L., Romero, M., Saarikoski, P., Van Handel, B., Huang, A., Li, X., & Mikkola, H. K. A. (2013). Expansion on stromal cells preserves the undifferentiated state of human hematopoietic stem cells despite compromised reconstitution ability. PloS One, 8(1), e53912.

Matsubara, A., Iwama, A., Yamazaki, S., Furuta, C., Hirasawa, R., Morita, Y., Osawa, M., Motohashi, T., Eto, K., Ema, H., Kitamura, T., Vestweber, D., & Nakauchi, H.

(2005). Endomucin, a CD34-like sialomucin, marks hematopoietic stem cells throughout development. J Exp Med, 202(11), 1483–92.

Mayani, H., & Lansdorp, P. M. (1994). Thy-1 expression is linked to functional properties of primitive hematopoietic progenitor cells from human umbilical cord blood. Blood, 83(9), 2410–7.

McKinney-Freeman, S., Cahan, P., Li, H., Lacadie, S. A., Huang, H.-T., Curran, M., Loewer, S., Naveiras, O., Kathrein, K., Konantz, M., Langdon, E., Lengerke, Zon, L., Collins, J., & Daley, G. Q. (2012). The transcriptional landscape of hematopoietic stem cell ontogeny. Cell stem cell, 11(5), 701–14.

Mikkola, H. K. A., & Orkin, S. H. (2006). The journey of developing hematopoietic stem cells. Development, 133(19), 3733–44.

Morrison, S. J., Hemmati, H. D., Wandycz, A. M., & Weissman, I. L. (1995). The purification and characterization of fetal liver hematopoietic stem cells. Proc Natl Ac Sci USA, 92(22), 10302–6.

Morrison, S. J., Uchida, N., & Weissman, I. L. (1995). The biology of hematopoietic stem cells. Annu Rev Cell Dev Biol, 11, 35–71.

Morrison, S. J., & Weissman, I. L. (1994). The long-term repopulating subset of hematopoietic stem cells is deterministic and isolatable by phenotype. Immunity, 1(8), 661–73.

Nakano, T., Kodama, H., & Honjo, T. (1994). Generation of lymphohematopoietic cells from embryonic stem cells in culture. Science, 265(5175), 1098–1101.

Rhodes, K. E., Gekas, C., Wang, Y., Lux, C. T., Francis, C. S., Chan, D. N., Conway, S., Orkin, S., Yoder, M., & Mikkola, H. K. A. (2008). The emergence of hematopoietic

stem cells is initiated in the placental vasculature in the absence of circulation. Cell stem cell, 2(3), 252–63.

Risueño, R. M., Sachlos, E., Lee, J.-H., Lee, J. B., Hong, S.-H., Szabo, E., & Bhatia, M. (2012). Inability of human induced pluripotent stem cell-hematopoietic derivatives to downregulate microRNAs in vivo reveals a block in xenograft hematopoietic regeneration. Stem cells, 30(2), 131–9.

Robin, C., Bollerot, K., Mendes, S., Haak, E., Crisan, M., Cerisoli, F., Lauw, I., Kaimakis, P.,Jorna, R., Vermeulen, M., Kayser, M., van der Linden, R., Imanirad, P., Verstegen, M., Nawaz-Yousaf, H., Papazian, N., Steegers, E., Cupedo, T., & Dzierzak, E. (2009). Human placenta is a potent hematopoietic niche containing hematopoietic stem and progenitor cells throughout development. Cell stem cell, 5(4), 385–95.

Schmitt, T. M., & Zúñiga-Pflücker, J. C. (2002). Induction of T cell development from hematopoietic progenitor cells by delta-like-1 in vitro. Immunity, 17(6), 749–56.

Shenoy, S. (2013). Umbilical cord blood: an evolving stem cell source for sickle cell disease transplants. Stem Cells Transl Med, 2(5), 337–40.

Suzuki, K., Watanabe, T., Sakurai, S.-i., Ohtake, K., Kinoshita, T., Araki, A., Fujita, T., Takei, H., Takeda, Y., Sato, Y., et al. (1999). A Novel Glycosylphosphatidyl Inositol-Anchored Protein on Human Leukocytes: A Possible Role for Regulation of Neutrophil Adherence and Migration. J Immunol 162, 4277-4284.

Tavian, M., Biasch, K., Sinka, L., Vallet, J., & Péault, B. (2010). Embryonic origin of human hematopoiesis. Int J Dev Biol, 54(6-7), 1061–5.

Tavian, M. & Péault, B. (2005). Embryonic development of the human hematopoietic system. Int J Dev Biol, 49(2-3):243-50.

Van Handel, B., Prashad, S. L., Hassanzadeh-Kiabi, N., Huang, A., Magnusson, M., Atanassova, B., Chen, A., Hamalainen, E., & Mikkola, H. K. A. (2010). The first trimester human placenta is a site for terminal maturation of primitive erythroid cells. Blood, 116(17), 3321–30.

Weissman, I. L. (2000). Stem cells: units of development, units of regeneration, and units in evolution. Cell, 100(1), 157–68.

FIGURE LEGENDS

Figure 3.1. A subpopulation of human fetal liver hematopoietic stem and progenitor cells express GPI-80/VNN2

A. Representative flow cytometry plot of human hematopoietic populations from week 15 fetal liver with surface markers CD34, CD38, and CD90. **B.** Analysis of human hematopoietic engraftment in the bone marrow of NSG mice by pan-hematopoietic marker CD45 ($p<0.01$). **C.** Quantile-Quantile plots comparing differentially expressed genes between P1 ($CD38^-CD90^+$) vs. P2 ($CD38^-CD90^-$), and P1 ($CD38^-CD90^+$) vs. P3 ($CD38^+CD90^-$). **D.** Top 20 cell surface proteins upregulated in $CD34^+CD38^-CD90^+$ HSPC vs. $CD34^+CD38^-CD90^-$ HPC. **E.** Quantitative RT-PCR of GPI-80 mRNA in $CD34^+CD38^-CD90^+$ population as compared to $CD34^+CD38^-CD90^-$ and $CD34^+CD38^+CD90^-$ cells ($p<0.01$). **F.** Representative flow cytometry plot of CD34+ enriched cells from 15 week developmental age human fetal liver (n=3) stained for CD34, CD38, CD90 and GPI-80.

Figure 3.2. GPI-80 expression defines HSPC with self-renewal and engraftment ability

A. *In vitro* self-renewal/expansion assay of GPI-80^+ and GPI-80^- HSPC co-cultured on OP9M2 stroma and analyzed at 2 and 4 weeks for the presence of undifferentiated HSPC is shown. Growth curves of total cellular expansion and expansion $CD34^+CD38^-CD90^+$ population on OP9M2 are shown (n=3). Representative flow cytometry plots of hematopoietic populations after 2 and 4 weeks of co-culture on OP9M2 stroma are

shown. **B.** Cell cycle analysis of FACS sorted fetal liver HSPC cultured on OP9M2 overnight and pulsed with BRDU is shown (n=3). Representative flow cytometry plots assessing BRDU incorporation in GPI^{-}80^{+} and GPI^{-}80^{-} cells are shown. **C.** Scheme of transplant assay for analysis of engraftment ability of GPI-80^{+} and GPI-80^{-} HSPC**.** Flow cytometry analysis of human hematopoietic engraftment in peripheral blood, spleen, and bone marrow of mice transplanted with GPI-80^{+} and GPI-80^{-}HSPC from human fetal liver is shown ($p<0.01$).

Figure 3.3. GPI-80 tracks self-renewing HSPC during human development

A. Representative flow cytometry plot of 15 week human fetal bone marrow with CD34, CD38, CD90 and GPI-80 is shown. Representative FACS plots and growth curves of cultured GPI-80^{+} and GPI-80^{-} HSPC from fetal bone marrow are shown (n=3). **B**. Representative flow cytometry plots of 7-8 week human fetal liver, 8 week human bone marrow, and 10 week human bone marrow cells with CD34, CD38, CD90 and GPI-80 are shown. **C.** Representative flow cytometry plots of 4 and 5 week placenta stained with CD34, CD45, CD90 and GPI-80 are shown. Frequencies of GPI-80^{+} HSPC of placental hematopoietic and endothelial populations at different stages are shown (n=3 4 wk placentas, n=3 5 wk placentas, and n=2 6 wk placentas). Representative flow cytometry plots of CD34^{+} placental cells after 2 week in culture on OP9M2 are shown. **D**. Model of timeline of emergence of GPI-80^{+} HSPC in the placenta and migration of GPI-80^{+} HSPC from the fetal liver into the fetal bone marrow is shown.

Figure 3.4. GPI-80 and ITGAM are required for the maintenance of undifferentiated HSPC

A. Quantile-quantile plot comparing differentially expressed genes between GPI-80^{+} and GPI-80^{-} HSPC is shown. **B.** Bar graphs showing the relative expression of transcription factors required for the development or maintenance of hematopoietic stem cells**. C.** Bar graphs showing the relative expression of transcription factors responsible for lineage commitment. **D.** Heat map illustrating top 20 annotated genes significantly and consistently up-regulated among replicates (n=3, p=0.05) in GPI-80^{+} HSPC. **E**. Representative 15 week fetal liver and 5 week placental tissue stained for CD34, CD38, CD90, GPI-80 and ITGAM are shown (placenta gated on CD45+). **F.** Representative ImageStream images of 15 week CD34^{+} fetal liver cells stained for CD90, GPI-80 and ITGAM are shown. **G.** Representative flow cytometry plots of CD34^{+} cell after lentiviral knockdown of GPI-80 or ITGAM are shown. Quantification of expansion of total cells and HSPC population after knockdown of GPI-80 or ITGAM are shown (n=3).

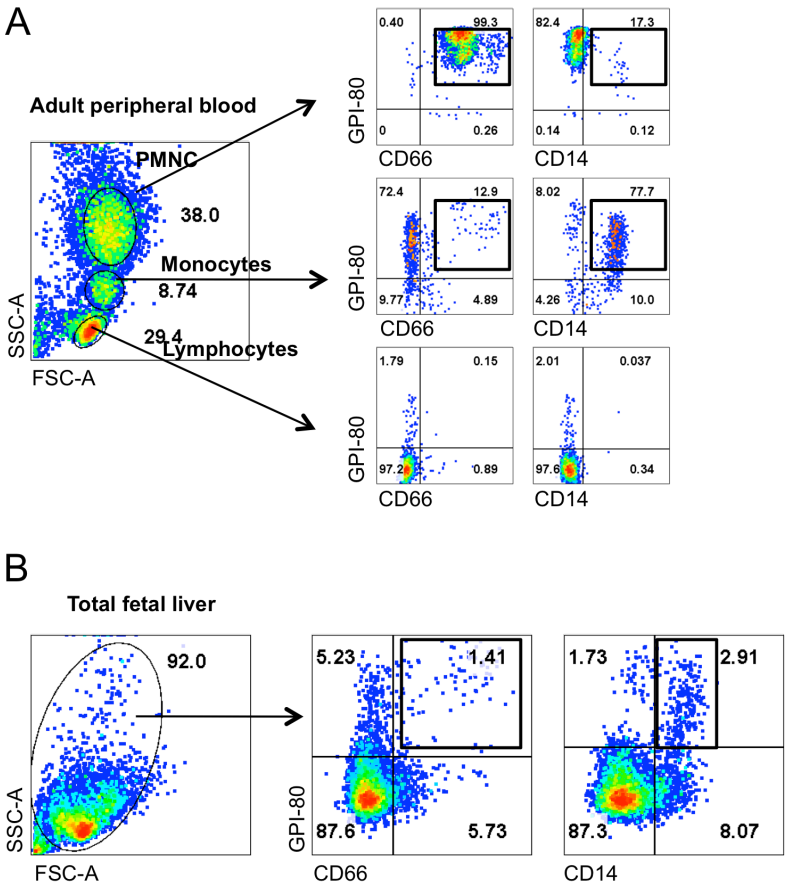

Figure S1. GPI-80 expression in myeloid cells. A. Representative flow cytometry plot of adult peripheral blood with CD66, CD14 and GPI-80 is shown, verifying expression of GPI-80 in adult peripheral blood myeloid cells. Cells gated from CD45+CD34- population. **B**. Representative flow cytometry plot from second trimester fetal liver with CD66, CD14 and GPI-80 is shown, documenting expression on fetal myeloid cells. Cells gated from CD45+CD34- population.

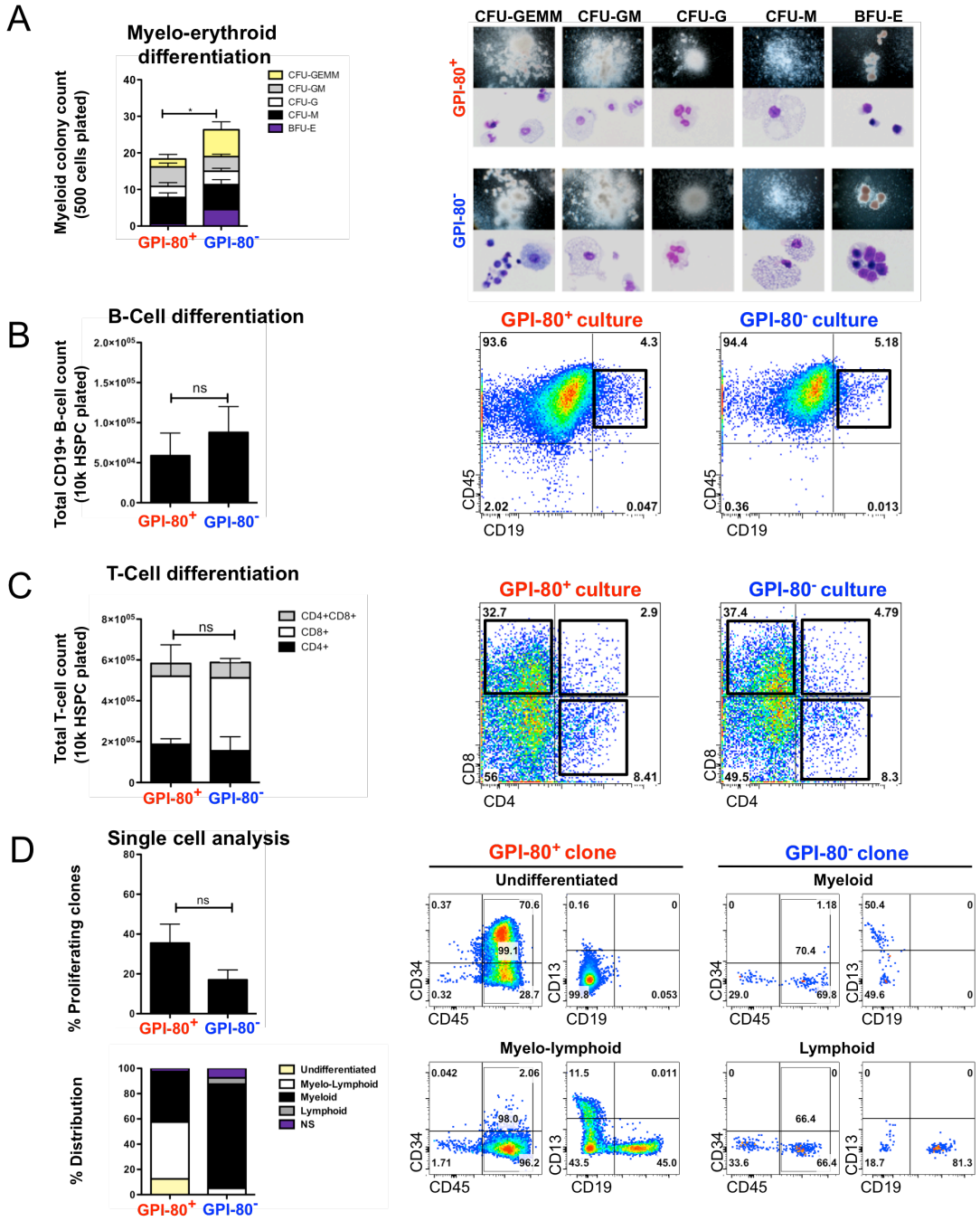

Figure S2. Multipotency of GPI-80⁺ HSPC. A. Myelo-erythroid differentiation potential of GPI-80⁺ and GPI-80⁻ HSPC on methylcellulose assay is shown (n=6, p=<0.05). **B.** Flow cytometry analysis for B-cell marker CD19 on GPI-80⁺ and GPI-80⁻ HSPC after 2 weeks on OP9M2 is shown (n=3). **C.** Flow cytometry analysis of T cell markers CD4 and CD8 after 2 weeks of HSPC culture on OP9-Dll1 (n=3). **D.** Myeloid and lymphoid potential of GPI-80⁺ and GPI-80⁻ HSPC at the single cell level is shown. Quantification of proliferating clones (defined as >200 cells, n=2 donors), distribution of clone types (40 clones analyzed), and representative clones from GPI-80⁺ and GPI-80⁻ HSPC after two weeks of culture on OP9M2 are shown. Though bulk cultures demonstrate multilineage potential of GPI-80⁻ HSPC, single cell analysis reveals enrichment of multipotential cells in the GPI-80⁺ population.

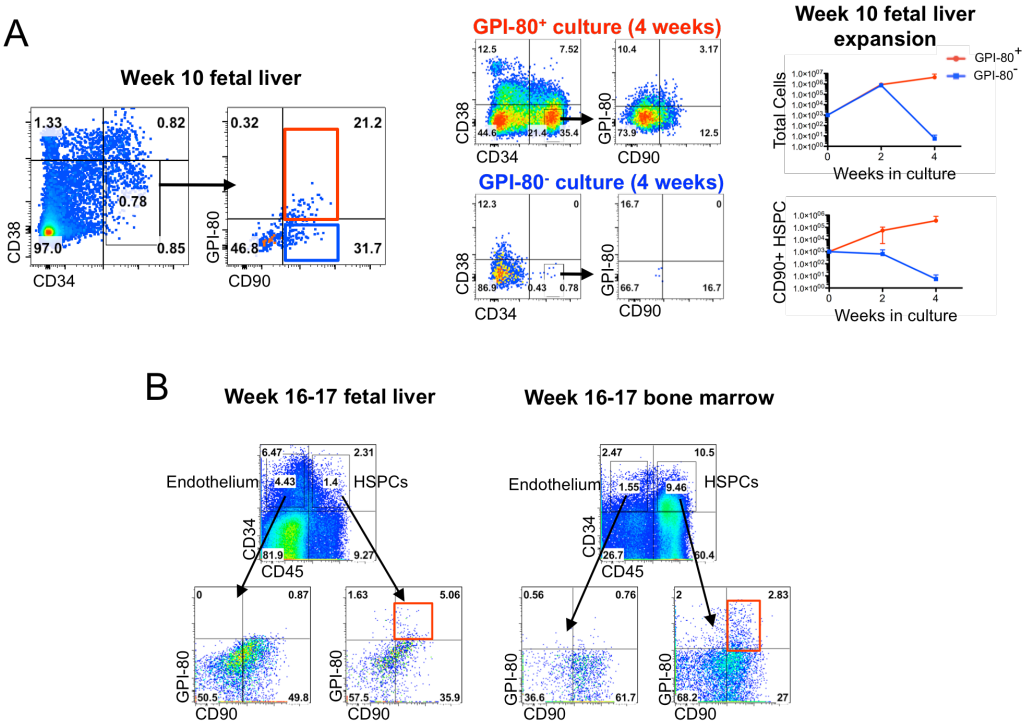

Figure S3. GPI-80 expression in fetal hematopoietic sites. A. Representative flow cytometry plot of week 10 fetal liver with CD34, CD38, CD90 and GPI-80 is shown. Representative FACS plots and growth curves of cultured GPI-80$^+$ and GPI-80$^-$ HSPCs from week 10 fetal liver are shown, documenting the association of GPI-80 with long-term self-renewal in first trimester tissue (n=3). **B.** Representative flow cytometry plots of second trimester total fetal liver and fetal bone marrow with CD45, CD34, CD90 and GPI-80 is shown, documenting that GPI-80 is largely restricted to the hematopoietic population.

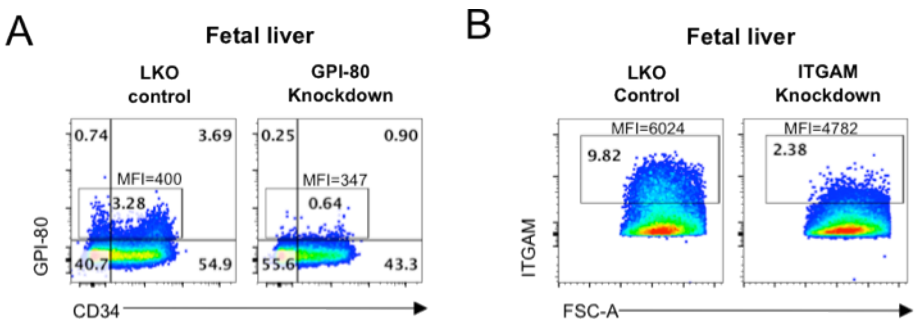

Figure S4. Lentiviral shRNA knockdown of GPI-80 and ITGAM. Representative flow cytometry plot of GPI-80 **(A)** and ITGAM **(B)** one week after lentiviral infection, documenting reduction of GPI-80 and ITGAM protein on the cell surface.

Table S1. Human engraftment in bone marrow of NSG mice transplanted with $CD90^+$ and $CD90^-$ HSPC

Mouse Number	Population transplanted (human fetal liver cells)	Percent CD45 engraftment (bone marrow)
1	$CD34^+CD38^-CD90^+$	35.3
2	$CD34^+CD38^-CD90^+$	69.9
3	$CD34^+CD38^-CD90^+$	56.8
4	$CD34^+CD38^-CD90^-$	0.3
5	$CD34^+CD38^-CD90^-$	0.1
6	$CD34^+CD38^-CD90^-$	0.1
7	$CD34^+CD38^+CD90^-$	0
8	$CD34^+CD38^+CD90^-$	0
9	$CD34^+CD38^+CD90^-$	0

Table S3. Human engraftment in bone marrow of NSG mice transplanted with GPI-80$^+$ and GPI-80$^-$ HSPC

Mouse Number	Population Transplanted (human fetal liver cells)	Percent CD45 Engraftment in Bone Marrow	Percent CD13$^+$,CD66$^+$ (of total cells)	Percent CD19$^+$ (of total cells)	Percent CD3$^+$ (of total cells)
1	CD34$^+$CD38$^-$ CD90$^+$GPI80$^+$	55.6	27.1	19.0	0.7
2	CD34$^+$CD38$^-$ CD90$^+$GPI80$^+$	44.6	17.1	19.1	1.0
3	CD34$^+$CD38$^-$ CD90$^+$GPI80$^+$	73.2	16.3	51.3	3.2
4	CD34$^+$CD38$^-$ CD90$^+$GPI80$^+$	38.6	6.4	18.2	0.6
5	CD34$^+$CD38$^-$ CD90$^+$GPI80$^-$	0.5	0.1	0.3	0.1
6	CD34$^+$CD38$^-$ CD90$^+$GPI80$^-$	0	0.1	0.1	0
7	CD34$^+$CD38$^-$ CD90$^+$GPI80$^-$	0.1	0.1	0.1	0

Supplementary Experimental Procedures

Isolation of CD34$^+$ cells from human fetal hematopoietic tissues. Fetal livers were mechanically dissociated using scalpels and syringes. Red blood cells were removed by use of a Ficoll gradient (Stem Cell Technologies), and CD34$^+$ cells were isolated using magnetic beads (Miltenyi Biotec, CD34 MicroBead Kit). Fetal bone marrow was ground in sterile mortars and CD34$^+$ cells were fractionated by FACS sorting. Placentas were mechanically dissociated and incubated with collagenase (Worthington), dispase and DNase (Van Handel et al, 2010) and CD34$^+$ cells were isolated magnetically. The stage of the hematopoietic tissues is indicated as developmental age, which is two weeks less than the gestational age (from last menstrual period).

Flow cytometry and sorting. 7-amino-actinomycin D was used to identify and remove dead cells. Mouse anti-human antibodies were used to detect CD34, CD90, CD45, CD66b, CD13, CD3, CD4 and CD8 (BD Biosciences), CD38, CD19 (eBioscience), GPI-80 (MBL International) and ITGAM (eBioscience). Cells were analyzed on BD LSRII flow cytometer, and cell sorting was conducted on BD Aria II.

Microarray. RNA was purified from sorted HSPC using RNeasy Mini Kit (QIAGEN). Extracted RNA was hybridized on Affymetrix arrays (u133plus2.0 array). Microarrays were completed by the Clinical Microarray Core, Department of Pathology & Laboratory Medicine at UCLA.

Bioinformatic analysis. Analysis of microarray results was performed as previously described (Van Handel et al, 2012). Briefly, R package *Limma* provided through Bioconductor (Gentleman et al, 2004). was used for assessing differential expression (> 2-fold and p-value <0.05). Robust Multiarray Averaging was used to obtain absolute expression mRNA levels (Bolstad et al, 2003). For genes with multiple probe sets, probe sets with the lowest p-value were chosen. Diagnostic plots using the Bioconductor package array QualityMetrics were generated to assess quality of all arrays. The normalized expression were standardized and analyzed in Cluster 3.0 and Java Treeview for heatmap visualization.

Colony forming assay. Sorted HSPC were plated on MethoCult GF+H443 (Stem Cell Technologies) containing SCF, GM-CSF, IL-3 and EPO, and supplemented with TPO (10ng/ml, Peprotech), 1% penicillin-streptomycin and 1% amphotericin B (GIBCO/Invitrogen). Myeloerythroid colonies were scored 14 days after plating.

Lymphoid differentiation assays. Sorted HSPC were differentiated into B-cells on OP9M2 stroma, whereas T cell differentiation was carried out on OP9-DL1. Lymphoid co-cultures were plated in media containing MEM-α (GIBCO/Invitrogen), 20% Fetal Bovine Serum (Hyclone) and 1% penicillin/streptomycin supplemented with SCF (25 ng/ml), FLT3 (10 ng/ml), (Peprotech) and IL-7 (20 ng/ml) (Invitrogen).

Single cell differentiation assay. Fetal liver HSPC were sorted into 96 well plates pre-seeded with 20,000 irradiated OP9-M2, in the presence of SCF (100 ng/ml), TPO (100

ng/ml, Flt3 (100 ng/ml) (Peprotech) and IL-7 (20 ng/ml) (Invitrogen). Wells that visually demonstrated cell expansion were collected and analyzed by FACS for myeloid, lymphoid and HSPC markers after 14 days.

***In vitro* self-renewal assay.** OP9M2 stromal cells were plated in media containing MEM-α (GIBCO/Invitrogen), 20% Fetal Bovine Serum of specific batches tested for HSC expansion (Hyclone or OMEGA), penicillin (100 U/ml), streptomycin (100 μg /ml) and glutamine (292μg/ml). For co-culture assays, OP9M2 stromal cells were irradiated at 2000 rads and plated in tissue-treated 24-well plates at a concentration of 50,000 cells/cm2. HSPC were plated in media (MEM-α, 20% FBS and 1% penicillin/strep) supplemented with TPO (25 ng/ml), FLT-3 (25 ng/ml), and SCF (25 ng/ml) (Peprotech). Half of the medium in each well was changed every other day. FACS analysis was used to evaluate the ability to maintain undifferentiated HSPC population in culture.

Cell cycle analysis. Freshly isolated $CD34^+$ cells from 15-17 weeks fetal livers were cultured overnight on OP9M2 stroma and then pulse labeled with 10μM BrdU for 35 min in culture. Cells were sorted for the indicated surface phenotypes and processed according to the FITC-BrdU flow kit (BD) instructions to detect the distribution between cell cycle stages.

Transplantation Assays. Human fetal liver hematopoietic populations were injected into sub-lethally irradiated (325 rad) NOD-scid IL2Rγ-null mice (Jackson Laboratories). Sorted subpopulations originating from 50,000 CD34+ cells were injected intravenously

in each mouse. Mice were bled retro-orbitally for analysis of peripheral blood at 6 and 12 weeks. 16 weeks after transplantation, mice were sacrificed and hematopoietic organs (bone marrow and spleen) were harvested and analyzed for human engraftment based on detection of human CD45, CD66b, CD13, CD3 (BD Biosciences), and CD19 (eBioscience). Experimental protocols involving mice were reviewed and approved by the UCLA Animal Research Committee (Protocol number 2005-109).

Production of shRNA lentiviral vectors. 293T cells were transfected with Lipofectamine 2000 (Invitrogen)-complexed plasmids (pLKO vectors: VSV-G: ΔR8.2 in a 2.5:1:1 ratio) in OPTI-MEM (Invitrogen). Viral supernatant was collected after 48 hours and ultracentrifuged at 20,200 rpm for 1.5 hrs. Viral pellet was resuspended in Serum-Free Expansion Medium (SFEM, STEMCELL Technologies) and stored at -80°C.

Lentiviral transduction protocol. $CD34^+$ cells were pre-stimulated for 6 hours in SFEM supplemented with SCF (100 ng/ml), TPO (100 ng/ml, and Flt3 (100 ng/ml) (Peprotech). Transduction was performed on 40 ug/ml RetroNectin (Takara)-coated plates according to manufacturer's protocol. For efficient transduction, $CD34^+$ cells were incubated twice sequentially with 5 µl of virus for 12 hours. After infection, cells were washed in PBS supplemented with 5% FBS and seeded onto OP9M2 as described above. Cells were selected with puromycin 1µg/ml starting 48h after first transduction for the duration of the experiment. shRNA knockdown of GPI-80 and ITGAM was verified by FACS and q-

RT-PCR. Two independent shRNA sequences for each gene that yielded robust knock-down and similar phenotype in HSPC culture were identified.

Amnis Image Stream flow cytometry. Samples were analyzed on an Image Stream 100 flow cytometer, and data was analyzed using IDEAS software (Amnis). $CD34^+$ cells magnetically isolated from human fetal liver were stained with CD90 (BD Biosciences), ITGAM (eBioscience) and GPI-80 (MBL International).

Supplemental References

Bolstad B. M., Irizarry R. A., Astrand M., Speed T. P. (2003). A comparison of normalization methods for high density oligonucleotide array data based on variance and bias. Bioinformatics 19: 185-193.

Gentleman R. C., Carey V. J., Bates D. M., Bolstad B., Dettling M., Dudoit S., Ellis B., Gautier L., Ge Y., Gentry J., Hornik K., Hothorn T., Huber W., Iacus S., Irizarry R., Leisch F., Li C., Maechler M., Rossini A. J., Sawitzki G., Smith C., Smyth G., Tierney L., Yang J. Y., Zhang J. (2004). Bioconductor: open software development for computational biology and bioinformatics. Genome biology 5: R80.

Van Handel B., Montel-Hagen A., Sasidharan R., Nakano H., Ferrari R., Boogerd C. J., Schredelseker J., Wang Y., Hunter S., Org T., Zhou J., Li X., Pellegrini M., Chen J. N., Orkin S. H., Kurdistani S. K., Evans S. M., Nakano A., Mikkola H. K. (2012). Scl represses cardiomyogenesis in prospective hemogenic endothelium and endocardium. Cell 150: 590-605.

Van Handel B., Prashad S. L., Hassanzadeh-Kiabi N., Huang A., Magnusson M., Atanassova B., Chen A., Hamalainen E. I., Mikkola H. K. (2010). The first trimester human placenta is a site for terminal maturation of primitive erythroid cells. Blood 116: 3321-3330.

Chapter 4:

Summary and Discussion

Summary and Discussion

Chapter 2: Defining a Mesenchymal Stem Cell System for Human HSPC Culture

Attempts at expanding human HSC in culture for use in clinic have had limited success, in part due to a lack of understanding of the microenvironment necessary to support HSC function. Largely from murine studies, the bone marrow niche has been shown to be composed of multiple cell types, including endothelial cells , mesenchymal stem cells and osteoblasts (Kiel et al., 2005; Ding et al., 2012, Ding & Morisson, 2013, Morrison & Scadden, 2014); however, the unique contribution of each component of the HSC niche has not been thoroughly dissected. Moreover, without specific markers to identify developing HSC throughout ontogeny, especially in human, it has proven difficult to define the niche components supportive of HSC self-renewal during fetal development when HSC are rapidly expanding.

In this work, we defined a co-culture system utilizing OP9M2 mesenchymal stem cell (MSC) stroma that supports dramatic expansion of undifferentiated human HSPC. Expanded HSC maintained the established HSC surface phenotype (CD34+CD38-CD90+) and retained proliferative potential and capacity for multilineage differentiation in culture for several weels. Promisingly, this culture system maintained engraftable HSC for over two weeks; however, co-culture with OP9M2 did not lead to significant expansion of the functional, transplantable HSC,

implying that majority of the in vitro expanded HSPC acquire defects that compromise their function. Our analysis showed that most of the known HSC transcription factors were maintained a surprisingly stable levels for over several weeks. However, we were able to identify changes in PBX governed genetic networks that may negatively affect HSC function; these changes may provide a molecular explanation for the compromised condition of HSC in culture.

This work demonstrates that the OP9M2 MSC niche can serve as a model system to study key components of human HSC maintenance and multilineage differentiation (see also Chapter 3), which is a major advance as mechanistic studies in human HSC are largely missing due to shortage of model systems that enables manipulation of human HSC. In terms of HSC expansion, further experiments aiming to maintain PBX function and its downstream networks in cultured HSC may improve future HSC culture, given that PBX acts as a regulator of self-renewal in HSC (Ficara, Murphy, Lin, & Cleary, 2008).

Given our discovery that many of the key transcription factors governing the development and maintenance of HSC are largely stable on HSPC expanded on mesenchymal stromal culture, our findings suggest that *in vitro* expansion of HSC may not be a completely unrealistic goal. We believe that comparative analysis between self-renewing HSC in their niche and HSC in culture will provide the insight necessary to define the key programs and signals that are missing from the *in vitro* system. In addition to directly manipulating the cell intrinsic regulatory programs in

cultured HSC, supplementing OP9 cultures with other niche cells, such as endothelial cells, may provide the signals necessary to upregulate factors necessary for HSC expansion. Furthermore, as bone marrow does not primarily function as a niche for HSC expansion, but for maintenance, it is possible that there are superior niche cells that could be utilized to expand HSC *in vitro*. It is possible that human fetal stromal lines derived from placenta or fetal liver, which are known sites of human HSC expansion during development, may be functionally superior, though a fetal stromal line that supports HSPC as well as OP9M2 has not yet been derived. Other niche cells that are specific to the fetal microenvironments such as placental trophoblasts of fetal liver hepatocytes may also provide unique insights and tools for HSC in vitro culture (Chhabra et al., 2012; Chou & Lodish, 2010). Nevertheless, the OP9M2 culture system serves now as a well-defined platform for studies to improve human HSPC expansion, and also provides an *in vitro* system for mechanistic studies of human HSPC proliferation and differentiation.

Chapter 3: GPI-80 Marks Self-renewing Human HSPC During Development

Human HSC surface markers have been poorly defined, and unspecific at best. Our work has led to the identification of GPI-80 as a novel marker for the self-renewing HSC during human development. Intriguingly, the GPI-80+ HSPC were the only cells in second trimester human fetal liver that showed robust multipotency at clonal level, had long-term self-renewal ability, and could engraft in immune-deficient

mice upon transplantation. We also found that GPI-80 expression is restricted to the hematopoietic cells in multiple fetal niches, demarcating HSC from the underlying endothelium in sites of HSC emergence and expansion. Furthermore, lentiviral knockdown of GPI-80 or ITGAM, and integrin that GPI-80 co-localizes and co-operates with, resulted in differentiation and loss of HSPC. As GPI-80 and ITGAM are utilized by neutrophils for adhesion to their environment, our data indicates that factors used in the function of terminally differentiated myeloid cells may be also be employed at the apex of the hematopoietic hierarchy by HSC for maintenance of stem cell properties.

GPI-80 provides a unique tool for tracking the self-renewing human HSPC during development, a critical period in which HSC are generated. As HSC become largely quiescent in the bone marrow during post-natal life, fetal HSC provide an exceptional and unique system for study of the transcriptional regulators of self-renewal that lead to HSC expansion. Though GPI-80+ HSPC and GPI-80- HSPC are strikingly similar in gene expression analysis, they behave starkly differently in both *in vitro* assays and *in vivo* transplantation settings; thus, the genes that are upregulated in GPI-80 HSPC provide strong candidates for conferring the key properties of self-renewal and engraftment. Promising preliminary investigation into genes that are upregulated in GPI-80 HSPC indicate that factors such as HIF3alpha and HLF are necessary for proper HSPC self-renewal; furthermore, our studies indicate that overexpression of these factors may lead to enhanced self-renewal of HSPC. Ongoing studies are focused on manipulation of these

transcriptional regulators to improve HSPC cultures, and exploring whether these factors could potentially be harnessed in the expansion of HSPC for clinical purposes.

As GPI-80 has been implicated as having a particular function in adhesion of myeloid cells and neutrophils through activation of Beta-2-integrin (Watanabe & Sendo, 2002) ; it is plausible that it functions through similar mechanisms also in the HSPC compartment, and the GPI-80/ITGAM complex is necessary for proper HSPC adhesion. Homing and migration assays comparing control GPI-80+ HSPCs and GPI-80 knockdown cells, as well as ITGAM knockdown cells, will provide data necessary for determining whether in HSPC, GPI-80 functions similarly in adhesion and extravasation.

Finally, we have found that GPI-80 also becomes upregulated in a subpopulation of ES-derived HSPC after their emergence of hemogenic endothelium when they are expanded on OP9M2 MSC stroma (data not shown). However, as previous studies and preliminary data from our lab demonstrate that functional HSC cannot be generated *in vitro* from human ES cells (Dravid & Crooks, 2011; Panopoulos & Belmonte, 2012), this data suggests that GPI-80 expression is necessary but not sufficient for self-renewal. Thus, the next step would be to perform focused studies on GPI-80+ subpopulation and analyze the transcriptional differences between the ES-derived HSPC and the fetal liver derived HSC. Gene expression comparison between non-engraftable ES-derived HSPC and the self-renewing, engraftable fetal

liver HSC will elucidate programs that are askew or improperly maintained by ES-derived HSPC, and bring us closer to correcting the defects and generating functional HSC in vitro. Over-expression of factors specific to fetal liver GPI-80 HSC in the ES system may be beneficial for generation of HSC capable of self-renewal.

Bibliography

Chhabra, A., Lechner, A., Ueno, M., Acharya, A., Van Handel, B., Wang, Y., Iruela-Arispe, M. L., Tallquist, M.D., Mikkola, H.K (2012). Trophoblasts regulate the placental hematopoietic niche through PDGF-B signaling. *Developmental Cell,* 22(3), 651-9.

Chou, S., & Lodish, H. (2010). Fetal liver hepatic progenitors are supportive stromal cells for hematopoietic stem cells. *PNAS,* 107(17), 7799-04.

Ding, L., Saunders, T. L., Enikolopov, G. & Morrison, S. J. (2012). Endothelial and perivascular cells maintain haematopoietic stem cells. Nature 481, 457–462.

Ding, L. & Morrison, S. J. (2013). Haematopoietic stem cells and early lymphoid progenitors occupy distinct bone marrow niches. Nature 495, 231–235.

Dravid, G. G., & Crooks, G. M. (2011). The challenges and promises of blood engineered from human pluripotent stem cells. *Advanced drug delivery reviews*, *63*(4-5), 331–41.

Ficara, F., Murphy, M. J., Lin, M., & Cleary, M. L. (2008). Pbx1 regulates self-renewal of long-term hematopoietic stem cells by maintaining their quiescence. *Cell stem cell*, *2*(5), 484–96.

Kiel, M. J., Yilmaz, O. H., Iwashita, T., Yilmaz, O. H., Terhorst, C., & Morrison, S. J. (2005). SLAM family receptors distinguish hematopoietic stem and progenitor cells and reveal endothelial niches for stem cells. *Cell*, *121*(7), 1109–21.

Morrison, S.J., & Scadden, D. T. (2014). The bone marrow niche for haematopoietic stem cells. *Nature* 505, 327-334.

Panopoulos, A. D., & Belmonte, J. C. I. (2012). Induced pluripotent stem cells in clinical hematology: potentials, progress, and remaining obstacles. *Current opinion in hematology*, *19*(4), 256–60.

Watanabe, T., & Sendo, F. (2002). Physical association of beta 2 integrin with GPI-80, a novel glycosylphosphatidylinositol-anchored protein with potential for regulating adhesion and migration. *Biochemical and biophysical research communications*, *294*(3), 692–4.

blood

2010 116: 3321-3330
Prepublished online July 13, 2010;
doi:10.1182/blood-2010-04-279489

The first trimester human placenta is a site for terminal maturation of primitive erythroid cells

Ben Van Handel, Sacha L. Prashad, Nargess Hassanzadeh-Kiabi, Andy Huang, Mattias Magnusson, Boriana Atanassova, Angela Chen, Eija I. Hamalainen and Hanna K. A. Mikkola

Blood (print ISSN 0006-4971, online ISSN 1528-0020), is published weekly by the American Society of Hematology, 2021 L St, NW, Suite 900, Washington DC 20036.

The first trimester human placenta is a site for terminal maturation of primitive erythroid cells

Ben Van Handel,[1] *Sacha L. Prashad,[1,2] *Nargess Hassanzadeh-Kiabi,[1] Andy Huang,[3] Mattias Magnusson,[1] Boriana Atanassova,[1] Angela Chen,[3] Eija I. Hamalainen,[1] and Hanna K. A. Mikkola[1,2,4]

[1]Department of Molecular, Cell and Developmental Biology, [2]Molecular Biology Institute, [3]Department of Obstetrics and Gynecology, and [4]Eli and Edythe Broad Center for Regenerative Medicine and Stem Cell Research, University of California Los Angeles, Los Angeles, CA

Embryonic hematopoiesis starts via the generation of primitive red blood cells (RBCs) that satisfy the embryo's immediate oxygen needs. Although primitive RBCs were thought to retain their nuclei, recent studies have shown that primitive RBCs in mice enucleate in the fetal liver. It has been unknown whether human primitive RBCs enucleate, and what hematopoietic site might support this process. Our data indicate that the terminal maturation and enucleation of human primitive RBCs occurs in first trimester placental villi. Extravascular ζ-globin$^+$ primitive erythroid cells were found in placental villi between 5-7 weeks of development, at which time the frequency of enucleated RBCs was higher in the villous stroma than in circulation. RBC enucleation was further evidenced by the presence of primitive reticulocytes and pyrenocytes (ejected RBC nuclei) in the placenta. Extravascular RBCs were found to associate with placental macrophages, which contained ingested nuclei. Clonogenic macrophage progenitors of fetal origin were present in the chorionic plate of the placenta before the onset of fetoplacental circulation, after which macrophages had migrated to the villi. These findings indicate that placental macrophages may assist the enucleation process of primitive RBCs in placental villi, implying an unexpectedly broad role for the placenta in embryonic hematopoiesis. (*Blood*. 2010;116(17):3321-3330)

Introduction

The hematopoietic system during embryonic development provides two important functions: rapid generation of terminally differentiated blood cells for the survival and growth of the embryo and establishment of a pool of undifferentiated hematopoietic stem cells (HSCs) for postnatal life. To achieve these goals, embryonic hematopoiesis is segregated into multiple waves that occur in several anatomical sites,[1] a process that is broadly conserved in vertebrates.[2,3] The yolk sac is the site of the first wave of embryonic hematopoiesis that generates both primitive red blood cells (RBCs) that deliver oxygen to the embryo and macrophages that assist in tissue remodeling and immune defense.[4] The second wave of hematopoiesis also commences in the yolk sac with the production of a transient pool of erythromyeloid progenitors. Although they lack self-renewal ability and lymphoid potential, they have an important function in fetal hematopoiesis as they rapidly differentiate into mature definitive erythroid and myeloid cells after migration to the fetal liver.[5,6] The third wave of hematopoiesis emerges in the major intra- and extraembryonic arteries, generating HSCs that can both self-renew and differentiate into all blood cell types, including lymphoid cells. HSCs subsequently colonize the fetal liver where they expand before eventually seeding the bone marrow. HSCs emerge in the AGM (aorta-gonad-mesonephros region) and attached vitelline and umbilical arteries,[7-11] the yolk sac, and the placenta. The capacity of the placenta for generation[12] and expansion[13-15] of multipotential hematopoietic stem/progenitor cells has been described recently in both mouse and human,[16-18] whereas its potential function as a primitive hematopoietic organ has not been evaluated.

The most important products of primitive hematopoiesis that are critical for the survival of the embryo are the primitive RBCs. Experimental evidence suggests that the yolk sac-derived primitive erythroid cells are specified directly from mesoderm with restricted hematopoietic potential, rather than from a multipotential HSC.[19-22] Primitive red cells differ from definitive red cells not only in their developmental origin, but also in their larger size and distinct globin expression pattern.[23] In mice, primitive RBCs can be identified by expression of εy-globin,[24] which is absent from definitive red cells derived from the fetal liver and the adult bone marrow that express β-major globin.[25] In human, primitive red cells uniquely express the α-like ζ-globin as well as the β-like ε-globin.[26] Furthermore, primitive red cells differ from definitive red cells in that they enter circulation as nucleated erythroblasts, whereas the definitive erythroid cells complete maturation and enucleation in their site of origin, the fetal liver[27] or bone marrow, before entering circulation (reviewed in Chasis[28]). It has been documented that this process occurs in "erythroblast islands" in association with macrophages, which digest the ejected RBC nuclei[27] and serve other supportive functions.[28] However, there is evidence that macrophages are not essential for RBC enucleation.[29] Although the long-standing dogma asserts that primitive red cells, or erythroblasts, remain nucleated and never mature into enucleated erythrocytes, it has been recently documented that primitive

Submitted April 12, 2010; accepted June 30, 2010. Prepublished online as *Blood* First Edition paper, July 13, 2010; DOI 10.1182/blood-2010-04-279489.

*S.L.P. and N.H.-K. contributed equally to this work.

The online version of this article contains a data supplement.

The publication costs of this article were defrayed in part by page charge payment. Therefore, and solely to indicate this fact, this article is hereby marked "advertisement" in accordance with 18 USC section 1734.

erythroblasts in mouse embryos do enucleate. In the process, a transient population of free nuclei termed pyrenocytes is generated.[30] The enucleation of primitive RBCs lay undiscovered for a century because it starts in mouse embryos at the same developmental time when definitive erythroid cells begin to enter circulation.[31] Although the site of enucleation of primitive red cells was unknown, association of primitive red cells and macrophages in the fetal liver, and the ability of the liver macrophages to ingest the nuclei of primitive red cells in vitro, suggested that fetal liver macrophages can support maturation of both primitive and definitive erythroblasts during mouse development.[30,32] In humans, the limited access to the early embryonic hematopoietic tissues has hindered our understanding of human developmental hematopoiesis. It is unknown if human primitive erythroblasts enucleate or which anatomical sites might support the enucleation process.

Here we show that human primitive RBCs do enucleate, segregating the nucleated erythroblast into a reticulocyte and a pyrenocyte. Our data reveal that primitive RBC enucleation occurs in the placental villous stroma in association with macrophages. The presence of macrophage progenitors in the chorionic plate of precirculation placentas suggests that the human placenta may autonomously generate the macrophages that migrate to the villi to assist the terminal maturation of primitive RBCs. These data indicate that the placenta has a broader role as a hematopoietic organ than previously appreciated, functioning as an integral component of both primitive and definitive hematopoiesis.

Methods

Tissue collection and procurement

Extra-embryonic and embryonic tissues were discarded material obtained from elective terminations of first and second trimester pregnancies performed by Family Planning Associates or University of California Los Angeles (UCLA) Medical Center. The gestational age of the specimen was determined by ultrasound. If this information was not available, the date from the last menstrual period and histologic features of the specimen were used to determine the duration of pregnancy. The age of the specimen is indicated in this work as developmental age, which is 2 weeks less than the gestational/clinical age. Tissues were harvested directly into sterile containers with phosphate-buffered saline (PBS) and transported on ice in PBS containing 5% fetal bovine serum (FBS; Hyclone), 0.1% ciprofloxacin HCl (10 μg/mL; Sigma-Aldrich), 1% amphotericin B (250 μg/mL; Invitrogen), and 1% penicillin (10 000 U/mL)–streptomycin (10 000 μg/mL; Invitrogen) and processed the same day.

Preparation of tissue sections

Tissues were fixed in 3.7% phosphate-buffered formalin (Protocol) for 12-16 hours, then rinsed with tap water and transferred to 70% ethanol for storage. Fixed specimens were embedded in paraffin and cut into 5-μm sections by the UCLA Translational Pathology Core Laboratory (TPCL). Hematoxylin/eosin (H&E) stainings were performed by TPCL.

Histologic analysis of erythroblast maturation

To assess RBC maturation, 5 random microscope fields were selected from each slide and photographed (Zeiss Axiovert 40 CFL with attached Canon Powershot G6 camera) at ×400 total magnification. RBCs were identified by an eosinophilic cytoplasm and designated as nucleated or enucleated (with or without a dark purple nucleus) and circulating or extravascular (inside or outside of blood vessels). Cells were annotated on printed photographs while viewed in the scope. All cells in each category were then summed across the fields for each slide. The enucleation ratios (ERs) were defined for each specimen by dividing the number of enucleated RBCs by the total number of RBCs counted. To compare the enucleation status of extravascular versus circulating RBCs, ERs were determined for both compartments for each specimen, and relative enrichment of enucleated cells in extravascular versus intravascular spaces was determined by dividing the ERs in the 2 compartments.

Preparation of single–cell suspensions from hematopoietic tissues

Single-cell suspensions were prepared from fresh specimens for use in culture assays or flow cytometry. Tissues were first mechanically dissociated by mincing with scalpels, then subjected to enzymatic dissociation in 10 mL of enzyme solution per gram tissue (2.5 U dispase [Invitrogen], 90 mg collagenase [Sigma-Aldrich], 5% FBS [Hyclone], 1% amphotericin B [250 μg/mL; Invitrogen], 1% penicillin [10 000 U/mL]–streptomycin [10 000 μg/mL; Invitrogen] and 0.1% ciprofloxacin HCl [10 μg/mL; Sigma-Aldrich]) for 30 minutes with agitation at 37°C. After 30 minutes, DNase I (0.075 mg/g tissue; Sigma-Aldrich) was added, and samples were incubated for an additional 30 minutes. Dissociated cells were then filtered through 70-μm mesh, washed with PBS, and counted.

Flow cytometry and cell sorting

Fluorescence-activated cell sorting (FACS) analysis was performed using single-cell suspensions prepared as described above. Intracellular FACS of RBCs was performed essentially as described,[33] with the following modifications. Cells were stained with antibodies against CD235 (1:100, fluorescein isothiocyanate or phycoerythrin [PE]; BD Biosciences) and CD71 (1:25, Alexa Fluor 647; Santa Cruz Biotechnology) before fixation by incubation with antibodies at 4°C for 20 minutes. After fixation and permeabilization, cells were stained with an anti–ζ-globin antibody (1:1000; a kind gift from T. Papayannapoulou, University of Washington Medical School) followed by an anti-mouse Alexa Fluor 488–conjugated secondary antibody (1:250; Invitrogen) or a fluorescein isothiocyanate–conjugated anti–ϵ-globin antibody (1:2000; Fitzgerald Industries). For ζ-globin analysis, cells were briefly postfixed with 1% formaldehyde. To detect erythroid cells at different stages of maturation, cells were stained with CD235 as above, and DRAQ5 (Biostatus Limited) was used at 5μM as directed. To detect hematopoietic progenitors, cells were stained with antibodies against CD43 PE (used at 1:25, mouse anti–human; Santa Cruz Biotechnology), and CD34 APC (1:50, mouse anti–human; BD Biosciences) diluted in 5% FBS (Hyclone). 7-Aminoactinomycin D (BD Biosciences) was added at a final dilution of 1:50 in all analyses of nonfixed cells. Stained cells were analyzed on a LSR II cytometer (BD Biosciences) and processed with FlowJo software Version 7.6.1 (TreeStar). Sorting for hematopoietic progenitors ($CD34^+CD43^+$) and RBC populations defined by DRAQ5 and CD235 was performed as above using a BD FACSAria II in the UCLA Broad Stem Cell Center Core facility.

In vitro erythroblast island formation assay

Island assays were performed essentially as described,[30] with the following modifications. Macrophages were labeled with CD68 PE and isolated from placental cell suspensions (6 weeks) using anti-PE magnetic beads (Miltenyi Biotec) according to manufacturer's instructions. Isolated macrophages were plated at a density of 2.5×10^4 cells per well in fibronectin-coated 8-well chamber slides (BD). Primitive RBCs ($CD235^+CD71^+$) were sorted from pooled 4- to 6-week placental suspensions, labeled with CellTracker Green (Molecular Probes), and combined with macrophages in chamber slides at a density of 1×10^5 cells per well in "association media" (30% plasma-derived serum, Iscove modified Dulbecco medium, 2mM glutamine, 0.15mM monothioglycerol, 1 ng/mL macrophage colony-stimulating factor, 2 U/mL erythropoietin, 300 mg/mL transferrin, and 40 ng/mL insulin-like growth factor 1) and cultured for 48 hours. Wells were washed 3× with PBS, fixed in ice-cold methanol for 5 minutes, and then stained for FXIII and DAPI (4′,6-diamidino-2-phenylindole).

Immunohistochemistry

For immunohistochemistry (IHC), unstained sections were deparaffinized and rehydrated through a xylene/alcohol gradient. Antigen retrieval was

performed in an antigen-dependent manner using a pressure cooker and a microwave. For CD235 (Santa Cruz Biotechnology), FXIII (Vector Laboratories), and CD68 (Santa Cruz Biotechnology) staining, slides were immersed in a 10mM Tris, 1mM EDTA (ethylenediaminetetraacetic acid), 0.05% Tween 20 solution, at pH 9.0, and microwaved on high for 8 minutes. For slides stained with ζ-globin and ϵ-globin (Fitzgerald Industries), microwave retrieval was performed in a 100mM Tris solution at pH 6.0. CD34 and cytokeratin (Vector Laboratories) staining was of equal quality with either retrieval technique. After cooling, endogenous peroxidases were quenched in a 0.9% solution of H_2O_2 in methanol for 20 minutes at room temperature. Slides were blocked in 5% normal horse serum in PBS, pH 7.4, containing 0.05% Tween 20 for 10 minutes. Primary antibodies were diluted in blocking buffer and incubated for 1 hour at room temperature (FXIII 1:50, CD235 1:75, cytokeratin 1:1200, and CD34 1:50) or overnight at 4°C (1:1500; ζ- and ϵ-globin). Biotinylated anti-rabbit (1:500; cytokeratin) or anti-mouse (1:500; all others) secondary antibodies were diluted in blocking buffer and incubated for 30 minutes at room temperature, then detected following manufacturer's instructions (Vector Laboratories). Nuclear counterstain (Fast Red; Vector Laboratories) was used as directed. Slides were dehydrated, mounted (Vectamount; Vector Laboratories), and imaged with an Olympus BX51 microscope and a DP72 camera.

Image acquisition information

For all brightfield micrographs, an Olympus BX51 microscope with an attached DP72 camera and DP72-BSW software (Version 2.2) were used to acquire images. For 100× images, a 10×/0.40 UPlanSApo objective was used, for 200× images, a 20×/0.75 UPlanSApo objective was used, and for 400× images a 40×/1.30 UPlanFLN oil objective was used. All slides were mounted with Vectamount (Vector Laboratories). ImageJ (Version 1.40g) was used to process images.

Immunofluorescence and confocal microscopy

For immunofluorescence, unstained sections were deparaffinized and rehydrated through a xylene/alcohol gradient. Antigen retrieval was performed at 95°C for 30 minutes each sequentially in 10mM Tris, 1mM EDTA, 0.05% Tween 20 solution, pH 9.0, followed by 10mM citrate solution in PBS, pH 6.0. After cooling, endogenous peroxidases were quenched in a 0.9% solution of H_2O_2 in methanol for 20 minutes at room temperature. Sections were permeabilized with 1% Triton X-100 in PBS for 1 hour, then blocked in tyramide blocking solution (Invitrogen) plus 1% Triton X-100 (TBST) for 1 hour. Slides were incubated with primary antibodies overnight at 4°C (1:1000, CD43 MT1, Santa Cruz Biotechnology; 1:1000, CD34 QBEnd/10, Vector Laboratories; 1:1000, CD235 11E4B7.6, Santa Cruz Biotechnology; 1:750, CD31 0.N.100, Santa Cruz Biotechnology; 1:1500, Flk1 A-3, Santa Cruz Biotechnology; 1:500, FXIII E980.1, Vector Laboratories; 1:2500, CD68 KP1, Santa Cruz Biotechnology; 1:1000, phosphatidylserine 1H6, Millipore). Slides were washed with 0.1% Tween in PBS (PBST) followed by incubation with biotinylated secondary antibodies (1:500; Vector Laboratories) in TBST for 30 minutes at room temperature. Slides were washed 3× with PBST followed by incubation with streptavidin–horseradish peroxidase (1:500 in TBST; Invitrogen) for 30 minutes at room temperature. Slides were washed 3× in PBST, then tyramide biotin-XX amplification was performed for 7.5 minutes as per manufacturer's instructions (Invitrogen). Slides were washed in PBST followed by incubation with ABC Elite (Vector Laboratories) for 30 minutes at room temperature. Slides were washed in PBST and incubated with tyramide-fluorophore for 7.5 minutes prepared as directed (Invitrogen). Slides were washed in PBS and incubated with 0.05M HCl for 20 minutes at room temperature to quench peroxidases. Slides were washed 3× in PBST, then blocked, and incubated with primary antibodies as above. After the final tyramide-fluorophore step, slides were washed in PBS then incubated with DAPI solution (5 μg/mL in PBS) for 5 minutes at room temperature. Slides were washed 3× with PBS, then mounted in ProLong Gold mounting medium (Molecular Probes), and stored at 4°C. TUNEL stains were performed by first deparaffinizing slides and performing antigen retrieval as above, then using the In Situ Cell Death Detection Kit AP (Roche) as directed. Subsequent stains were then performed using the same immunofluorescent protocol. Confocal images were obtained on a Zeiss LSM 510 equipped with 405, 488, 543, and 633 nm lasers. Images were processed with ImageJ software Version 1.40g (National Institutes of Health).

Electron microscopy

Individual or small groups of villi were dissected away from fresh placental samples and immersed in electron microscopy (EM) fixative (2% glutaraldehyde and 1% paraformaldehyde in PBS) at 4°C overnight. Second-trimester fetal liver tissues were used as controls. Ultrathin sections were cut and viewed in a JEOL 100CX transmission electron microscope (JEOL USA). Images were captured on a Gatan UltraScan 2k*2k camera (Gatan), developed, and scanned at 1200 dots per inch.

Clonogenic progenitor assays

Single-cell suspensions were prepared as described above. Cell populations sorted based on CD34 and CD43 expression were plated in MethoCult GF$^+$ H4435 methylcellulose (StemCell Technologies) containing stem cell factor, granulocyte macrophage colony-stimulating factor, interleukin-3, and erythropoietin supplemented with 1:2000 thrombopoietin (10 μg/mL; Peprotech), 1% penicillin-streptomycin (Invitrogen), 1% amphotericin B (Invitrogen), and 0.1% ciprofloxacin HCl (Sigma-Adrich). Cultures were incubated at 37°C and 5% CO_2 for 14 days, and colonies were scored based on classical morphologic characteristics. Cytospins of individual colonies were performed using a Shandon Cytospin 4 (Thermo Electron Corporation) followed by May-Grunwald Giemsa staining (Sigma-Aldrich).

PCR for fetal-maternal identity

To verify the fetal origin of hematopoietic colonies derived from placental samples, colonies were picked from methylcellulose assays, lysed, and tested first for the 2 sex chromosomes: the SRY gene on the Y chromosome and the HTR2C gene on the X chromosome by polymerase chain reaction (PCR) amplification. The primers used were SRY-F (5′-TAATACGACTCACTATAGGGAGAATAAGTATCGACCTCGTCGGAA-3′), and SRY-R (5′-AATTAACCCTCACTAAAGGGAGACACTTCGCTGCAGAGTACCGA-3′), and HTR2C-F (5′-TAATACGACTCACTATAGGGAGAGTGGTTTCAGATCGCAGTAA-3′), HTR2C-R (5′-AATTAACCCTCACTAAAGGGAGAATATCCATCACGTAGATGAGAA-3′). Both SRY and HTR2C primers were combined in one PCR, which was performed as follows: the initial denaturation was done at 95°C for 15 minutes, followed by 15 cycles of amplification, which included a 30-second denaturation step at 95°C, a 64°C annealing step for 30 seconds, and a 1-minute extension step at 68°C. For the first 15 cycles, the temperature was decreased by 0.5°C per cycle. This was followed by 24 cycles done as follows: a 30-second denaturation step at 95°C, a 56°C annealing step for 30 seconds, and an extension for 1 minute at 68°C. The final extension was done at 72°C for 10 minutes. In the absence of a signal from the Y chromosome, microsatellite PCR was used to verify that placental colonies differed in their genotype from the maternal decidua. For the MTC118 microsatellite PCR, the primers used were MCT118A (5′-GTCTTGTTGGAGATGCACGTGCCCCCTTGC-3′) and MCT118B (5′-GAAACTGGCCTCCAAACACTGCCCGCCG-3′). The PCR conditions were as follows: the initial denaturation was done at 95°C for 15 minutes and was followed by 31 cycles, which consisted of a 1-minute denaturation step at 94°C, a 62°C annealing step for 1 minute, and a 1-minute extension step at 72°C. As above, the final extension was done at 72°C for 10 minutes. All PCRs were completed in a total volume of 25 μL, and HotStar *Taq* DNA polymerase was used. Gels were imaged and digitized using a BioDoc-It Imaging System (UVP).

Results

Enucleated primitive RBCs populate the placental villous stroma during the first trimester

To determine whether human primitive RBCs enucleate, we assessed the enucleation status of RBCs in the placenta, which is an

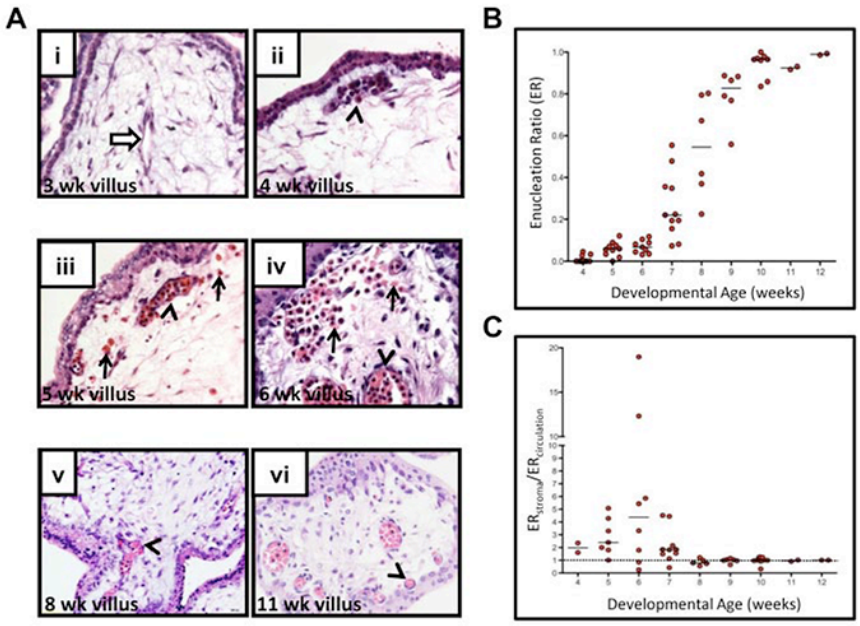

Figure 1. The first trimester placental stroma becomes populated by extravascular RBCs that enucleate. (A) Localization and enucleation status of erythroid cells in the placenta was determined by H&E staining. At 3 weeks of developmental age (i), placental blood vessels had started to form and were devoid of RBCs (white arrow). By 4 weeks (ii), nucleated RBCs had appeared in the placental vasculature (arrowhead). Between 5-7 weeks of developmental age, RBCs were also found in the villous stroma (arrows) with increasing frequency (iii-iv), and many were enucleated, whereas most circulating RBCs still retained their nuclei (arrowheads). Toward the end of first trimester, RBCs were found mainly in circulation (arrowheads in v-vi). All images shown were acquired at 400× original magnification. (B) Calculation of ERs (number of enucleated RBCs divided by the total number of RBCs counted, see "Histologic analysis of erythroblast maturation") for the placental RBC pool for each week of development revealed a marked change in their maturation state between 4 and 8 weeks. Bars represent median for each age. (C) Analysis of enucleation ratios of RBCs in circulation (inside blood vessels) or extravascular (in placental stroma) revealed an enrichment of enucleated RBCs in the extravascular stroma during 5-7 weeks of development. Dotted line at 1 indicates equal representation of enucleated cells in both compartments, and bars represent the median at each age.

accessible fetal tissue that can be used to investigate circulating blood cells from the early first trimester onward. The status of fetoplacental circulation was determined by flow cytometry (supplemental Figure 1, available on the *Blood* Web site; see the Supplemental Materials link at the top of the online article) by identifying precirculation specimens based on the absence of $CD235^+CD71^+$ fetal erythroblasts. H&E stained sections from placentas were used for quantitative analysis of RBC enucleation and localization status at different ages (Figure 1). As expected, erythroblasts were detectable in the placental vasculature by 4 weeks of developmental age (corresponding to 6 weeks clinical age). By 5 weeks of developmental age, a fraction of the RBCs had lost their nucleus. Interestingly, at this stage some of the erythroid cells were found in the stroma of the placental villi rather than contained within placental vessels (Figure 1Aiii). The frequency of extravascular RBCs in the villous stroma was highest between 6 and 7 weeks, coincident with an increase in the overall frequency of enucleated RBCs in the placenta. When both the enucleation status and localization (circulating or extravascular) of RBCs in the placenta was scored, an enrichment of enucleated RBCs in the placental extravascular stroma in comparison to blood vessels was observed (ie, ER was higher) at 5-7 weeks of development, with the peak at 6 weeks (Figure 1C). Toward the end of the first trimester, most RBCs were contained in the vessels, and very few RBCs with a nucleus were present. The enrichment of enucleated RBCs in the placental stroma at the time when enucleation of RBCs starts raised the hypothesis that circulating erythroblasts may extravasate into the placental stroma for the purpose of terminal maturation and enucleation.

Based on the developmental timing when extravascular RBCs are found in the placenta and the fact that these RBCs initially possess a nucleus, we hypothesized that they represent the primitive erythroid lineage. To test this, an antibody against ζ-globin, which is characteristic for primitive RBCs, was used along with CD235 (Figure 2A,C) to mark primitive erythroid cells. Flow cytometry for ζ-globin in combination with CD71 and CD235 confirmed that the earliest RBCs in the placenta express ζ-globin and are of the primitive lineage (Figure 2A). To investigate the localization of primitive RBCs in hematopoietic tissues, adjacent sections were stained for ζ-globin and CD235 to identify erythroid cells, while CD34 staining was used to delineate endothelial cells that separate vascular lumens from stromal regions (Figure 2A,C). From the time when RBCs first appear in the placental vessels through 6 weeks of age, when many of these cells were found in the extravascular stroma and had started to enucleate, essentially all RBCs in the placenta expressed ζ-globin (Figure 2A) and ϵ-globin (supplemental Figure 2A). Furthermore, flow cytometry for ϵ-globin confirmed that ϵ-$globin^+$ primitive RBCs enucleate (supplemental Figure 2B). Staining with 2 other endothelial markers, CD31 and Flk1, confirmed the lack of blood vessels surrounding primitive RBCs in the villous stroma (Figure 2B). In contrast, all $CD235^+$ cells in the yolk sac and the fetal liver at 5-5.5 weeks were contained within the vasculature (Figure 2C), whereas the first $CD235^+$ RBCs found in the liver parenchyma at 6.5 weeks were ζ-$globin^{neg}$ definitive erythroid cells (Figure 2Ciii,iiii′). These data suggest that at the time when primitive erythroid cells start to enucleate, they are highly enriched in the placental villous stroma compared with the liver parenchyma. By 11 weeks, most RBCs in the placenta were enucleated, contained in vessels, and no longer expressed ζ-globin (Figure 2Av,v′), whereas most of the RBCs in the fetal liver were devoid of ζ-globin expression and resided in the liver parenchyma (Figure 2Biv,iv′). Importantly, TUNEL staining implied that there was no significant cell death among the extravascular RBCs in the placenta (supplemental Figure 3A). Moreover, staining for phosphatidylserine (PTDS), a lipid exposed both on the surface of apoptotic cells and on the nuclear membrane surrounding ejected RBC nuclei,[34] verified that there was little apoptosis among the extravascular primitive RBCs and that some of the RBCs had begun to expose PTDS on the nuclear membrane (supplemental Figure 3B). Altogether, these data suggested that human primitive erythroid cells may enucleate in the placental villous stroma.

Enucleation of human primitive RBCs in the placental villous stroma generates a transient population of pyrenocytes

During enucleation, RBCs segregate their contents into 2 compartments: a reticulocyte and a pyrenocyte. Analysis of H&E stained

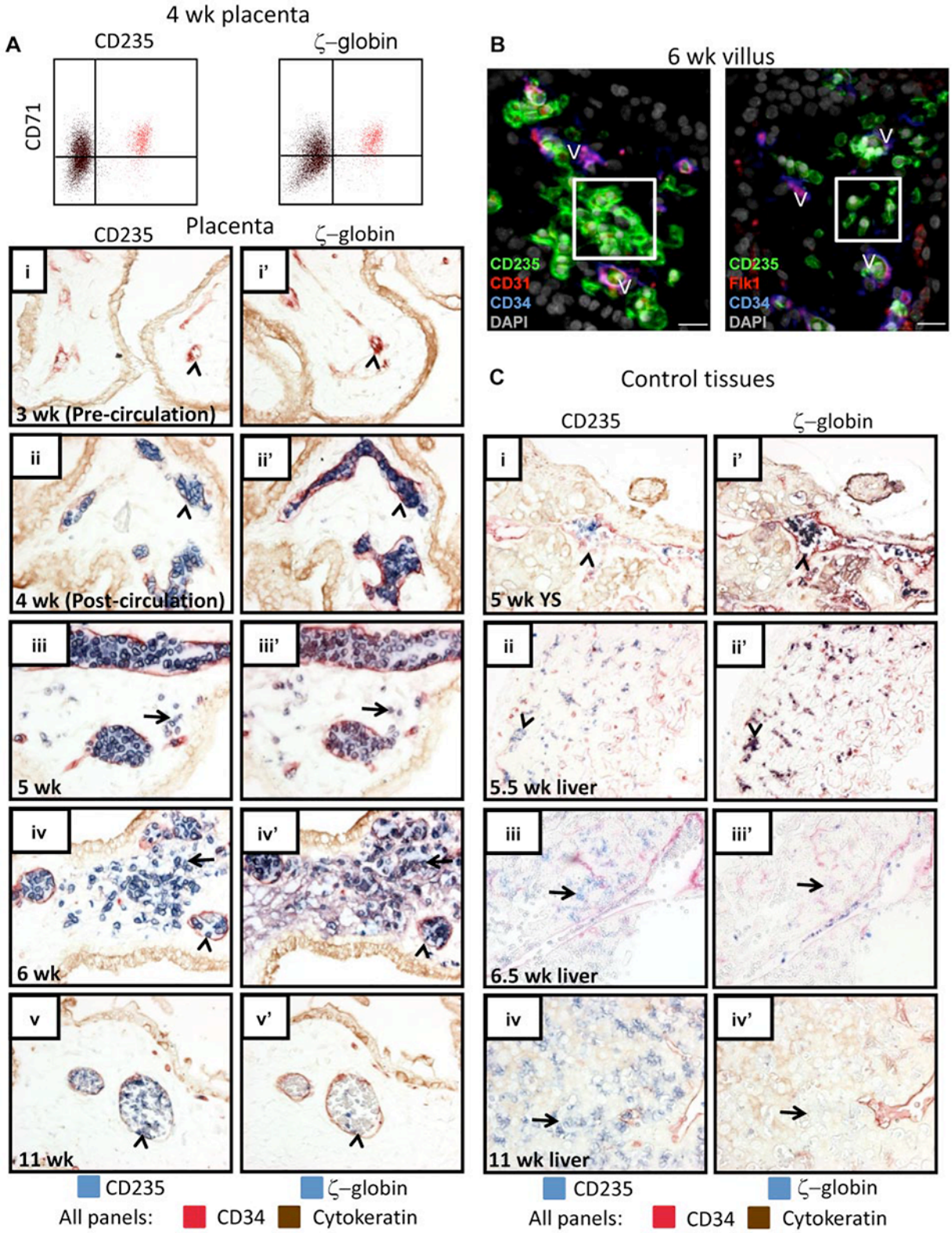

Figure 2. RBCs in the placental villous stroma are of the primitive erythroid lineage. (A) Intracellular flow cytometry confirmed that the CD235$^+$CD71$^+$ erythroid cells in the early first trimester placenta were ζ-globin expressing primitive RBCs (colored cells are the same in both FACS plots). IHC of adjacent tissue sections demonstrated that the RBCs observed in the placental villous stroma were of the primitive lineage. In precirculation placentas (i-i′), no ζ-globin$^+$CD235$^+$ cells were found in placental blood vessels (arrowheads). The first cells in the vasculature (arrowheads) were CD235$^+$ (II) and ζ-globin$^+$ (ii′). At 5 weeks of age, all RBCs in the placenta expressed ζ-globin (iii vs iii′) and some were localized to the placental stroma (arrows). By 6 weeks many more primitive RBCs were observed in the villous stroma (arrows in iv-iv′). At 11 weeks, the placental RBC pool comprised mostly ζ-globin$^-$ RBCs that were contained in blood vessels (arrowheads in v-v′). Images were acquired at 400× original magnification. (B) Immunofluorescence using 3 different endothelial markers, CD31, Flk1, and CD34, confirmed the extravascular localization of placental RBCs (white boxes). V indicates blood vessels; scale bars, 20 μm. (C) Staining of yolk sac and fetal liver at the developmental stages when RBC extravasation was prominent in the placenta did not reveal major populations of ζ-globin$^+$ extravascular primitive RBCs (i-iii). By 11 weeks, the liver had generated ζ-globin$^-$ definitive RBCs (iv-iv′). Arrowheads mark circulating RBCs; arrows mark RBCs in the fetal liver parenchyma. Images were acquired at 200× original magnification.

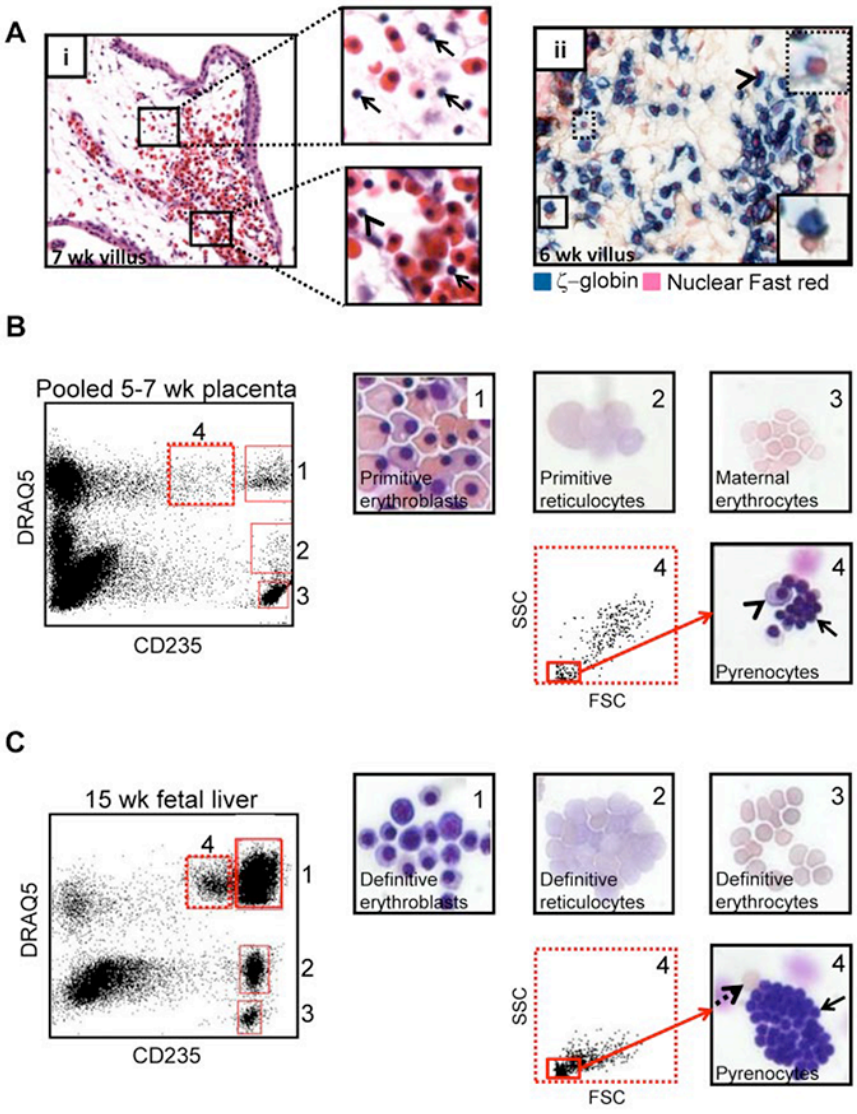

Figure 3. Primitive RBCs eject their nuclei in the placental villous stroma. (A) H&E staining of 7-week placenta (i) suggested the presence of free RBC nuclei (pyrenocytes) in the extravascular stroma of placental villi (top inset arrow) as well as less frequent pyrenocytes and primitive RBCs with pyknotic nuclei in circulation (bottom inset, arrow and arrowhead, respectively). Staining for ζ-globin and the nuclear counterstain Fast red (ii) demonstrated that pyrenocytes in the villous stroma were associated with ζ-globin$^+$ primitive RBCs (solid boxed inset arrowhead) or contained a small amount of ζ-globin (dotted boxed inset). Images were acquired at 400× original magnification. (B) The presence of primitive pyrenocytes in the placenta was further verified by cell sorting using the nucleic acid dye DRAQ5 in conjunction with CD235. Subgating for small cells in the CD235^{med}DRAQ5$^+$ (dotted gate 4) fraction permitted purification of primitive pyrenocytes from the placenta. Arrow marks pyrenocytes; arrowhead points to an erythroblast that cosorted with pyrenocytes. Images were acquired at 400× original magnification. (C) The same sorting strategy allowed the isolation of definitive pyrenocytes from the fetal liver. Solid arrow marks pyrenocytes, and dashed arrow indicates an enucleated erythrocyte that cosorted with the pyrenocytes. Images were acquired at 400× original magnification.

placental sections revealed that the placental villous stroma contained a large number of what appeared to be free red cell nuclei (Figure 3Ai top inset) at the time when primitive RBC enucleation was occurring. Occasional free nuclei were also found both in placental (Figure 3Ai bottom inset) and systemic (supplemental Figure 4) circulation. IHC for ζ-globin followed by a nuclear counterstain suggested that the free red cell nuclei in the placenta were primitive pyrenocytes due to their close association with ζ-globin$^+$ RBCs (Figure 3Aii). To confirm the presence of pyrenocytes in the placenta, FACS was combined with May-Grunwald Giemsa staining. Analysis of dissociated placental specimens from 5-7 weeks of developmental age, the time of maximal primitive RBC enucleation, based on CD235 and the nucleic acid dye DRAQ5 allowed the identification and sorting of distinct stages of primitive RBC maturation (Figure 3B): CD235$^+$DRAQ5$^+$ erythroblasts (gate 1), CD235$^+$DRAQ5^{lo} reticulocytes (gate 2), and CD235^{med}DRAQ5$^+$ pyrenocytes (gate 4). At this developmental stage no definitive fetal RBCs have circulated to the placenta, and CD235$^+$DRAQ5^{neg} maternal erythrocytes (gate 3) are the only enucleated RBCs that lack both DNA and RNA. As a control, the same sorting strategy was applied to second trimester fetal liver, which is an active hematopoietic site with ongoing definitive erythroid maturation (Figure 3C). A similar maturation profile, with the addition of fully mature fetal erythrocytes, was observed in the fetal liver.

Placental macrophages associate with extravascular primitive RBCs

As macrophages are known to associate with erythroblasts and digest enucleated RBC nuclei during definitive erythropoiesis in the fetal liver[27] and bone marrow, we investigated whether the enucleation of primitive erythroblasts in the human placenta also occurs in physical association with macrophages. IHC revealed a close association between placental macrophages (identified by factor XIII [FXIII]) and RBCs (CD235; Figure 4Ai) in the extravascular stroma of the placental villi in vivo. Furthermore, sorted placental macrophages were able to bind primitive erythroblasts in vitro (supplemental Figure 5). Macrophage–red cell clusters in the placental stroma were prominent at 5-7 weeks of developmental age. At 6.5 weeks, few macrophages were present in the fetal liver (Figure 4Aii). At 5.5 weeks, when enucleated primitive RBCs had already appeared in the placental stroma, there were rare, if any, FXIII$^+$ or CD68$^+$ macrophages in the fetal liver, whereas the

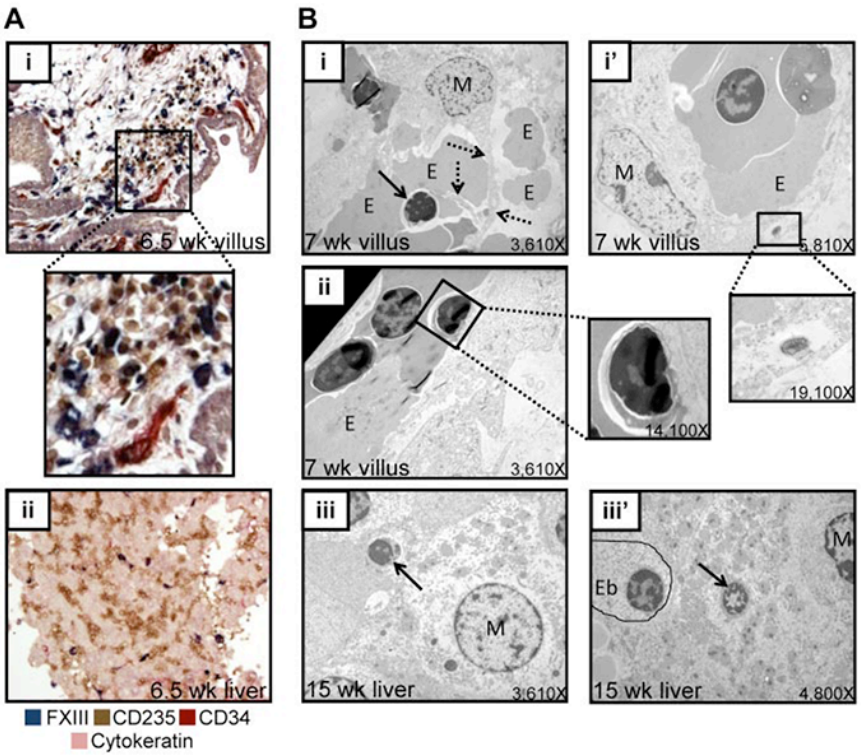

Figure 4. Primitive RBCs enucleate in the placental stroma in close association with placental macrophages. (A) Immunohistochemical staining of 6.5-week placental sections for macrophages (FXIII, blue), RBCs (CD235, brown), endothelial cells (CD34, red), and trophoblast (cytokeratin, purple) demonstrated the congregation of macrophages and RBCs in the extravascular stroma in placental villi (i; a higher magnification inset of the boxed area is also shown), whereas at the same developmental age very few macrophages were found in the fetal liver (ii). Images were acquired at 200× original magnification. (B) EM performed on 7-week placental villi demonstrated both direct physical interactions between placental macrophages and erythroblasts (i). Dashed arrows indicate macrophage cytoplasmic projection, solid arrow denotes ejected nucleus; M, macrophage; E, erythroid cell. as well as macrophages containing ingested nuclei (i′ inset) and pyrenocytes in circulation (ii inset). These macrophage-RBC associations were reminiscent of RBC maturation during definitive erythropoiesis in the fetal liver, where both free pyrenocytes (iii arrow) and engulfed nuclei (iii′ arrow; Eb, erythroblast) were present. All original magnifications for EM micrographs are as indicated.

placenta was readily populated by these cells (supplemental Figure 6). EM of placental villi demonstrated cytoplasmic projections from macrophages contacting extravascular erythroblasts (Figure 4Bi), forming structures reminiscent of erythroblast islands in the fetal liver (Figure 4Biii). Furthermore, both placental and fetal liver macrophages were observed to both engulf and digest nuclei (Figure 4Bi′,iii′). Free red cell nuclei were also detected by EM both in the placenta villous stroma (Figure 4Bi) and placental circulation (Figure 4Bii) as well as the fetal liver (Figure 4Biii). These data suggest that placental macrophages may function in primitive erythropoiesis to digest ejected primitive RBC nuclei.

Fetal macrophage progenitors are found in the precirculation placenta

Given the association of placental macrophages with primitive RBC enucleation, we next asked at what developmental stage macrophages entered the placenta. IHC for FXIII demonstrated that rare macrophages were present already in precirculation specimens in the chorionic plate (Figure 5Ai). With increasing developmental age, macrophages became more numerous and populated both the chorionic plate (Figure 5Aii-iii) and the villi (Figure 5Aii′-iii′). To determine whether macrophage progenitors were present in the placenta, colony-forming assays were performed (Figure 5B). This analysis revealed that clonogenic macrophage progenitors are present in the placenta even before the onset of fetoplacental circulation. XY and microsatellite PCR confirmed that these progenitors were fetal in origin (Figure 5C). FACS and methylcellulose colony assays demonstrated that only $CD34^+CD43^+$ cells were capable of giving rise to a hematopoietic colony (supplemental Figure 7A). Flow cytometry confirmed that $CD34^+CD43^+$ progenitors are present in the placenta already in precirculation specimens (supplemental Figure 7B). Immunofluorescence revealed putative macrophage-committed progenitors expressing CD34, CD43, and either FXIII or CD68, in the chorionic plate of precirculation specimens (Figure 5Di-i′), suggesting that macrophages are generated de novo in the placenta or migrate there as progenitors through the extraembryonic mesoderm. By 6 weeks, most macrophages in the chorionic plate and villi no longer expressed CD34 (Figure 5Dii-ii′), and the frequency of macrophage progenitors, as determined by colony-forming assays, decreased (Figure 5B and supplemental Figure 7C). In summary, these results imply that macrophage progenitors populate the chorionic plate of the placenta before the onset of fetoplacental circulation, and their progeny migrate into the villous stroma and participate in the terminal stages of the enucleation process of primitive RBCs.

Discussion

The identification of the human placenta as a hematopoietic organ has provided an accessible tissue to permit the study of early human embryonic hematopoiesis. In addition to being a source of definitive hematopoietic stem/progenitor cells,[16-18] the placenta contains a large pool of primitive RBCs, making the study of RBC enucleation and embryonic globin regulation in vivo feasible.[35] Here we show that the first trimester human placenta has an unexpected role in primitive erythroblast maturation. Our data reveal that circulating primitive erythroblasts extravasate into the stroma of placental villi and enucleate there in association with macrophages. The presence of clonogenic macrophage progenitors in the chorionic plate of precirculation placentas raises the possibility that macrophages may be generated de novo in the placenta and mature there, after which they migrate to the villi to physically interact with primitive RBCs and ingest primitive pyrenocytes. These data suggest that the first trimester human placenta, in addition to its newly identified function in definitive hematopoiesis, also has an integral role in primitive hematopoiesis (Figure 6).

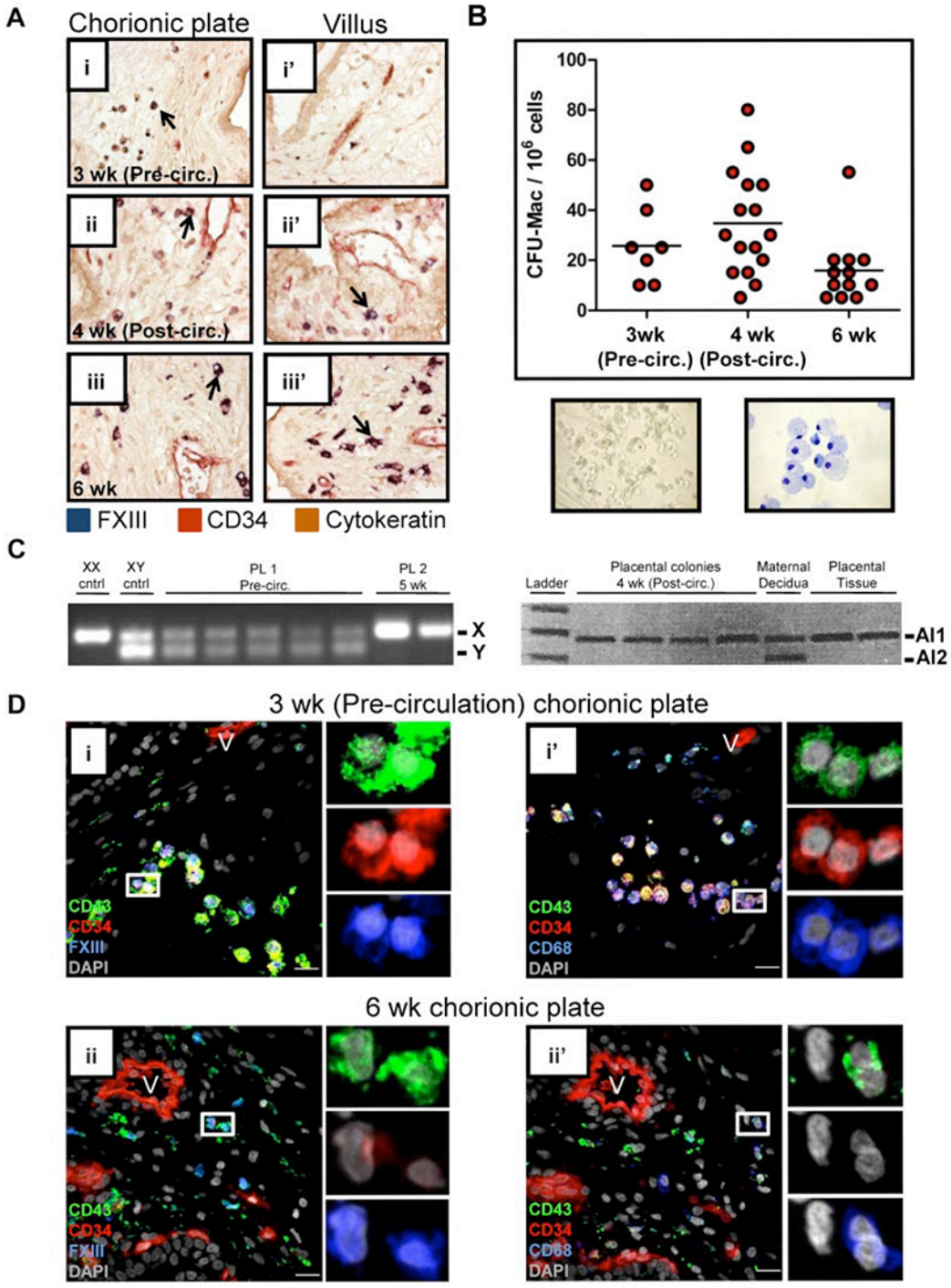

Figure 5. The human placenta contains macrophage progenitors before the onset of fetoplacental circulation. (A) IHC of placental sections revealed the progressive migration of FXIII$^+$ macrophages (arrows) from the chorionic plate (i) into the villi (ii′-iii′). Images were acquired at 200× original magnification. (B) Methylcellulose colony-forming assays documented the presence of clonogenic macrophage progenitors in the chorionic plate of the human placenta before the onset of fetoplacental circulation. A representative macrophage colony (original magnification, ×100) and May-Grunwald Giemsa–stained cytospin of a macrophage colony (original magnification, ×400) are shown. (C) PCR performed on single colonies from methylcellulose for the Y chromosome was able to demonstrate the fetal origin of placental colonies from male (sample 1, XY) but not female (sample 2, XX) specimens. In the case of an XX specimen, informative microsatellites, defined by differences in the number of repeats contained in alleles (AI1 and AI2) inherited from each parent could be used to verify the fetal origin of placental progenitors. Of 176 colonies picked and analyzed (ranging from precirculation to 8 weeks developmental age), none was found to be maternal (data not shown). (D) Immunofluorescent staining of placental sections demonstrated the presence of macrophage-committed progenitors (CD34$^+$CD43$^+$FXIII$^+$ and CD34$^+$CD43$^+$CD68$^+$ cells; i and i′ insets, respectively) in the chorionic plate of precirculation specimens. Later in development, placental macrophages no longer expressed CD34. V indicates blood vessels; scale bars, 20 μm.

Our study shows that human primitive erythroid cells, like their murine counterparts, ultimately enucleate.[30-32,36] This suggests strong parallels between primitive erythroid maturation in human and mice, albeit with possible differences in the site of enucleation. Previous work with mouse embryos has suggested that enucleation of primitive RBCs may take place in the bloodstream[31] or the fetal liver.[30,32,36] Our data revealed that during human development, the placenta is a major, and possibly the first, site of primitive erythroid

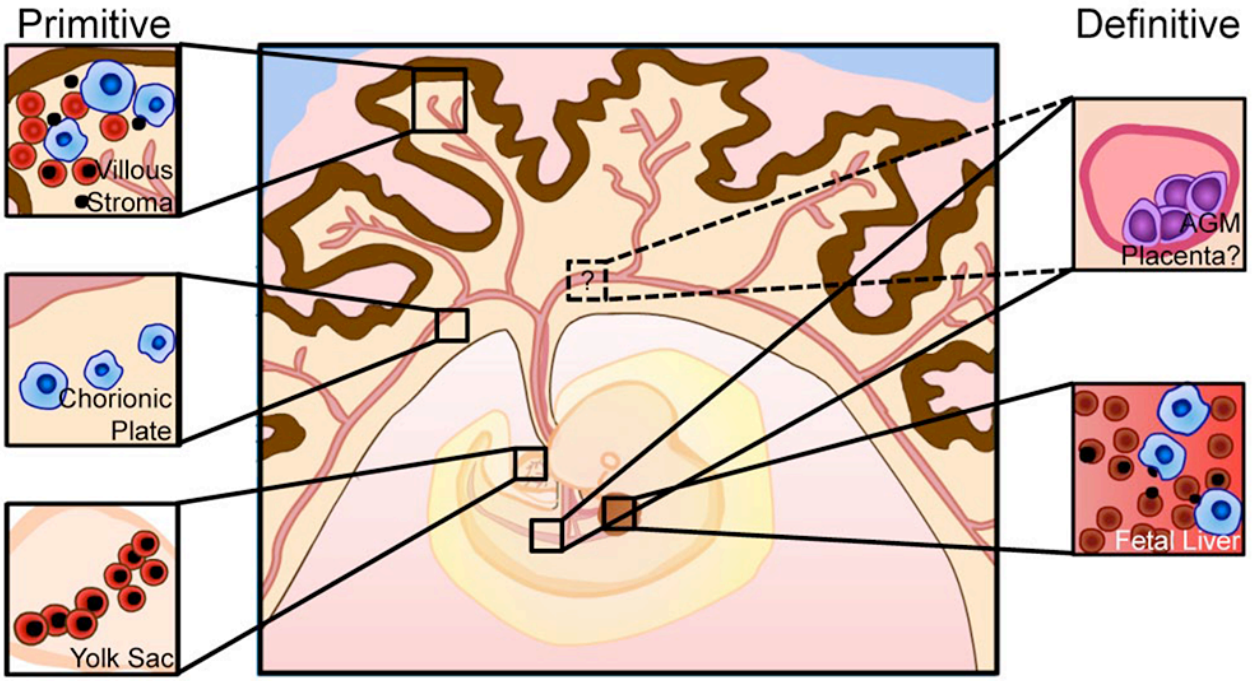

Figure 6. Updated model of human embryonic hematopoiesis. Primitive erythroid cells are generated in the yolk sac (bottom left) and enter circulation with an intact nucleus. Macrophage progenitors appear in the chorionic plate of the placenta (middle left) and generate mature macrophages that migrate to the placental villi. Primitive erythroblasts and macrophages convene in the extravascular stroma of the placental villi to facilitate terminal maturation and enucleation of primitive RBCs and clearance of ejected nuclei (top left), in a similar manner to definitive RBC maturation in the fetal liver (bottom right). Concurrently, definitive HSCs are generated in the dorsal aorta, umbilical and vitelline arteries, and potentially in the placenta, and colonize the fetal liver for expansion and differentiation.

enucleation based on the enrichment of enucleated RBCs in the placental stroma (Figure 1) and the lack of extravascular RBCs in the early fetal liver (Figure 2). Furthermore, the relative paucity of macrophages in the fetal liver at the time when enucleation of primitive red cells is already occurring (Figure 4 and supplemental Figure 6) suggests that the human fetal liver may not be able to assist erythroblast enucleation until later in development. Despite overt differences in placental architecture[37] in mice and humans, it is possible that the murine placenta also supports enucleation of primitive RBCs. Although this possibility was not examined in previous work, our data suggest that the murine placenta harbors major populations of macrophages and pyrenocytes at the time when enucleation of primitive RBCs occurs (E12.5-E16.5) and may also support primitive erythroblast maturation (A. Chhabra, A. Lechner, B.V.H., M. Tallquist, H.K.A.M., manuscript in preparation).

The presence of macrophages (Hofbauer cells) in the human placenta has been recognized for a long time,[38,39] but their origin has been unknown. Our data revealed the presence of macrophages and macrophage committed progenitors in the chorionic plate of the placenta even before fetoplacental circulation has started, suggesting that the macrophages may be generated de novo in the placenta and later migrate to the villi to promote the terminal maturation and enucleation of primitive RBCs. Placental Hofbauer cells are thought to have multiple functions, including the promotion of vascularization via the production of vascular endothelial growth factor[40] and angiopoietin-2.[41] These factors may also affect definitive hematopoietic stem/progenitor cells in the placenta, either directly or indirectly via the vascular niche. In addition, the localization of placental macrophages at the site of fetal-maternal exchange and their documented expression of iron transport and storage proteins[42] is suggestive of a potential role for placental macrophages in early iron transport to the embryo, but investigation of this hypothesis is beyond the scope of the present work. Together, these data indicate that Hofbauer cells may be generated in situ in the placenta and highlight their dynamic roles in early embryonic hematopoiesis and development.

Although the placenta has not been traditionally regarded as a hematopoietic organ, these findings together with the recent reports of the human placenta as a source of definitive hematopoietic stem/progenitor cells imply an important and much broader role for the human placenta in development beyond its well-established function in RBC oxygenation and iron transport. These findings have opened up new avenues to investigate the mechanisms that direct hematopoietic specification, hematopoietic stem/progenitor development and expansion, as well as terminal erythroid maturation during early human development and may help to understand the etiology of pregnancy complications that originate from defects in placental development and function.

Acknowledgments

The authors thank James Palis for insightful discussions about experimental design and data as well as critical reading of the manuscript and Thalia Papayannapoulou for the gift of the anti-ζ-globin antibody. The authors also thank the staff of the UCLA Translational Pathology Core Laboratory for assistance in specimen preparation and Marianne Cilluffo for expert assistance with EM.

This work was supported by a California Institute for Regenerative Medicine (CIRM) New Faculty Award (RN1-00 557-1) and an NIH/National Heart, Lung, and Blood Institute (NHLBI) RO1 (HL097766-01) to H.K.A.M. B.V.H was supported by the NIH Ruth Kirschstein National Research Service Award (GM007185), and S.L.P. was supported by the Howard Hughes Medical Institute

Gilliam fellowship. M.M. was supported by the Swedish Research Council and the Tegger Foundation.

Authorship

Contribution: B.V.H. designed and performed research and wrote the manuscript; S.L.P. designed and performed research; N. H.-K., A.H., M.M., B.A., and E.H. performed research; A.C. provided vital reagents; and H.K.A.M. designed and supervised research and wrote the manuscript.

Conflict-of-interest disclosure: B.V.H., A.H., and M.M. are cofounders of and own significant financial stakes in Novogenix Laboratories, LLC. The remaining authors declare no competing financial interests.

Correspondence: Hanna Mikkola, 621 Charles E. Young Dr S, LSB 2204, Los Angeles, CA 90095; e-mail: hmikkola@mcdb.ucla.edu.

References

1. Mikkola HK, Orkin SH. The journey of developing hematopoietic stem cells. *Development.* 2006; 133(19):3733-3744.
2. Cumano A, Godin I. Ontogeny of the hematopoietic system. *Annu Rev Immunol.* 2007;25:745-785.
3. Orkin SH, Zon LI. Hematopoiesis: an evolving paradigm for stem cell biology. *Cell.* 2008;132(4): 631-644.
4. McGrath KE, Palis J. Hematopoiesis in the yolk sac: more than meets the eye. *Exp Hematol.* 2005;33(9):1021-1028.
5. Yokota T, Huang J, Tavian M, et al. Tracing the first waves of lymphopoiesis in mice. *Development.* 2006;133(10):2041-2051.
6. Bertrand JY, Jalil A, Klaine M, Jung S, Cumano A, Godin I. Three pathways to mature macrophages in the early mouse yolk sac. *Blood.* 2005;106(9): 3004-3011.
7. Cumano A, Dieterlen-Lievre F, Godin I. Lymphoid potential, probed before circulation in mouse, is restricted to caudal intraembryonic splanchnopleura. *Cell.* 1996;86(6):907-916.
8. Godin I, Cumano A. The hare and the tortoise: an embryonic haematopoietic race. *Nat Rev Immunol.* 2002;2(8):593-604.
9. Jaffredo T, Nottingham W, Liddiard K, Bollerot K, Pouget C, de Bruijn M. From hemangioblast to hematopoietic stem cell: an endothelial connection? *Exp Hematol.* 2005;33(9):1029-1040.
10. Medvinsky A, Dzierzak E. Definitive hematopoiesis is autonomously initiated by the AGM region. *Cell.* 1996;86(6):897-906.
11. Muller AM, Medvinsky A, Strouboulis J, Grosveld F, Dzierzak E. Development of hematopoietic stem cell activity in the mouse embryo. *Immunity.* 1994;1(4):291-301.
12. Rhodes KE, Gekas C, Wang Y, et al. The emergence of hematopoietic stem cells is initiated in the placental vasculature in the absence of circulation. *Cell Stem Cell.* 2008;2(3):252-263.
13. Gekas C, Dieterlen-Lievre F, Orkin SH, Mikkola HK. The placenta is a niche for hematopoietic stem cells. *Dev Cell.* 2005;8(3):365-375.
14. Alvarez-Silva M, Belo-Diabangouaya P, Salaun J, Dieterlen-Lievre F. Mouse placenta is a major hematopoietic organ. *Development.* 2003;130(22): 5437-5444.
15. Ottersbach K, Dzierzak E. The murine placenta contains hematopoietic stem cells within the vascular labyrinth region. *Dev Cell.* 2005;8(3):377-387.
16. Barcena A, Muench MO, Kapidzic M, Fisher SJ. A new role for the human placenta as a hematopoietic site throughout gestation. *Reprod Sci.* 2009; 16(2):178-187.
17. Barcena A, Kapidzic M, Muench MO, et al. The human placenta is a hematopoietic organ during the embryonic and fetal periods of development. *Dev Biol.* 2009;327(1):24-33.
18. Robin C, Bollerot K, Mendes S, et al. Human placenta is a potent hematopoietic niche containing hematopoietic stem and progenitor cells throughout development. *Cell Stem Cell.* 2009;5(4):385-395.
19. Kinder SJ, Tsang TE, Quinlan GA, Hadjantonakis AK, Nagy A, Tam PP. The orderly allocation of mesodermal cells to the extraembryonic structures and the anteroposterior axis during gastrulation of the mouse embryo. *Development.* 1999; 126(21):4691-4701.
20. Ueno H, Weissman IL. Clonal analysis of mouse development reveals a polyclonal origin for yolk sac blood islands. *Dev Cell.* 2006;11(4):519-533.
21. Huber TL, Kouskoff V, Fehling HJ, Palis J, Keller G. Haemangioblast commitment is initiated in the primitive streak of the mouse embryo. *Nature.* 2004;432(7017):625-630.
22. Palis J, Yoder MC. Yolk-sac hematopoiesis: the first blood cells of mouse and man. *Exp Hematol.* 2001;29(8):927-936.
23. Palis J. Ontogeny of erythropoiesis. *Curr Opin Hematol.* 2008 May;15(3):155-161.
24. Kingsley PD, Malik J, Emerson RL, et al. "Maturational" globin switching in primary primitive erythroid cells. *Blood.* 2006;107(4):1665-1672.
25. Leder A, Kuo A, Shen MM, Leder P. In situ hybridization reveals co-expression of embryonic and adult α globin genes in the earliest murine erythrocyte progenitors. *Development.* 1992;116(4): 1041-1049.
26. Peschle C, Mavilio F, Care A, et al. Haemoglobin switching in human embryos: asynchrony of ζ-α and epsilon-gamma-globin switches in primitive and definite erythropoietic lineage. *Nature.* 1985; 313(5999):235-238.
27. Kawane K, Fukuyama H, Kondoh G, et al. Requirement of DNase II for definitive erythropoiesis in the mouse fetal liver. *Science.* 2001;292(5521): 1546-1549.
28. Chasis JA, Mohandas N. Erythroblastic islands: niches for erythropoiesis. *Blood.* 2008;112(3): 470-478.
29. Spike BT, Dibling BC, Macleod KF. Hypoxic stress underlies defects in erythroblast islands in the Rb-null mouse. *Blood.* 2007;110(6):2173-2181.
30. McGrath KE, Kingsley PD, Koniski AD, Porter RL, Bushnell TP, Palis J. Enucleation of primitive erythroid cells generates a transient population of "pyrenocytes" in the mammalian fetus. *Blood.* 2008;111(4):2409-2417.
31. Kingsley PD, Malik J, Fantauzzo KA, Palis J. Yolk sac-derived primitive erythroblasts enucleate during mammalian embryogenesis. *Blood.* 2004; 104(1):19-25.
32. Isern J, Fraser ST, He Z, Baron MH. The fetal liver is a niche for maturation of primitive erythroid cells. *Proc Natl Acad Sci U S A.* 2008;105(18): 6662-6667.
33. Thorpe SJ, Thein SL, Sampietro M, Craig JE, Mahon B, Huehns ER. Immunochemical estimation of haemoglobin types in red blood cells by FACS analysis. *Br J Haematol.* 1994;87(1):125-132.
34. Yoshida H, Kawane K, Koike M, Mori Y, Uchiyama Y, Nagata S. Phosphatidylserine-dependent engulfment by macrophages of nuclei from erythroid precursor cells. *Nature.* 2005;437(7059):754-758.
35. Sankaran VG, Menne TF, Xu J, et al. Human fetal hemoglobin expression is regulated by the developmental stage-specific repressor BCL11A. *Science.* 2008;322(5909):1839-1842.
36. Fraser ST, Isern J, Baron MH. Maturation and enucleation of primitive erythroblasts during mouse embryogenesis is accompanied by changes in cell-surface antigen expression. *Blood.* 2007;109(1):343-352.
37. Georgiades P, Ferguson-Smith AC, Burton GJ. Comparative developmental anatomy of the murine and human definitive placentae. *Placenta.* 2002;23(1):3-19.
38. Kappelmayer J, Bacsko G, Kelemen E, Adany R. Onset and distribution of factor XIII-containing cells in the mesenchyme of chorionic villi during early phase of human placentation. *Placenta.* 1994;15(6):613-623.
39. Ingman K, Cookson VJ, Jones CJ, Aplin JD. Characterisation of Hofbauer cells in first and second trimester placenta: incidence, phenotype, survival in vitro and motility. *Placenta.* 31(6):535-544.
40. Demir R, Kayisli UA, Seval Y, et al. Sequential expression of VEGF and its receptors in human placental villi during very early pregnancy: differences between placental vasculogenesis and angiogenesis. *Placenta.* 2004;25(6):560-572.
41. Seval Y, Sati L, Celik-Ozenci C, Taskin O, Demir R. The distribution of angiopoietin-1, angiopoietin-2 and their receptors tie-1 and tie-2 in the very early human placenta. *Placenta.* 2008;29(9): 809-815.
42. Bastin J, Drakesmith H, Rees M, Sargent I, Townsend A. Localisation of proteins of iron metabolism in the human placenta and liver. *Br J Haematol.* 2006;134(5):532-543.